UNIVERSITA' VITA-SALUTE SAN RAFFAELE

CORSO DI DOTTORATO DI RICERCA INTERNAZIONALE IN MEDICINA MOLECOLARE

Curriculum in Neuroscience and Experimental Neurology

DIFFERENCES IN BRAIN STRUCTURE AND FUNCTION IN PRIMARY HEADACHE DISORDERS: A MULTIMODAL MRI STUDY

DoS: Prof. Maria Assunta Rocca

Second Supervisor: Prof. Messoud Ashina

Tesi di DOTTORATO di RICERCA di Roberta Messina

matr. 013823

Ciclo di dottorato XXXIV

SSD MED/26

Anno Accademico 2020/2021

CONSULTAZIONE TESI DI DOTTORATO DI RICERCA

La sottoscritta/ *I*	Roberta Messina
Matricola / *registration number*	013823
nata a/ *born at*	Erice
il/*on*	19/03/1987

autore della tesi di Dottorato di ricerca dal titolo / *author of the PhD Thesis entitled*

DIFFERENCES IN BRAIN STRUCTURE AND FUNCTION IN PRIMARY HEADACHE DISORDERS: A MULTIMODAL MRI STUDY

☐ AUTORIZZA la Consultazione della tesi / AUTHORIZES *the public release of the thesis*

☒ NON AUTORIZZA la Consultazione della tesi per 8 mesi /DOES NOT AUTHORIZE *the public release of the thesis for 8 months*

a partire dalla data di conseguimento del titolo e precisamente */ from the PhD thesis date, specifically*

Dal / *from* 01/01/2022 Al / *to* 01/08/2022

Poiché /*because*:

□ l'intera ricerca o parti di essa sono potenzialmente soggette a brevettabilità/ *The whole project or part of it might be subject to patentability;*

X ci sono parti di tesi che sono già state sottoposte a un editore o sono in attesa di pubblicazione/ *Parts of the thesis have been or are being submitted to a publisher or are in press;*

□ la tesi è finanziata da enti esterni che vantano dei diritti su di esse e sulla loro pubblicazione/ *the thesis project is financed by external bodies that have rights over it and on its publication.*

Data /Date 20/10/2021 Firma/Signature Roberta Messina

DECLARATION

This thesis has been composed by myself and has not been used in any previous application for a degree. Throughout the text I use both 'I' and 'We' interchangeably.

- The present work "Neural correlates of visuospatial processing in migraine: does the pain network help?" (Chapter 3) was performed by Roberta Messina in partial fulfilment of the requirements for obtaining the PhD degree at Vita-Salute San Raffaele University, Milano, Italy. The present work has already been published in Molecular Psychiatry (PMID: 33837270, DOI: 10.1038/s41380-021-01085-2).
- The present work "Dysregulation of multisensory processing stands out from an early stage of migraine: a study in pediatric patients" (Chapter 4) was performed by Roberta Messina in partial fulfilment of the requirements for obtaining the PhD degree at Vita-Salute San Raffaele University, Milano, Italy. The present work has already been published in Journal of Neurology (PMID: 31745724, DOI: 10.1007/s00415-019-09639-9).
- The present work "Clinical correlates of hypothalamic functional changes in migraine patients" (Chapter 5) was performed by Roberta Messina in partial fulfilment of the requirements for obtaining the PhD degree at Vita-Salute San Raffaele University, Milano, Italy. The present work is currently in press and will be published soon in Cephalalgia.
- Results of the study "Biomarkers of migraine and cluster headache: differences and similarities" (Chapter 6) were performed in collaboration with Prof PJ Goadsby, Dr CH Sudre and Prof S Ourselin, NIHR-Wellcome Trust King's Clinical Research Facility and School of Biomedical Engineering & Imaging Sciences, King's College London, London, UK.

  Clinical and MRI data used for this part of the project were collected by Roberta Messina at the King's College London in the context of her Postgraduate Specialisation in Neurology.

All sources of information are acknowledged by means of reference.

Acknowledgements

At the end of this journey, I'd like to dedicate this achievement to my grandparents, Vincenzo and Rita. Even if they are not here anymore, I'm sure they will be making a toast in my honor.

I also would like to dedicate a few words to all the people who have contributed to my course and given their support:

My DoS, Prof Rocca, for having supported my research work in the last 10 years and for her precious advice.

Prof Filippi, for his valuable guidance and the professional growth opportunities he has offered to me over these years.

I thank Prof. Messoud Ashina for sharing with me his expertise, his supervision and interest to my PhD project.

I also would like to thank Dr. Colombo for having supported my clinical activities and Dr. Cetta for her help.

A very special gratitude goes out to all the people working in the Neuroimaging Research Unit for sharing with me their competence and for their constant support and their friendship.

Most importantly, I want to thank my parents and my sister for being my biggest supporters and for tolerating me in every circumstances. A special thanks to my grandmother, Rosa, for her unconditional love, my uncles, aunts, cousins and my brother-in-law, for their encouragement.

I also would like to thank all my friends who, have supported me and for their affection.

Finally, I'd like to thank all the participants who have kindly taken part to this project.

"The mind is not a vessel to be filled, but a fire to be kindled"

Plutarch

ABSTRACT

Over the last decades, migraine research has progressed extremely thanks to the advancement in brain imaging techniques, yielding new insights into brain changes associated with the acute and interictal phase of migraine. Although previous MRI studies have broadened the understanding of migraine pathophysiology, a few unanswered questions need further investigations. During my PhD project, I have provided new insights into cerebral mechanisms underlying visuospatial processing in interictal migraine patients. During a visuospatial task, migraine patients may implement some adaptive mechanisms to maintain an adequate performance. Interestingly, these compensatory mechanisms involved the same brain regions that are usually implicated in nociception, suggesting the presence of a common brain network for visuospatial and pain processing. A crucial question that is still unresolved is whether interictal functional and structural brain alterations could be brain traits that predispose to the development of migraine or a brain state secondary to the recurrence of migraine attacks. This PhD project revealed the presence of functional alterations in brain networks implicated in pain, multisensory and cognitive processing in pediatric patients with migraine. The existence of an early dysregulation of the main sensory and cognitive brain networks suggests that these functional patterns could be a phenotypic biomarker of migraine. During my PhD, I have also focused the attention on the hypothalamus, a key area involved in migraine pathophysiology. I demonstrated that, during the interictal phase, the hypothalamus modulates the activity of pain and visual processing areas in migraine patients. Of note, the hypothalamic-cortical interplay changes dynamically over time according to patients' clinical features. Finally, I have tried to cast light on the important unanswered question regarding the specificity of brain functional and structural imaging alterations revealed in migraine patients. Combining machine learning techniques and multimodal MRI modalities, I showed that functional biomarkers, including the hypothalamic and periaqueductal functional networks, are shared by migraine and cluster headache patients, while the thalamo-cortical pathway is likely to be the neural substrate that differentiates these two forms of primary headaches with their distinct clinical features. Taken together these results support the idea that migraine is a complex neurological disorder that involves the interplay of brain traits, as well as dynamic brain changes that influence the course of the disease.

TABLE OF CONTENTS

ACRONYMS AND ABBREVIATIONS

AD	Axial diffusivity
BOLD	Blood oxygenation level dependent
BPM	Biological Parametric Mapping
CBF	Cerebral blood flow
CGRP	Calcitonin gene related peptide
CSD	Cortical spreading depression
cAMP	Cyclic adenosine monophosphate
cGMP	Cyclic guanosine monophosphate
DARTEL	Diffeomorphic Anatomical Registration using Exponentiated Lie algebra
DLPFC	Dorsolateral prefrontal cortex
DMN	Default mode network
DTI	Diffusion tensor imaging
ECN	Executive control network
EEG	Electroencephalogram
FA	Fractional anisotropy
FC	Functional connectivity
FlA	Flip angle
FLAIR	Fluid attenuated inversion recovery
FOV	Field of view
FMRI	Functional magnetic resonance imaging
FPN	Frontoparietal network
FWE	Family-wise error
GM	Grey matter
HARS	Hamilton Anxiety Rating Scale
HDRS	Hamilton Depression Rating Scale
HIT-6	Headache Impact Test
IC	Independent components
ICA	Independent component analysis
IoS	Patients with decreased or stable attack frequency at follow-up
IT	Inversion time
K_{ATP}	ATP-sensitive potassium
LV	Lesion volume
MD	Mean diffusivity
MIDAS	Migraine Disability Assessment questionnaire
MNI	Montreal Neurological Institute
MRI	Magnetic resonance imaging
MWA	Migraine with aura
MWoA	Migraine without aura
NRS	Numerical Rating Scale
OFG	Orbitofrontal gyrus

PACAP	Pituitary adenylate cyclase-activating peptide
PAG	Periaqueductal grey matter
pCASL	Pseudo-continuous Arterial Spin Labeling
PET	Positron emission tomography
PPTH	Persistent posttraumatic headache
RCTs	Randomized controlled trials
RD	Radial diffusivity
ROI	Regions of interested
RS	Resting state
RT	reaction time
SD	Standard deviation
SMN	Sensorimotor network
SPECT	Single photon emission computerized tomography
SPM	Statistical parametric mapping
STN	Spinal trigeminal nucleus
SVM	Support vector machine
TE	Echo time
TR	Repetition time
VIP	Vasoactive intestinal peptide
WM	White matter
WMHs	White matter hyperintensities
Wo	Patients with increased attack frequency at follow-up

LIST OF FIGURES AND TABLES

Supplementary Table 3.1.2	Regions showing significant increasing or decreasing activation associated to the angle discrimination task in migraine patients and controls
Supplementary Table 3.1.3	Regions showing significant increasing or decreasing activation associated to the colour discrimination task in migraine patients and controls
Table 4.1.1	Main demographic and clinical characteristics of the subjects enrolled in the study
Table 4.1.2	Global mean values and standard deviation of RS FC values of brain resting-state networks in controls and patients with migraine, expressed as Z-scores
Table 4.1.3	Regions showing significant RS FC differences between patients with migraine and controls in the RS networks of interest
Table 4.1.4	Within-group and between-group correlation coefficients (*r*) among the RS networks of interest in migraine patients and controls.
Table 5.1.1	Main demographic and clinical characteristics of migraine patients and controls enrolled in the study
Table 5.1.2	Regions showing significant decrease of hypothalamic resting state functional connectivity in patients with migraine compared to controls at baseline, as well as among subgroups of patients
Table 5.1.3	Regions showing significant hypothalamic resting state functional connectivity changes in the whole group of migraine patients over time, as well as in subgroups of patients
Supplementary Table 5.1.1.	Main baseline demographic and clinical characteristics of the subgroups of patients and controls that were studied longitudinally and those who were studied only at baseline
Supplementary Table 5.1.2	Regions showing positive resting state functional connectivity with the hypothalamus in migraine patients and controls at baseline
Supplementary Table 5.1.3	Regions showing significant decrease of hypothalamic resting state functional connectivity at baseline between migraine patients on and not on preventive treatments considered separately and controls
Supplementary Table 5.1.4	Regions showing significant decrease of hypothalamic resting state functional connectivity at baseline between the subgroups of migraine patients and controls that were studied at the two study time points, as well as among different subgroups of migraine patients
Supplementary Table 5.1.5	Regions showing significant longitudinal hypothalamic resting state functional connectivity changes in the subgroup of patients who were not taking preventive treatments at baseline and follow-up
Table 6.1.1	Demographic and clinical characteristics of controls and patients

Table 6.1.2	Classification performance of the most discriminative models differentiating headache patients from controls, as well as migraine from cluster headache patients
Table 6.1.3	Regional resting state functional connectivity differences between migraine patients and controls, as well as between cluster headache and migraine patients
Supplementary table 6.1.1	Regional thalamic resting state functional connectivity differences between patients with cluster headache and controls within the left thalamic RS FC IC4

1. INTRODUCTION

1.1 Primary headache disorders

Headache is a common neurological disease, which affects 46% of the global population, and is a major cause of disability (1). In 1988, the committee of the International Headache Society proposed a valid and comprehensive classification of headaches based on the type of symptoms and their modes of presentation. This classification identifies three main categories of headaches: primary headaches, secondary headaches and neuralgia and facial pain (2). Primary headaches, like migraine and cluster headache, encompass approximately two-thirds of all headache disorders (3). An increasing awareness of the importance of primary headache disorders has led to a growing interest in understanding their physiopathology and developing new therapies.

1.2 Migraine

Migraine is the second most prevalent primary headache disorder after tension type headache, affecting 1 billion people worldwide. Migraine is now widely recognized as a complex disorder characterized by recurrent episodes of pain and neurological symptoms that arise from the activation of distinct brain networks and the subsequent release of signaling molecules (4).

1.2.1 Epidemiology

Around 15% of the general population suffer from migraine with a male-to-female ratio of 1:3 (4). The onset of the disease peaks in both sexes between the ages of 30 and 39 years. Migraine affects also school-aged children and people aged 60 years or over with a prevalence of around 3-6% (5). It is interesting to note that migraine prevalence is stable over time, suggesting that it is a fluctuating disorder characterized by periods of remission interposed by relapses. The prevalence of migraine tends to decline with increasing age, especially in women (6).

Migraine has been graded as the second cause of years lived with disability worldwide and the leading cause of disability in people younger than 50 years, that is the time in life when we are most productive (7). The economic impact of migraine is enormous. In Europe, the costs attributed to migraine range between €50 to €111 billion, including indirect costs attributable to reduced productivity and absenteeism and direct costs, such

as medical examinations, drugs, and hospitalization. Moreover, there are also intangible costs associated to the emotional, family and lifestyle impact that the disease causes on the affected individual (5).

Approximately 1-2% of the general population is affected by a chronic form of migraine, defined by the International Classification of Headache Disorders as having at least 15 headache days per month of which at least 8 meeting the criteria for migraine, for more than 3 months (2). Around 3% of patients with episodic migraine can experience an increase in migraine attack frequency and evolve into the chronic form of the disease. Twenty-six percent of chronic migraine patients remit to the episodic form within 2 years (8). Key risk factors for migraine progression are obesity, age, baseline high attack frequency, female sex, snoring, stressful life events, low educational status and overuse of acute migraine drugs (9).

There is ample evidence showing an association between migraine and psychiatric comorbidities, such as depression and anxiety, as well as other chronic pain conditions, respiratory and cardiovascular problems (5, 10). Usually, comorbidities occur more often in patients with chronic migraine than episodic migraine, and they can serve as risk factors for migraine chronification (11).

1.2.2 Etiopathogenesis

Migraine is a multifactorial disease in which numerous environmental factors interact with a strong genetic substrate. Migraine heritability has been estimated to be around 42% (12). Several population-based family and twin studies demonstrated that first degree relatives of migraine patients are more likely to suffer from migraine than relatives of matched controls (13). A subject with a first-degree relative with migraine without aura has a 1.9-fold increase of relative risk of migraine, whereas in the case of migraine with aura the risk of the disease is 4 times higher (14). Of note, the relative risk increases with increased migraine severity, earlier age of onset, and the presence of migraine aura (15).

Genome-wide association studies found a higher risk of migraine in variants of genes implicated in synaptic plasticity, glutamatergic neurotransmission and vascular mechanisms (16, 17). While common forms of migraine are polygenic, familial hemiplegic migraine, a rare subtype of migraine with aura characterized by motor weakness that may last for several days, is monogenic (18). The genes that have been

recognized as causal for familial hemiplegic migraine are the CACNA1A gene (chromosome 19p13), encoding the 1αA subunit of P/Q type calcium channels, the ATP1A2 gene (chromosome 1q), which codes for the α2 subunit of the sodium-potassium ATPase pump, and the SCN1A gene (chromosome 2q24), which codes for the voltage gated sodium channel (19). These mutations result in higher levels of potassium and glutamate in the synaptic cleft that increase neuronal excitability and the susceptibility for the onset of migraine aura (13).

The genetic component interacts with environmental factors thus leading to an increase in the susceptibility of migraine. Many patients report an association between the presence or absence of specific exogenous or endogenous factors, called triggers, and the onset of a migraine attack. The most frequent triggers described by migraine patients are behavioural triggers (e.g. stress, fasting, sleep disturbances), dietary triggers (e.g., chocolate, wine, tyramine), environmental triggers (e.g., weather changes, visual stimuli or odours) and, especially in females, hormonal changes (20).

1.2.3 Physiopathology

Although numerous studies have advanced our understanding of migraine pathogenesis, the mechanisms responsible for migraine initiation are still unclear. Migraine was first considered a vascular disease. In 1940, the pioneering work of Ray and Wolff (21) found that electrical, chemical and mechanical stimulation of cranial arteries caused migraine-like headaches, implying that dilation of extracranial and intracranial vessels can activate trigeminal nociceptors, resulting in migraine pain perception. This theory was initially supported by the demonstration that ergotamine, a substance with a vasoconstrictor action, was able to block migraine attacks (22). However, it has been shown that the administration of strong vasodilators, like the calcitonin gene related peptide (CGRP) and vasoactive intestinal peptide (VIP), induce a modest vasodilation to activate perivascular trigeminal afferents (13). Moreover, magnetic resonance angiography studies (23, 24) showed that the migraine pain is associated to small arterial intracranial dilatation that is not affected by triptan administration and is not related to extracranial dilatation. These findings suggest that vascular mechanisms are neither sufficient, nor necessary to trigger a migraine attack (25).

The trigeminovascular system is an important player of the migraine attack. First order trigeminovascular neurons, located in the trigeminal ganglion, peripherally innervate the meninges and intracranial arteries and centrally project to second order trigeminovascular neurons located in the brainstem and the upper cervical spinal cord (26). In 1984, Moskowitz proposed the theory that a sterile neurogenic inflammation of the dura mater could cause the migraine pain (27). According to this theory, an early activation of first order trigeminovascular neurons releases vasoactive and endogenous inflammatory substances, like CGRP, substance P, VIP, histamine, and prostaglandins, at the level of the dura, which further increase the local blood flow and cause platelet aggregation, mast cell degranulation and plasma protein leakage. The inflammatory reaction, in turn, sensitizes and activates the trigeminovascular pathway at the level of the trigeminal ganglion, trigeminal cervical complex, thalamus, and other brain areas involved in pain perception (4, 27). However, this theory could not explain premonitory symptoms that occur before the onset of headache pain. In addition, drugs targeting the neurogenic dural inflammation were ineffective as acute and preventive treatments for migraine (28, 29).

Recent advances have shifted our understanding of migraine as a "neuro-vascular" disorder where neuronal alterations trigger the vascular changes and sensitization of the trigeminovascular pathway. It has been suggested that the migraine attack originates from an altered switching between hypo- and hyperexcitable states of brainstem and hypothalamic regions, which modulate the cellular and vascular functions of other brain areas (13). Brainstem areas, including the locus coeruleus, dorsal pons, rostral ventral medulla, superior salivatory and periaqueductal grey matter (PAG), the hypothalamus, thalamus, and cortical networks are key players of the migraine attack. Dysfunction in these brain networks can activate the trigeminovascular system and modulate autonomic responses and vascular changes, leading to the perception of pain (13, 30). Thalamic, hypothalamic and cortical alterations can explain the sensory hypersensitivity, homeostatic and cognitive changes experienced by patients during their migraine attack (13).

There is ample evidence suggesting that the cortical spreading depression (CSD) is the physiological substrate of migraine aura. CSD was first described in 1944 by Leao as a depolarization wave that is transmitted centrifugally, through the most superficial layers, to the adjacent cortical areas, without following any vascular or functional pattern. This

wave of depolarization initially produces neuronal and glial cells hyperexcitability, but then causes a depression of cortical activity that will last about 5-10 minutes. CSD propagates with a speed of 3 mm/second and lasts about a minute (31). In conjunction with the CSD, major metabolic, ionic and vascular changes are observed. With the progressive diffusion of the depolarization wave there is an increase in extracellular hydrogen ions and potassium, in the release of nitric oxide, serotonin, arachidonic acid and glutamate, as well as a decreases in intracellular sodium (32). The metabolic/ionic changes are accompanied by an increased blood flow, which is followed by sustained oligemia (13). The similarities found between CSD and patients' description of their migraine visual aura as a propagating wave of scotoma with scintillating borders that spread across the visual field at a rate of 3 mm/min has reinforced the hypothesis that the CSD could be the pathogenetic substrate of migraine with aura (32, 33). Neuroimaging studies have also confirmed the association between CSD and migraine aura showing a wave of occipital oligemia that progressively moved in about 15-45 minutes to the anterior brain regions, with a speed of 2 mm/minute, during the aura phase (34, 35). What could be the role of CSD in the headache phase of migraine with aura and whether CSD has a pathogenetic role also in migraine without aura it is still unclear. There is evidence showing that the CSD can activate and sensitize perivascular trigeminovascular afferents that transmit nociceptive impulses to the brainstem and cortical pain processing areas, thus explaining the headache pain present in both types of migraine with and without aura (36). The CSD can also modulate the activity of the brainstem, thalamus and trigeminovascular system with and without activation of meningeal nociceptors, suggesting its involvement also in migraine without aura (37-39).

Numerous preclinical and human provocation models have identified signalling pathways that could contribute to the genesis of the migraine attack (4, 40). The CGRP, pituitary adenylate cyclase-activating peptide (PACAP) and nitric oxide are potent vasodilators, which are broadly disseminated in the trigeminovascular system. There is evidence showing that the plasma concentration of CGRP and PACAP is elevated during spontaneous migraine attacks (41, 42). Furthermore, it has been shown that intravenous infusion of CGRP or PACAP induces migraine attacks in around 60% of migraine patients (43, 44), while the administration of glyceryl trinitrate, a nitric oxide donor, or phosphodiesterase 3 and 5 inhibitors reached an induction rate of approximately 80% (45-

47). Interestingly, all these molecules activate the intracellular cyclic guanosine monophosphate (cGMP) and cyclic adenosine monophosphate (cAMP) signalling pathways, which modulate the opening of ion channels, like the ATP-sensitive potassium (K_{ATP}) channels (40, 48). This evidence suggests that ion channels involved in nociceptive transmission, mainly potassium channels, might be the final common signalling pathway involved in migraine attack generation. This hypothesis was further confirmed by later studies showing that almost all patients with migraine (95-100%) developed a migraine attack after the administration of K_{ATP} or large (big)-conductance calcium-activated potassium ($BK_{Ca)}$ channel opener (49, 50). The exact site of action of these signalling molecules is still unknown. It is plausible that they may exert their action both peripherally, at the level of the smooth muscle cells of intracranial arteries, and centrally, in the perivascular trigeminal primary afferents (4, 40).

1.2.4 Clinical manifestations

Although head pain is the core symptom characterizing the migraine attack, migraine patients can also experience a plethora of non-headache symptoms starting before pain onset or persisting after headache resolution. Migraine is classically divided into different phases: the premonitory, aura, headache, postdrome, and interictal phases (13, 51).

The headache phase of the migraine attack may last form 4 to 72 hours and include a unilateral or bilateral, throbbing pain of moderate or severe intensity, which can be exacerbated by physical activity. During the attack, there must also be at least one of nausea and/or vomiting, phonophobia and photophobia (2). Other symptoms often experienced by migraine patients are osmophobia, cutaneous allodynia and cranial autonomic symptoms, comprising conjunctival injection, forehead/facial sweating, nasal congestion and lacrimation (52, 53).

Before the onset of the headache, numerous patients may experience premonitory symptoms that may last for up to 3 days. The prodromes typically consist of mood changes, such as the presence of a state of anxiety, depression or irritability, difficulty in concentration, food cravings, repetitive yawning, increased sensitivity to external stimuli, cranial autonomic symptoms and neck stiffness (54). The most commonly reported premonitory symptoms are yawning, mood change and tiredness (55). Although the migraine attack consists of distinct phases, premonitory symptoms may often continue

during the aura and headache phases (56). Recent studies have questioned whether triggers commonly reported by patients may actually be premonitory symptoms of the migraine attack (54). It has been shown that migraine patients who perceive lights, odours and foods as trigger factors, report the corresponding symptoms of photophobia, osmophobia and food cravings in the premonitory phase, suggesting that some premonitory symptoms may be misinterpreted as triggers by patients (57-59).

Around 30% of patients experience migraine aura before the onset of the headache pain. Aura symptoms may also occur in conjunction with the headache pain or in isolation without a subsequent headache (60, 61). Migraine aura consists of fully reversible, focal neurological symptoms that develop gradually over ≥5 minutes and last less than 60 minutes. The International Classification of Headache Disorders distinguish four types of migraine with aura according to the presence of visual, sensory, speech, motor, brainstem or retinal symptoms (2). The visual aura occurs in more than 90% of patients. It usually begins with the vision of jagged or zigzag lines that propagate from the centre of the visual field to the periphery, or vice versa and that sometimes are followed by central scotoma. Isolated scotomas, disturbances of visual perception and flashing lights can also be described by some patients (33, 61, 62). Less common are the sensory aura, which consists of unilateral paraesthesia or numbness that starting from the hand travels up to the entire upper limb and can spread to the ipsilateral face and tongue, and the dysphasic aura that comprise transient speech or language problems. Nonvisual aura symptoms can occur in unison with the visual disturbances or, less frequently, in isolation (63). Retinal migraine, migraine with brainstem aura and hemiplegic migraine are other subtypes of migraine aura that occur rarely and may comprise monocular visual disturbances, diplopia, hypacusia, tinnitus, ataxia, dysarthria, decreased level of consciousness, vertigo and moto weakness (2).

Many patients report that a variety of symptoms, including fatigue, sensory hypersensitivity, concentration difficulties, mood changes and neck stiffness, may persist for up to 24 hours after headache pain resolution, thus characterizing the postdrome phase (64, 65).

There is evidence showing that migraine patients might experience cognitive impairment and sensory hypersensitivity even during the interictal phase (13, 66-68). The

cognitive domains that are most affected in migraine patients are visuospatial ability, attention, executive functions, processing speed and memory (69, 70).

1.2.5 Diagnostic procedures

The first step for a correct diagnosis of migraine is to collect an accurate anamnestic history. The type of pain, its location, how long it has been present, if it always manifests itself with the same characteristics, if there are other symptoms associated with the pain and which are the factors that worsen the presentation are aspects that help clinicians to distinguish primary from secondary headaches and to identify the type of primary headache. A careful physical and neurological examination are also of fundamental importance to evaluate the possible presence of focal neurological signs and exclude other underlying diseases (71).

Diagnostic tests, including electroencephalogram (EEG), head computed tomography or brain magnetic resonance imaging (MRI), are warranted for patients with migraine only if the history or examination suggests the presence of a secondary headache. Interictal EEG is indicated only if the clinical history raises the suspicion of epilepsy as a possible differential diagnosis. Ictal EEG is indicated when headache may be a symptom of epileptic seizures or during aura episodes with confusion or decreased level of consciousness (72). Neuroimaging techniques should be considered in case of sudden onset headache, in patients older than 50 years with a new headache, patients with atypical headache features, a history of seizure, significant change in headache characteristics, an abnormal neurologic examination, other associated systemic symptoms or conditions (72, 73).

1.2.6 Treatment approaches

Migraine attacks can be highly disabling and can significantly impair function. Correct choice of medications is essential key component of the management of migraine patients. Migraine treatments primarily aim to relieve pain, restore function, and reduce headache frequency (74). For treatment decisions it is important to consider the severity and frequency of attacks, attack-related disability, previous treatment history, patient preferences, the presence of comorbidities, the use of concomitant medications and potential trigger factors (59, 75).

The objectives of acute migraine therapies include the reduction of pain, the control of associated symptoms (e.g., nausea, vomiting, phono and photophobia) and a rapid recovery to normal performance (76). Acute migraine therapies should be taken when the headache pain starts, to increase the chance of getting a good response. First-line drugs to treat mild-to-moderate migraine attacks include acetaminophen, non-steroidal anti-inflammatory drugs and caffeinated analgesic combinations, which are non-specific medications. These drugs inhibit the synthesis of prostaglandins in the perivascular area, thus blocking the increase of vessel permeability and the release of vasoactive amines (77). The effectiveness of common analgesics can be increased with the concomitant administration of prokinetic or antiemetic drugs, such as metoclopramide or domperidone, which increase analgesics absorption and reduce the nausea that could be experienced by patients during their attacks (78).

Triptans and ergotamine preparations are migraine-specific treatments that should be administrated for moderate or severe attacks or in case of failure of first-line drugs during mild-to-moderate episodes of migraine (75). Triptans are selective agonists for the 5-$HT1_B$ and 5-$HT1_D$ type serotonin receptors, which were first developed as selective cranial vasoconstrictors (79). Following studies showed that triptans can also modulate the activation of peripheral trigeminal nociceptors (80), reduce the release of vasoactive peptides (81) and exert a central modulatory effect on the brainstem, thalamus and cortical pain processing regions (80, 82, 83). Contraindications to the use of triptans include cerebro- or cardiovascular diseases, uncontrolled hypertension or ischemic bowel disease (56).

Novel acute therapies have been recently developed. These drugs include lasmitidan, a 5-$HT1_F$ receptor agonist, and gepants, small-molecule CGRP receptor antagonist, which all have documented effectiveness and safety for the treatment of the acute migraine attack (84).

The goals of migraine prevention are to reduce the duration, severity and frequency of the migraine attacks (75). Migraine prophylaxis should be start in patients who have four or more headache days per month, highly disabling attacks, and in those patients who do not respond to acute therapies or who have contraindications to acute treatments (85). Preventive therapies for migraine are considered successful if they reduce the frequency of migraine attacks by at least 50%. A significant improvement in attack duration and

severity, as well as in patients' quality of life, suggest also a positive response to migraine prevention (85).

Preventive drugs most commonly used for migraine prevention include oral beta-blockers, antidepressants, anticonvulsants, angiotensin II receptor antagonist inhibitors and calcium-channel blockers (86). Oral preventive treatments should be continued for at least 2 to 6 months, starting at a low dose that can be gradually increased until the therapeutic effect or the ceiling dose is reached (85). If migraine attacks are well controlled, preventive medications can be discontinued after approximately 6 months of treatments (78).

Another well-established therapeutic option for chronic migraine is botulinum toxin type A. This treatment consists of the intramuscular injection of 155 units of botulinum toxin type A that are administrated in different sites of the head and neck every 12 weeks (74). Treatment response to botulinum toxin type A should be evaluated after 6 to 9 months of treatment (4).

Based on recent studies showing a key involvement of CGRP in migraine pathophysiology, new therapies designed specifically for migraine have been introduced. These novel treatments are injectable monoclonal antibodies targeting the CGRP ligand or its receptor (fremanezumab, galcanezumab, eptinezumab, erenumab). Randomized controlled trials (RCTs) demonstrated that these drugs are safe, well-tolerated and effective in reducing the migraine attack frequency and patients' disability in patients with episodic and chronic migraine (87, 88). Recent data obtained from RCTs and real-world studies suggest that the benefits of anti-CGRP mAbs should be assessed after 3 to 6 months of treatment (4, 89). Clinical trials evaluating the role of small molecule CGRP receptor antagonists, atogepant and rimegepant in migraine prevention are ongoing (90).

Another promising migraine treatment option that has been developed recently is neuromodulation. Non-invasive devices, including electrical trigeminal nerve, single-pulse transcranial magnetic and noninvasive vagus nerve stimulation, have been demonstrated to be effective in reducing the migraine attack frequency and treating the acute migraine attack (75, 91). Nutraceutical compounds and psychological treatments are also valid therapies for those patients who have a preference for non-pharmacologic treatments, have low tolerance, or have medical contraindications to certain pharmacologic interventions (91).

1.3 Principles of magnetic resonance imaging

Although MRI is not recommended for routine use in the diagnosis of migraine, the application of advanced MRI techniques has played a decisive role in the study of migraine physiopathology.

1.3.1 Principles of functional MRI

Since 1990, the in vivo use of functional imaging has greatly enriched our knowledge about brain function providing information about heamodynamic changes. Blood constitutes are an excellent source of natural contrast for MRI thanks to the characteristics associated to the blood oxygenation level dependent (BOLD) mechanism. The haemoglobin saturation rate affects the T2 relaxation time of the blood, thus influencing the MRI signal. The activation of a certain brain area causes an increase in neuronal and glial metabolism and a corresponding increase in regional cerebral blood flow (CBF). The oxygen consumption is lower than the increase of blood flow, determining an increase in the ratio between oxygenated and deoxygenated haemoglobin, which enhances the MRI signal (92). The analysis of functional MRI (fMRI) images provides information about the extent of activation and functional interaction of brain areas involved in the performance of a given task, as well as brain regions in a rest condition (93).

Single photon emission computerized tomography (SPECT) and positron emission tomography (PET) identify and quantify the gamma rays released indirectly by radiolabeled molecules (tracers) injected into the body, thus providing information on the function and metabolism of brain tissues (94).

Perfusion MRI techniques use exogenous tracers (e.g., Gd-DTPA) or endogenous arterial water (pseudo-continuous Arterial Spin Labeling - pCASL) to quantify the regional CBF changes that are coupled to regional neural activity (95).

1.3.2 Principles of quantitative structural MRI techniques

Today, thanks to the introduction of modern techniques capable of analysing MR images, it is possible to study in-vivo brain morphometry, quantify macro- and microscopic structural alterations and evaluate the presence of any changes over time.

Volume-based morphometric approaches, like voxel-based morphometry, provide a voxel-by-voxel comparison of the regional grey and white matter (GM and WM) volume of the brain between different groups of subjects. Surface-based approaches allow investigating the laminar organization of the cerebral cortex and its division into columns, providing information about morphometric measures, such as the cortical thickness, cortical surface area and the gyrification index, on a vertex-by-vertex basis (96).

Diffusion-weighted MRI is a quantitative technique that is based on water diffusion in biological tissues. Water diffusion is conditioned by the size of the interstice and the presence of semi-permeable barriers that impose a directionality to the molecules. The diffusion coefficient provides information about the water movement in a translational motion. In most biological tissues, the water diffusion cannot be considered isotropic and the diffusion coefficient differ across the distinct directions. Pathological conditions can modify tissue integrity thus reducing the barrier to free water motion and increasing the value of the diffusion coefficient (97). An accurate quantification of water diffusion across biological tissues can be assessed in terms of a tensor (98), with a main axis and two smaller axes related to its depth and width. The diffusivity along the main axis is also known as parallel or axial diffusivity (AD), while the diffusivities along the two minor axes are frequently averaged to obtain the radial diffusivity (RD). The extent of water diffusion can be expressed by the mean diffusivity (MD) and the degree of anisotropy, which reflects the underlying tissue organization, can be calculated by the fractional anisotropy (FA).

1.4 The role of MRI in the understanding of migraine pathophysiology

Over the last decades, migraine research has progressed significantly thanks to the advancement in brain imaging techniques, yielding new insights into the brain mechanisms underlying the pathogenesis of migraine. Human provocation models and imaging techniques have allowed the capture of brain changes associated with the constellation of symptoms characterizing the acute phases of the migraine attack and have highlighted brain functional and structural alterations of the interictal phase (99).

1.4.1 Imaging the premonitory phase

PET and fMRI studies demonstrated an early activation of the hypothalamus, PAG, dorsal pons, frontal, temporal and occipital cortical areas in migraine patients experiencing nitroglycerine-triggered premonitory symptoms (100, 101). An early activation of the hypothalamus could mediate premonitory symptoms like fatigue, food craving, yawning and thirst, and explain the higher susceptibility to homeostatic changes described by some patients during the prodromal phase (54, 100). A crucial involvement of the hypothalamus in the premonitory phase of migraine has also been confirmed by fMRI studies during trigemino-nociceptive stimulation, showing an increased hypothalamic activity and altered functional interaction between the hypothalamus and the spinal trigeminal nucleus (STN) during the preictal phase in migraine patients studied daily for a month (102, 103).

There is also evidence of functional reorganization of the thalamo-cortical and pontine-cortical networks during the prodrome phase, which may be involved in mediating emotional, cognitive, autonomic and sensory symptoms. On the other hand, the photophobia and nausea could origin from an increased activation of the occipital cortex and rostral ventral medulla (54, 100, 104, 105). Interestingly, recent evidence showed an increased resting state (RS) functional interaction between the nucleus accumbens and the dorsal amygdala, rostral pons, parahippocampus and hippocampus during the preictal phase, suggesting the presence of early functional changes in dopamine-mediated descending pain control networks (106).

1.4.2 Imaging the pain phase

The activity of the dorsal pons and hypothalamus fluctuates throughout the migraine cycle, supporting their role in migraine attack generation and in facilitating the onset of the pain phase. Early PET studies (83, 107) showed a higher activation of the dorsal rostral pons and hypothalamus during the headache phase of spontaneous migraine attacks that persisted after complete pain-resolution induced by triptans injection, thus suggesting that these regions could be putative drivers of the migraine attack. More recently, fMRI studies (102, 106) showed a significant interaction between the pons and hypothalamus during the pain phase in migraine patients studied at rest and during

trigeminal nociceptive stimulation. Specifically, the most posterior part of the hypothalamus has been suggested to be involved in the onset of the migraine pain (108).

Several studies evaluating migraine patients during spontaneous (109, 110) and triggered (100, 101, 111) migraine attacks have reinforced the importance of the pons in the headache phase of migraine. A higher functional coupling between the pons and the ipsilateral primary somatosensory cortex has been found in migraine patients with aura during spontaneous headache (109). The pons showed also an increased functional connectivity (FC) with pain processing brain areas, including the cerebellum, STN, cingulate and frontal cortex in migraine patients with and without aura during nitroglycerin-triggered attacks (101).

Two other key actors of migraine pain are the trigeminovascular system and thalamus. After trigeminal nociceptive stimulation, migraine patients showed a gradient-like activity in the STN: migraine patients had decreased STN activation during the interictal phase, which increased over the pain-free migraine period (112). Interestingly, the amplitude of the STN signal could predict the time interval between headache attacks, suggesting an association between the oscillating behavior of the STN and the onset of the headache phase (112). During spontaneous migraine attacks without aura, the posterior thalamus displayed aberrant connection with the insula, frontal, and parietal pain processing regions (113). Furthermore, there is evidence that extracephalic cutaneous allodynia experienced by some patients during the ictal phase of their attacks may be mediated by a greater activity of the trigemino-thalamic circuit (114). A diffusion tensor imaging (DTI) study (115) showed dynamic microstructural changes of the thalamus during the different phases of a migraine episode: migraine patients had higher thalamic FA and lower MD during the interictal phase, but these values returned to normal during the pain phase. These changes could be the structural counterpart of the thalamic functional plasticity seen in migraine patients.

Beyond the involvement of single brain regions, recent evidence highlighted functional alterations of brain networks known to be involved in the attentional, cognitive and emotional aspects of pain in migraine patients studied during spontaneous and PACAP-induced migraine attacks (116-118).

MRI studies have also had a fundamental role in exploring the hemodynamic changes of cerebral and meningeal vessels associated to the headache phase in migraine patients.

Early PET and SPECT studies reported contradictory results on CBF changes in migraine patients with and without aura (25, 35, 119). Subsequent magnetic resonance angiography studies (23, 24) demonstrated that migraine pain is only associated with a slight dilatation of the middle cerebral, internal carotid and middle meningeal arteries, and is not associated to extracranial arterial dilatation.

1.4.3. Imaging the aura phase

The theory of migraine as a brain disorder rather than a vascular disease has been reinforced by fMRI techniques showing an association between CSD and migraine aura. Patients with induced and spontaneous visual aura attacks showed an increased BOLD-response that starting from occipital extrastriate brain areas (area MT/V3A) progressed contiguously over the cortex during checkerboard visual stimulation. The initial increased BOLD-response was followed by a reduction. Similar to CSD, the velocity of the BOLD signal change was approximately 3 mm/min, confirming the hypothesis that CSD is the electrophysiological correlate of migraine aura (62). Another study (114) found a higher BOLD response during positive aura symptoms (e.g., visual flashing) and a lower response during negative aura symptoms (e.g., dizziness), suggesting that different aura symptoms are linked to different patterns of neuronal activity.

1.4.4 Imaging the interictal phase

Many conventional and advanced MRI approaches have been applied to the study of migraine patients during the interictal phase (99). Conventional MRI studies using T2-weighted and fluid-attenuated inversion recovery (FLAIR) scans reported a higher prevalence of small, punctuate, round or oval shaped WM hyperintensities (WMHs) in migraine patients compared to controls (120-122). These results were not confirmed by other studies, suggesting that other aetiologies rather than migraine, like cardiovascular risk factors, might explain the presence of these alterations (123-125). WMHs of migraine patients usually involve the deep or periventricular WM (120). A few studies described also infarct-like hyperintensities involving deep brain structures and the cerebellum in migraine patients with and without aura (123, 126). Whether the occurrence of WMHs might be influenced by potential risk factors, such as the female gender, longer disease duration, higher migraine attack frequency and presence of migraine aura is still a matter

of debate (123, 127-129). Discordant results have also been found regarding the progression of WMHs in migraine patients (122, 130, 131). There is evidence suggesting that some of the mechanisms contributing to the occurrence of WMHs in migraine patients include neurogenic inflammation, increased neuronal activation and metabolic dysfunction (132). Other plausible mechanisms are endothelial dysfunction, atherosclerotic risk factors, cardiac abnormalities, like atrial septal defect and patent foramen ovale, and focal oligemia related to an altered cerebrovascular reactivity (123, 133, 134).

Several voxel-based and surface-based morphometry studies have shown the coexistence of regions of decreased and increased GM volume, cortical thickness, and cortical surface area in visual and nociceptive brain areas, such as the brainstem, thalamus, cerebellum, basal ganglia, hippocampus, frontal, parietal, temporal, and occipital areas, in migraine patients studied during the interictal phase (99). During this phase of migraine, patients showed also volumetric alterations of frontal and parietal areas involved in executive abilities and attentional processing (135, 136).

Microstructural alterations of the trigeminothalamic, thalamo-cortical, corpus callosum, frontal, parietal and temporal WM tracts have been found in interictal migraine patients, indicating an involvement of the trigeminal somatosensory and pain modulatory networks (137-140). There is also evidence showing that migraine patients with and without aura experience FA abnormalities in WM regions close to motion-processing visual areas, the superior colliculus and the lateral geniculate nucleus (141). Moreover, compared to controls and patients with migraine without aura, migraine patients with aura showed a specific involvement of the visual processing networks, as reflected by reduced FA and increased MD of the optic radiations (142).

Consistent with morphometric findings, a vast number of fMRI studies have shown that an altered functional activity of visual and pain processing brain regions might contribute to abnormal sensory processing in interictal migraine patients (143). Several studies using experimental pain stimulation have explored the neural substrate of pain perception in migraine patients, showing abnormal activation of the cingulate cortex (involved in the affective response to pain), somatosensory cortex, insula, thalamus (contributing to the sensory-discriminative aspects of pain perception), and prefrontal cortex (participating to the cognitive processing of pain) (143-145). Widespread

functional alterations in limbic (146, 147) and sensory-motor (148, 149) networks that might influence pain experience in migraine patients have also been described. It is interesting to note that recent evidence showed a higher activation of higher-order visual processing brain areas during trigeminal noxious heat stimulation in migraine patients with aura, thus reinforcing the presence of a common neuroanatomical and functional framework between the visual and nociceptive trigeminovascular system (150). Alterations in pain inhibitory/modulatory areas, including the thalamus, PAG, insula, somatosensory and anterior cingulate cortex, may lead to an imbalance in the inhibition and facilitation of pain signalling, thus explaining the impaired habituation to repetitive painful stimuli and the development of cutaneous allodynia in patients with migraine (151-154). Interestingly, a RS fMRI study (155) showed that reduced functional coupling between brain regions of the default mode (DMN) and executive control (ECN) networks could predict the development of cutaneous allodynia in migraine patients without aura after 3 years.

Although many studies have investigated the role of the hypothalamus in the acute phases of the migraine attack, only one small study has explored its involvement in the interictal phase showing an altered hypothalamic functional coupling with cortical regions implicated in pain processing, sympathetic and parasympathetic functions (156). Moreover, whether the hypothalamic functional alterations are associated with clinical features of migraine patients has not been investigated so far.

Similarly to what has been shown during the premonitory and pain phase of migraine, several fMRI studies reported an altered functional activation of cognitive brain networks, like the DMN and ECN, in migraine patients studied between migraine attacks (157, 158). The ECN and DMN are implicated in attentive and executive functions, such as working memory, attention and interoception (157, 158).

An important question that we still need to answer is whether interictal functional and structural brain alterations result from the recurrence of migraine attacks, representing a brain state, or are a brain trait that predisposes to the development of migraine (159). Two recent morphometric studies (140, 160) demonstrated that pediatric migraine patients, like adult migraine patients, have volumetric and microstructural alterations in GM regions and WM tracts involved in visual and pain processing. A morphometric MRI study (161) compared migraine twins with aura to their migraine-free

co-twins and unrelated migraine-free twins, which served as controls, showing a significant thicker cortex in V2 and V3A visual areas that were not associated to the frequency of headache or aura attacks (99). Taken together these findings support the hypothesis that morphometric alterations of key brain regions may be inherent traits associated with migraine pathophysiology. On the other hand, other studies revealed an association between brain alterations and patients' clinical features, such as disease duration and migraine attack frequency, implying that mechanisms of central reorganization might occur in response to the disease burden (151, 162, 163). This hypothesis is further reinforced by the demonstration of longitudinal brain morphometric changes over the years. There is evidence showing that migraine patients developed both increased and decreased volume of nociceptive regions over a period of 4 years, which were related to patients' disease activity (164). Overall, these results suggest that brain alterations observed using morphometric imaging techniques might derive from the interaction between predisposing brain traits and experience-dependent responses.

A further crucial question is whether MRI brain abnormalities are unique to migraine or are common to other headache and chronic pain disorders. Distinct patterns of brain activation, GM and WM morphometry have been found in migraine patients in comparison to patients with other types of headaches, like tension-type or persistent posttraumatic headache (PPTH), as well as compared to patients with other chronic pain conditions (165-170). However, there is evidence showing that some functional alterations involving pain processing brain networks, such as the frontal-parietal, DMN and sensorimotor (SMN) networks, are not migraine specific but are associated to the recurrent experience of pain (170).

A valuable strategy to identify MRI biomarkers of migraine is to use machine learning techniques. A few machine learning studies based on RS fMRI or morphometric MRI data have been used to discriminate migraine patients from controls, as well as migraine patients from patients with PPTH (169-173). The FC of brain regions implicated in the processing of the affective components of pain discriminated migraine patients from controls with an accuracy of 86% (169). Classifiers containing MRI measures of brain regional volumes, cortical thickness and cortical surface area of nociceptive areas were able to classify patients with chronic migraine from controls and from episodic migraine patients with an accuracy of 86% and 84%, respectively (171, 174). Recently, a

classification model combining clinical, WM microstructural and cortical morphometric data provided an accuracy of 78% for distinguishing migraine patients from patients with PPTH (172).

2. AIM OF THE WORK

Although previous MRI studies have broadened the understanding of migraine pathophysiology, a few unanswered questions need further investigations. In this perspective, my PhD project aimed to address the following unsolved issues:

(a) Which are the neural correlates of neuropsychological manifestations of migraine during the interictal phase?

(b) Are interictal functional MRI alterations predisposing traits or are the consequence of the recurrence of migraine attacks?

(c) Are patients' clinical characteristics influenced by the interictal functional activity of key players of the acute migraine attack? Do the functional activity of these key regions change over time? Do these changes influence migraine progression over the years?

(d) Is it possible to identify biomarkers that discriminate migraine from cluster headache patients?

In particular, the specific aims of this project were:

(a) To explore migraine patients' performance during a visuospatial task and investigate the activity of brain areas involved in visuospatial processing using an active fMRI paradigm;

(b) To elucidate whether interictal brain functional alterations might represent a predisposing trait to migraine, investigating RS FC of large-scale brain networks in pediatric migraine patients at an early stage of the disease and their correlation with patients' clinical features;

(c) To investigate the association between interictal RS functional activity of the hypothalamus and patients' clinical features, as well as explore whether such functional alterations might change over time and affect disease progression over the years;

(d) To identify MRI biomarkers that best distinguish migraine from cluster headache patients, using a machine learning approach and multimodal MRI modalities, and test whether the discrimination accuracy could be improved combining MRI and clinical data.

3. NEURAL CORRELATES OF VISUOSPATIAL PROCESSING IN MIGRAINE PATIENTS

3.1. Neural correlates of visuospatial processing in migraine: does the pain network help? Messina *et al.*, Mol. Psychiatry 2021.

This chapter describes the work published in Molecular Psychiatry (PMID: 33837270, DOI: 10.1038/s41380-021-01085-2).

Molecular Psychiatry
https://doi.org/10.1038/s41380-021-01085-2

ARTICLE

Neural correlates of visuospatial processing in migraine: does the pain network help?

Roberta Messina[1,2,3] · Alessandro Meani[1] · Gianna C. Riccitelli[4] · Bruno Colombo[2] · Massimo Filippi[1,2,3,5,6] · Maria A. Rocca[1,2,3]

Received: 26 November 2020 / Revised: 1 March 2021 / Accepted: 26 March 2021

Abstract

Migraine patients frequently report cognitive symptoms during the different phases of migraine. The most affected cognitive domains are visuospatial abilities, processing speed, attention and executive functions. We explored migraine patients' performance during a visuospatial task and investigated the activity of brain areas involved in visuospatial processing. A functional magnetic resonance imaging (MRI) visuospatial task, including an angle and a colour discrimination paradigm, was administrated to 17 headache-free migraine patients and 16 controls. Correlations between functional MRI abnormalities and subjects' performance, clinical and neuropsychological variables were also investigated. Deficits at visuospatial cognitive tests were present in around 20% of patients. Migraine patients maintained a preserved behavioural performance (reaction time and number of correct responses) during the angle discrimination task, while they performed less correctly in the colour task compared to controls ($p = 0.05$).

The comparison of angle vs. colour task revealed an increased activity of the right insula, bilateral orbitofrontal cortex and medial frontal gyrus, and decreased activity of the bilateral posterior cingulate cortex in migraine patients compared to controls. In migraine patients, a better performance in the angle task was associated with higher activation of the right insula and orbitofrontal cortex, as well as with decreased activation of the right posterior cingulate cortex. Our results suggest an adaptive functional plasticity that might help migraine patients to overcome impaired visuospatial skills and preserve an adequate performance during a visuospatial task. These compensatory mechanisms seem to take advantage of recruiting brain areas that are commonly involved also in nociception.

Introduction

Migraine is one of the main causes of neurological disability worldwide. Migraine is not simply a disease characterized by recurrent pain attacks, but migraine patients can also experience sensory hypersensitivities, cranial autonomic symptoms, cognitive, mood and homeostatic changes (30). Cognitive and neuropsychiatric symptoms, such as concentration difficulty, irritability, anxiety and unhappiness, are frequently reported by migraine patients during the premonitory, headache and postdrome phase of the migraine attack (54). Previous clinical studies demonstrated cognitive impairment in migraine patients, which can be influenced by disease severity, also during the inter-ictal phase (66, 67). However, other studies have not confirmed these findings (69, 175). The most affected cognitive domains in migraineurs are visuospatial abilities, processing speed, attention, memory and executive functions (69, 70).

Cognitive dysfunction in migraine patients can be associated with functional and structural MRI alterations in brain networks related to cognition (135, 149, 176). Numerous fMRI studies have shown an aberrant functional activation of the DMN and ECN in migraine patients during and between migraine attacks. The ECN and DMN are known to underlie executive and attentive functions, such as interoception, attention and working memory (101, 176). Morphometric alterations of frontal and parietal areas involved in the control of executive abilities and in attentional processing have also been reported using volumetric MRI analysis (135, 136).

Visual functions have been widely studied in migraine (177). Besides visual symptoms often experienced by patients with migraine, such as photophobia and visual aura, there is evidence also showing deficits in visual memory, visuomotor and visuospatial skills in these patients during and outside a migraine attack (69, 70, 178). Using MRI, functional and structural alterations in different areas of the visual network have been demonstrated in migraine patients with and without aura (177).

In this study, we wished to explore migraine patients' performance during a visuospatial task and investigated the activity of brain areas subserving visuospatial processing. Our working hypothesis was that abnormal recruitment of visuospatial processing brain networks might occur in migraine patients and such altered recruitment might be associated with the clinical and neuropsychological manifestations of the disease. To study those brain areas specifically involved in visuospatial processing and

their abnormalities, we applied an active fMRI paradigm including an angle and a colour discrimination task. The colour task was used as a control task to highlight visuospatial processing functions. A better understanding of the mechanisms underlying cognitive deficits in migraine patients may pave the way to the development of novel therapeutic strategies.

Materials and Methods

Participants. We prospectively studied 22 right-handed patients with episodic migraine and 20 right-handed, education-, age- and sex-matched controls with a normal neurological exam. Patients were recruited consecutively from the migraine population attending the Outpatient Clinic, Neurology Unit of the IRCCS San Raffaele Scientific Institute (Milan, Italy). Controls were recruited among consented friends, university students and hospital workers. All patients met the criteria of the International Classification of Headache Disorders for the diagnosis of migraine (179).

Exclusion criteria for both patients and controls were hypertension, hypercholesteremia, diabetes mellitus, vascular/heart disease, other major systemic, neurologic, or psychiatric conditions, use of illicit drugs, or use of drugs affecting the central nervous system. Controls with a history of headache disorders, except from low-frequency tension-type headache, were excluded from the study. To avoid possible confounding interferences with fMRI results, pharmacological preventive treatments for migraine were not allowed during the previous three months. Only patients who were having nutraceuticals were included. To minimize the risk of measuring MRI alterations related to the acute phase of the migraine attack, all patients had to be headache-free at the time of the MRI and for at least 24 hours before the exam. Most of the patients also denied having headache the day following the MRI. Three patients were excluded from the study because they were experiencing headache the day of the MRI exam. Images of two patients and four controls were excluded due to MRI artefacts or movements during fMRI acquisition. Seventeen migraine patients and 16 controls were included in the final analysis.

Clinical and neuropsychological assessment. Prior to the MRI exam, all patients were assessed by a neurologist and a neuropsychologist. A detailed clinical history, including

patients' disease duration and migraine attack frequency, was obtained. The average headache pain intensity was assessed using the Numerical Rating Scale (NRS) (180). Patients' disability was quantified using the Migraine Disability Assessment (MIDAS) (181) and the 6-item Headache Impact Test (HIT-6) (182). Seven patients had a diagnosis of migraine with and without aura, while ten had only migraine without aura. Eight patients suffered from a right-sided migraine, three migraine patients had left-sided migraine and all remaining patients had bilateral migraine. Ten patients had a positive familial history of migraine. At the time of MRI, two patients were taking nutraceuticals containing ginkgolide B.

During neuropsychological evaluation, attention and information processing speed (Trail Making Test (183) and Coding Test (184, 185)), executive functions (Wisconsin card sorting test (186)), visual constructive skills (Judgment of Line Orientation test (187)), mnestic verbal (Rey Auditory Verbal Learning Test), and visuospatial cognition (Rey–Osterrieth Complex Figure Test [ROCF] Recall Task (188)), including visuospatial memory, were tested. For each participant, the results from neuropsychological tests were scored using a standardized method based on a comparison with the percentile distribution of values from normal controls (189). Test scores $\leq 5°$ percentile of normal population, according to age, sex, and education-adjusted Italian norms, were considered abnormal (189). Depression and anxiety were evaluated using the Hamilton Depression Rating Scale (HDRS) (190) and Hamilton Anxiety Rating Scale (HARS) (191). Patients with a score ≥ 8 at HDRS were considered depressed (190), while a score ≥ 18 at HARS suggests the presence of anxiety (191).

Ethics approval and consent to participate. This study was approved by the Local Ethical Committes on human studies and all subjects provided written informed consent prior to study participation.

Experimental design. A block-design fMRI study, including an angle and a colour discrimination task, was administered to all subjects during the MRI. The colour task was used as a control task to highlight visuospatial processing functions. The paradigm consisted of a schematized clock with different angular disparities and two white or yellow hands (192). Depending on the task, targets were defined as clock with angles less

than or equal to 60° (angle discrimination task) or clock with yellow hands (colour discrimination task) (**Fig. 3.1.1**). For both tasks, subjects were instructed to press a button whenever they recognized the target. Prior to each task, a visual instruction clue (Angle or Colour) was presented for 2 seconds. The paradigm included 7 blocks of each task lasting 36 seconds and presented in a pseudo-random order. Each block consisted of 4 target and 6 non-target stimuli with a variable interstimulus interval and presented in a pseudo-random order. Each activation block was followed by a period of rest, during which the same clock image without hands was shown for 10 seconds. Stimuli were administered by a program implemented with Presentation® software, version 12 (Neurobehavioural System). Stimuli were back-projected onto a screen in the scanner room; subjects looked at the stimuli through a mirror standard system located on the scanner head coil. Responses were registered using a 2-button fMRI compatible response-box, held with the right hand. For each task, we assessed behavioural variables including the mean reaction time (RT), which is associated with information processing speed, and accuracy, measured as percentage of correct responses, of each subject.

MRI acquisition. Using a 3.0 Tesla Intera scanner (Philips Medical Systems, Best, The Netherlands), the following sequences of the brain were obtained: 1) T2*-weighted single-shot EPI sequence during a visuospatial task (repetition time (TR)=2000 ms, echo time (TE)=30 ms, flip angle (FlA)=85°, field of view (FOV)=240mm2, matrix=128x128, 336 sets of 33 contiguous axial slices, with a thickness of 4 mm); 2) T2-weighted turbo-spin echo (TR/TE=3000/120 ms, FlA=90º, matrix size=512x512, FOV=230 mm^2, 28, 4 mm thick, contiguous slices); 3) FLAIR (TR/TE=11000/120 ms, inversion time=2800 ms, FlA=90°, matrix size=256x256, FOV=230 mm^2, 28, 4 mm thick, contiguous slices); and 4) 3D T1-weighted fast field echo (TR/TE= 25/4.6 ms; FlA=30°; matrix size= 256x256; FOV= 230x230 mm^2; 220 contiguous slices with voxel size= 0.89x0.89x0.8 mm).

MRI analysis. The presence of WMHs was assessed on T2-weighted scans, using FLAIR scans to increase confidence in their identification. The volume of T2-hyperintensities (LV) was measured using a local thresholding segmentation technique (Jim 8; Xinapse Systems Ltd., Colchester, UK).

fMRI data were analysed using the statistical parametric mapping (SPM12) software. fMRI images were realigned to the mean one to correct for subject motion, co-registered to the 3D T1-weighted image and spatially normalised by applying the non-linear warping parameters used to transform the 3D T1-weighted scan to the MNI standard space. Finally, fMRI images were smoothed with a 10-mm, 3D-Gaussian filter. Subjects were included in the subsequent statistical analysis if they had a maximum translation/rotation lower than 3.0 mm/5 degrees in the x, y, z planes (1 patient and two controls excluded at this stage). Changes in BOLD contrast associated with the performance of the angle and colour discrimination task were assessed on a voxel-by-voxel basis, using the general linear model and the theory of Gaussian fields. A first-level design matrix, including motion parameters as regressors, was built and specific effects were tested by applying appropriate linear contrasts. For each subject, we investigated areas showing increasing activation (or deactivation) associated to each experimental condition (angle or colour). The main effect related to visuospatial task performance was assessed by contrasting the angle versus the colour discrimination task (angle *vs* colour).

To correct fMRI activations for local GM volume, GM was segmented from 3D T1-weighted images of each study subject using SPM12 and registered to a population-specific template using the Diffeomorphic Anatomical Registration using Exponentiated Lie algebra (DARTEL) method (177). Finally, GM maps were normalized to the MNI space, resampled to equalize voxel sizes with fMRI data (2x2x2 mm^3) and smoothed with an 8 mm Gaussian kernel.

Statistical analysis

Based on the number of participants for estimating fMRI changes in headache disorders reported in the literature (193), we estimated that at least 15 patients should have been included in the study.

The Q-Q plots and Kolmogorov-Smirnov and Shapiro-Wilk tests were used to assess whether continuous data were normally distributed. Since the distribution of the data was not normal, within- and between-group differences in demographic and behavioural variables were assessed using the Wilcoxon signed-rank and Mann-Whitney test, respectively. The Fisher exact test was used for categorical variables. The correlation between clinical (disease duration, migraine attack frequency, MIDAS, HIT-6, and NRS

scores), neuropsychological (anxiety scores, depression scores, attentive, executive, processing speed, memory and visuospatial performance, corrected for age, sex and education) and fMRI behavioural (RT and accuracy) variables was investigated using the Spearman rank correlation test *(*version 26.0; SPSS software, IBM, Armonk, NY). P values were adjusted for multiple comparisons using the Bonferroni correction.

ANCOVA models were used to estimate within- and between-group activations/deactivations associated to each experimental condition (angle or colour), as well as their contrast (angle *vs* colour) using the Biological Parametric Mapping (BPM) toolbox (194). All models were adjusted for age, sex and voxel-wise GM probability maps.

Using the BPM software, in migraine patients, multiple linear regression models, adjusted for age, sex and voxel-wise GM probability maps, were used to assess the association between fMRI alterations and behavioural (RT and accuracy), clinical (disease duration, migraine attack frequency, MIDAS, HIT-6, and NRS scores) and neuropsychological (anxiety scores, depression scores, attentive, executive, memory and visuospatial domain performance) variables.

Results were tested both at $p < 0.001$, uncorrected, and at $p < 0.05$, FWE corrected.

Results

The main demographic and clinical characteristics of migraine patients and controls are summarized in **Table 3.1.1**. Age (p=0.09), sex (p=0.4) and education (p=0.4) were not statistically different between migraine patients and controls.

The performance of patients at all neuropsychological tests is summarized in **Supplementary Table 3.1.1**. Three patients (19%) showed impaired visuospatial processing abilities and four patients (25%) had an abnormal visuospatial memory performance. One patient (6%) showed abnormal verbal memory performance and another one (6%) showed impaired information processing speed. None of the patients had deficits in visual constructive, attention and executive tests. Five patients (31%) were depressed and two of them suffered also from anxiety (12%).

In migraine patients, impaired visuospatial processing skills were associated to higher pain severity (r=-0.57, p=0.03).

Eight migraine patients and seven controls had small, aspecific, punctate WMHs (migraine patients: mean lesion volume=0.46 ml, standard deviation (SD) 1.35; controls: mean lesion volume=0.11 ml, SD 0.19). The volume of WM hyperintensities did not differ between migraine patients and controls (p=0.8).

Behavioural analysis of visuospatial performance during fMRI. The mean RT of the colour discrimination task was shorter than that of the angle discrimination task in both patients and controls (migraine patients: p<0.001; controls: p<0.001). There were no significant within-group differences in the accuracy of the angle and colour discrimination task (migraine patients: p=0.07; controls: p=0.2). The percentage of correct responses in the colour task was significantly lower in migraine patients compared to controls (**Table 3.1.1**). There were no significant between-group differences in the accuracy of the angle discrimination task and in the mean RT of the angle and colour discrimination tasks (**Table 3.1.1**). In migraine patients, longer RT of the angle discrimination task was associated with older age (r=0.50, p=0.04), while longer RT of the colour discrimination task was associated with higher migraine attack frequency (r=0.48, p=0.05) and longer disease duration (r=0.54, p=0.02).

Visuospatial fMRI analysis. Brain regions significantly activated or deactivated during the angle and colour discrimination task in migraine patients and controls are shown in **Fig. 3.1.2**, **Supplementary Table 3.1.2** and **Supplementary Table 3.1.3**. Regions showing significant differences between the angle and colour discrimination task within the group of migraine patients and controls are reported in **Table 3.1.2.** Both patients and controls showed an increased activation in the right parietal lobule during the execution of the angle compared to the colour discrimination task. The opposite comparison showed that, compared to the angle discrimination task, both migraine patients and controls had an increased activation of the left postcentral gyrus while performing the colour task.

Compared to controls, migraine patients showed an increased activation of the right insula, bilateral orbitofrontal cortex and medial superior frontal gyrus in the comparison angle versus colour discrimination task (**Table 3.1.3** and **Fig. 3.1.2**). They also had decreased activation of the bilateral posterior cingulate cortex when comparing the angle versus the colour discrimination task (**Table 3.1.3** and **Fig. 3.1.2**).

In patients with migraine, a better performance in the angle discrimination task was associated with higher activation of the right insula (percentage of correct responses at the angle task: r=0.84, $p<0.001$, uncorrected) and orbitofrontal cortex (percentage of correct responses at the angle task: r=0.83, $p<0.001$, uncorrected), and with decreased activation of the right posterior cingulate cortex (RT for the angle task: r=0.84, $p<0.05$, clusterwise FWE-corrected). We also found a significant association between the decreased activity of the left posterior cingulate cortex and shorter disease duration (r=0.93, $p<0.05$, clusterwise FWE-corrected), as well as between the increased activation of the left medial superior frontal gyrus and lower scores in visuospatial memory tests (r=-0.87, $p<0.05$, voxelwise FWE-corrected).

No correlation was found between brain fMRI activations and pain intensity, migraine disability, anxiety and depression scores.

Discussion

Here, we applied an active fMRI paradigm to explore the neural substrates of visuospatial processing in migraine patients. By using the colour paradigm as control task, we have removed any nonspecific effects of attention or motor response and have restricted our interest to those areas specifically involved in visuospatial processing. In line with the literature (69, 70), around 20 percent of our migraine patients showed selective deficits in visuospatial cognition during the neuropsychological evaluation. Patients with impaired visuospatial processing skills were those who had more painful migraine attacks. The novel finding of this study is that migraine patients implement an adaptive functional recruitment of brain areas subserving visuospatial processing to maintain an adequate performance during a visuospatial task.

Visuospatial processing brain networks are made by a dorsal pathway, which travels from the occipital lobe to fronto-parietal areas, and a ventral pathway, connecting occipital and temporal regions. The dorsal pathway directs visual information to sensorimotor processing areas involved in spatial perception, navigation and visually guided action, while the ventral pathway is responsible for the identification of object features, such as colour and shape, and for assigning meaning to visual information (195). Consistent with previous studies, we found that, during the execution of an angle discrimination task, both patients and controls showed an increased activation of the right

parietal lobule, which is an area of the dorsal system with a key role in spatial perception (192). Interestingly, when we compared migraine patients to controls, we found that patients with migraine had an increased recruitment of cortical areas, including the anterior insula, orbitofrontal and medial frontal cortex, engaged in visuospatial processing. The insula is a core area of the limbic system which prioritizes processing of behaviourally relevant stimuli, with implications for the allocation of spatial processing resources (196, 197). The medial frontal cortex, including the pre-supplementary motor area, is involved in planning eye movements, spatial reorienting, stopping, and switching responses (198, 199). There is evidence showing that the orbitofrontal cortex processes visual and spatial information through parietal and occipital connections. This frontal area directs the attention to visuospatial cues during goal-directed decisions and actions (200, 201). The higher activation of frontal and limbic areas we have found in migraine patients may represent a compensatory mechanism to maintain adequate performance during the angle discrimination task. This hypothesis is supported by the preserved performance of migraine patients during the angle discrimination task and the association we have observed between the increased activation of the insula and orbitofrontal cortex and higher correct responses at the angle task. It is also interesting to note that the activation of frontal areas is more evident in those patients who performed worst in visuospatial memory tests during the neuropsychological evaluation, suggesting the presence of a greater adaptive response in these patients.

We also observed deactivation of areas belonging to the default mode network (202), such as the posterior cingulate cortex, in both patients and controls during the execution of the angle discrimination task. It has been shown that the posterior cingulate cortex is deactivated during the performance of visual discrimination tasks, and that this deactivation was associated with a better task achievement (203). This area of the cingulum has a key role in shifting the attention from different stimuli and in the processing of internal and external information (204). Here, the deactivation of this area was more pronounced in migraine patients and was associated with a faster response in the angle discrimination task, as well as with shorter disease duration. This is likely to reflect another adaptive mechanism that might help migraine patients, especially those with a recent onset of the disease, to better perform in visuospatial tasks. It is also noteworthy that the deactivation of the posterior cingulate cortex we have observed in

patients at an early stage of migraine might represent a phenotypic biomarker of the disease. This suggests that brain functional adaptive mechanisms might be the result of a balance between predisposing traits and disease-related processes.

It is worth noting that, during the visuospatial task, migraine patients recruited brain areas that are usually also involved in nociception. A large body of evidence has shown an involvement of the insula, cingulate and frontal cortex in the perception of the sensory-discriminative and emotional aspects of pain (205). Previous studies have demonstrated that migraine patients experience an altered functional activation of the posterior cingulum, insula and frontal areas, which can influence the severity of the pain during the migraine attack (99, 116, 149). The insula is a key area of the brain network that subserves cognition-emotion integration. The orbitofrontal cortex is involved in affective pain modulation and, together with the posterior cingulate cortex, is part of the modulatory circuits related to attention (136, 149). The compensatory activation or deactivation of these cortical areas we have observed here might be strengthen by the recurrent involvement of these regions in modulating the migraine pain. The cognitive demands associated to the visuospatial task might have facilitated the recruitment of those brain regions involved in attentional modulation of pain. Supporting this hypothesis, we found that migraine patients with impaired visuospatial abilities are those patients who report more severe migraine attacks and who benefit most from these adaptive mechanisms.

Another interesting finding was that migraine patients, especially those with a higher disease activity, performed worse in the colour discrimination task compared to controls. However, the worse execution was not associated to functional alterations of colour processing brain areas. Previous studies have shown abnormalities in colour perception in migraine patients with and without aura (206, 207). In the future, the use of a fMRI paradigm that specifically investigates the processing of colour may provide new insights into colour perception in these patients.

The main limit of the study is its relatively small sample size. Moreover, both migraine patients with and without aura were enrolled in the study. Larger future studies are warranted to confirm our results and to investigate whether patients with and without aura present different visuospatial processing mechanisms.

Overall, our results have highlighted an adaptive functional plasticity that is likely to help migraine patients to overcome impaired visuospatial skills and to preserve an adequate performance during a visuospatial task. These compensatory mechanisms take advantage of recruiting a brain network that is repeatedly activated to process the migraine pain. Our findings could provide new perspectives to understand cognitive impairment in migraine patients and might pave the way to novel psychological approaches that, along with pharmacological treatments, can be effective for treating migraine patients.

Table 3.1.1. Main demographic, clinical and behavioural characteristics of the subjects enrolled in the study.

	Controls	**Migraine patients**	***p* values patients *vs* controls**
Women/Men	11/5	14/3	0.4
Age (years)	25.1 (24-39)	27.7 (25-46)	0.09
Education (years)	18 (16-18)	17 (16-18)	0.4
Attack frequency per month	-	3.5 (1.7-4.5)	-
Disease duration (years)	-	12.4 (8-26)	-
MIDAS score	-	21 (3-26)	-
HIT-6 score	-	63 (58-65)	-
NRS score	-	7 (6-7)	-
Percentage of correct responses for the angle discrimination task (%)	99% (96-99)	96 (89-99)	0.09
Percentage of correct responses for the colour discrimination task (%)	99 (99-100)	99 (95-99)	0.05*
RT for the angle discrimination task (seconds)	0.72 (0.66-0.77)	0.78 (0.64-0.85)	0.3

RT for the colour discrimination task (seconds)	0.62 (0.59-0.64)	0.68 (0.54-0.75)	0.2

Abbreviations: HIT-6 = 6-item Headache Impact Test; MIDAS = Migraine Disability Assessment; NRS = Numerical Rating Scale, RT = Reaction time.

Measures are reported as medians and interquartile ranges (25th–75th percentiles). Sex is reported as frequencies.
*Mann-Whitney test, $p<0.05$.

Table 3.1.2. Regions showing significant differences between the angle and colour discrimination task within the group of migraine patients and controls.

Migraine patients				
Angle *vs* colour discrimination task				
Cerebral regions showing increasing activations during the angle task	**Brodmann area**	***t* values***	**Cluster extent (no. of voxels)**	**MNI coordinates (X, Y, Z)**
R superior parietal lobule	7	10.03	1582	22, -72, 56
L orbitofrontal gyrus	46	9.60	175	-44, 50, -4
L superior parietal lobule	7	8.15	921	-28, -66, 54
R inferior temporal gyrus	37	7.66	151	52, -54, -14
Cerebellum (vermis)	-	7.45	199	-8, -76, -30
R middle frontal gyrus	45	7.16	169	48, 32, 28
R orbitofrontal gyrus	47	4.99**		46, 42, -8
R medial frontal gyrus	6	6.78	217	4, 28, 40
L cerebellum (pyramis)	-	6.43	45	-32, -68, -32
L fusiform gyrus	37	6.05	46	-46, -64, -14
R insula	13	6.02	12	34, 24, -4
R middle frontal gyrus	8	5.90	12	32, 6, 60

Colour *vs* angle discrimination task				
Cerebral regions showing increasing activations during the colour task	**Brodmann area**	***t* values***	**Cluster extent (no. of voxels)**	**MNI coordinates (X, Y, Z)**
L postcentral gyrus	48	6.41	52	-54, -12, 14
Cerebral regions showing decreasing activations during the angle task	**Brodmann area**	***t* values***	**Cluster extent (no. of voxels)**	**MNI coordinates (X, Y, Z)**
R inferior frontal gyrus	48	9.68	225	52, -8, 14
R posterior cingulate cortex	23	6.67	696	6, -56, 20
L posterior cingulate cortex	23	6.45		-2, -46, 30
Controls				
Angle *vs* colour discrimination task				
Cerebral regions showing increasing activations during the angle task	**Brodmann area**	***t* values***	**Cluster extent (no. of voxels)**	**MNI coordinates (X, Y, Z)**
R superior parietal lobule	7	7.76	198	24, -74, 54
Colour *vs* angle discrimination task				
Cerebral regions showing increasing activations during the colour task	**Brodmann area**	***t* values***	**Cluster extent (no. of voxels)**	**MNI coordinates (X, Y, Z)**

L inferior frontal gyrus	48	6.50	163	-40, -30, 20
L postcentral gyrus	48	6.17		-56, -16, 20
Cerebral regions showing decreasing activations during the angle task	**Brodmann area**	***t* values***	**Cluster extent (no. of voxels)**	**MNI coordinates (X, Y, Z)**
R inferior frontal gyrus	48	8.11	81	52, -8, 14
R superior temporal gyrus	41	6.25	29	50, -40, 12

*Age- and sex-adjusted linear model (p<0.05, voxelwise FWE-corrected for multiple comparisons).
**Age- and sex-adjusted linear model (p<0.001, uncorrected).

Abbreviations: L=left, R=right.

Table 3.1.3. Regions showing significant differences between migraine patients and controls in the comparison angle versus colour discrimination task.

Migraine patients *vs* controls				
Cerebral regions showing increasing activation during the angle task	**Brodmann area**	***t* values***	**Cluster extent (no. of voxels)**	**MNI coordinates (X, Y, Z)**
L orbitofrontal gyrus	47	6.66	566	-44, 48, -6
R medial superior frontal gyrus	8	5.68	1615	6, 32, 38
L medial superior frontal gyrus	8	4.67		-6, 24, 50
R orbitofrontal gyrus	47	5.35	911	46, 40, -8
R insula	13	4.71		36, 24, -6
Cerebral regions showing decreasing activation during the angle task	**Brodmann area**	***t* values***	**Cluster extent (no. of voxels)**	**MNI coordinates (X, Y, Z)**
L posterior cingulate cortex	31	4.85	784	-2, -42, 38
R posterior cingulate cortex	31	4.72		6, -48, 40

*Age- and sex-adjusted linear model (p<0.05, clusterwise FWE-corrected for multiple comparisons).

Abbreviations: L=left, R=right.

Fig. 3.1.1. Experimental task during fMRI. The functional MRI paradigm consisted of a schematized clock with different angular disparities and two white or yellow hands. **A)** During the angle discrimination task, targets were defined as clocks with angles less than or equal to 60°. **B)** During the colour discrimination task, targets were defined as clocks with yellow hands.

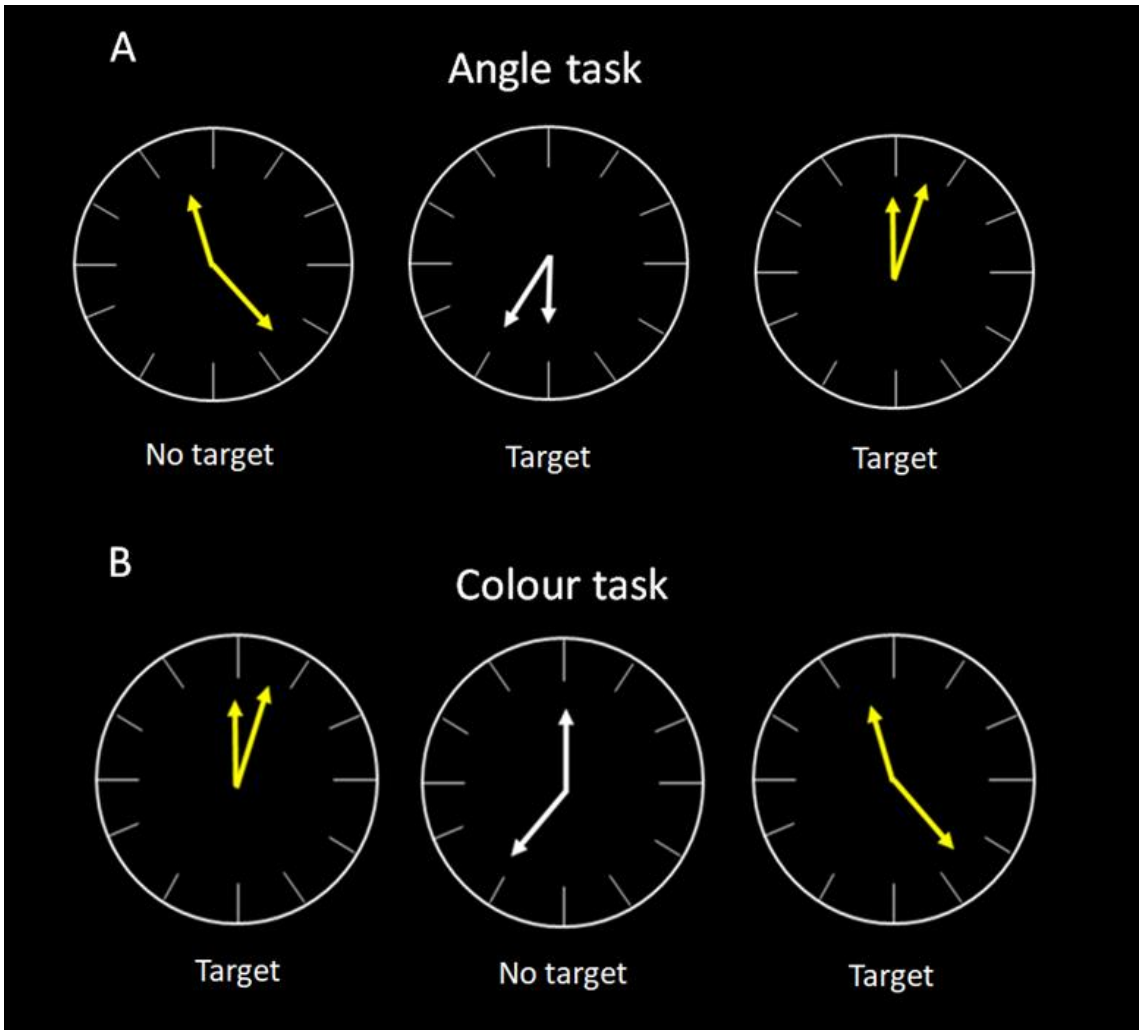

Fig. 3.1.2. Visuospatial fMRI analysis. A) Brain regions significantly activated or deactivated during the angle discrimination task in migraine patients and controls (p<0.05, voxelwise FWE-corrected for multiple comparisons), represented on a high resolution T1-weighted template**.** Regions of increased activation are shown in orange (colour-coded for their t values), and regions of deactivation are represented in cyan (colour-coded for their t values). **B)** Brain regions significantly activated or deactivated during the colour discrimination task in migraine patients and controls (p<0.05, voxelwise FWE-corrected for multiple comparisons), represented on a high resolution T1-weighted template. Regions of increased activation are shown in orange (colour-coded for their t values), and regions of deactivation are represented in cyan (colour-coded for their t values). **C)** Brain regions showing significant differences between migraine patients and controls in the comparison angle versus colour discrimination task (p<0.05, clusterwise FWE-corrected for multiple comparisons), represented on a high resolution T1-weighted template. Regions of increased activation in migraine patients during the angle discrimination task are shown in violet (colour-coded for their t values), and regions of decreased activation in migraine patients during the angle discrimination task are represented in green (colour-coded for their t values).
Abbreviations: L=left, R=right.

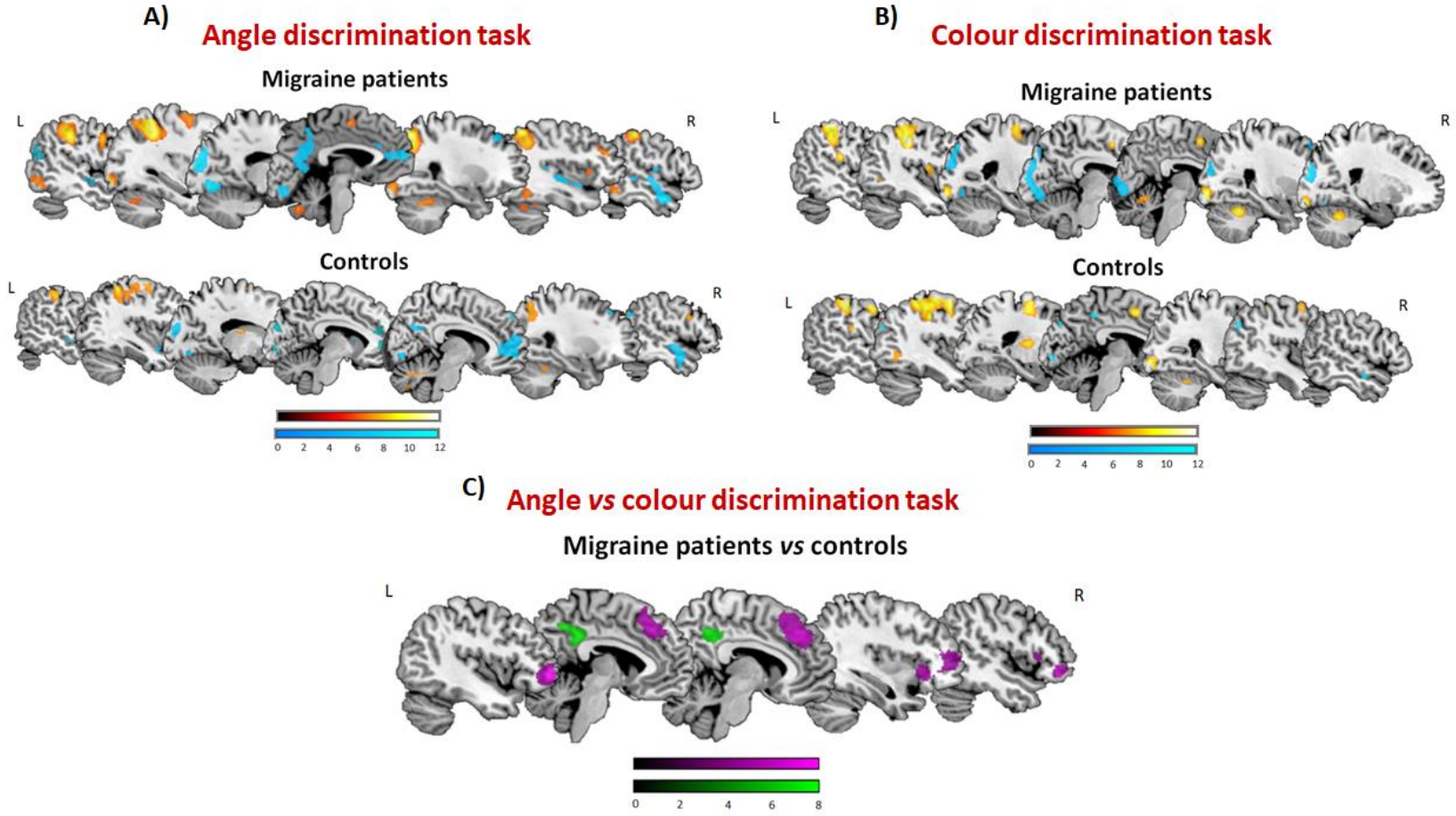
A)
Angle discrimination task
Migraine patients
L
R
Controls
L
R
0 2 4 6 8 10 12
B)
Colour discrimination task
Migraine patients
L
R
Controls
L
R
0 2 4 6 8 10 12
C)
Angle vs colour discrimination task
Migraine patients vs controls
L
R
0 2 4 6 8

Supplementary Table 3.1.1. Neuropsychological tests in migraine patients.

Cognitive domain	Neuropsychological test	Number of patients (%) with impairment
Attention and information processing speed	Trail Making Test	0
	Coding Test	1 (6%)
Executive functions	Wisconsin Card Scoring Test	0
Visual constructive skills	Judgment of Line Orientation Test	0
Verbal memory	Rey Auditory Verbal Learning Test	1 (6%)
Visuospatial cognition	Rey-Osterrieth Complex Figure Test - Copy Task	3 (19%)
	Rey-Osterrieth Complex Figure Test - Recall Task	4 (25%)
Depression	Hamilton Depression Rating Scale	5 (31%)
Anxiety	Hamilton Anxiety Rating Scale	2 (12%)

Supplementary Table 3.1.2. Regions showing significant increasing or decreasing activation associated to the angle discrimination task in migraine patients and controls.

Migraine patients				
Cerebral regions showing increasing activation	**Brodmann area**	***t* values***	**Cluster extent (no. of voxels)**	**MNI coordinates (X, Y, Z)**
L inferior parietal lobule	40	11.57	2253	-38, -46, 52
R superior parietal lobule	7	10.96	1935	30, -64, 50
L inferior occipital gyrus	18	8.71	865	-30, -92, -10
L fusiform gyrus	37	8.57		-44, -64, -16
L cerebellum (pyramis)	-	7.20		-28, -64, -30
R middle frontal gyrus	45	8.69	143	44, 38, 22
R cerebellum (culmen)	-	8.33	756	34, -48, -26
R cerebellum (declive)	-	7.31		8, -74, -28
Cerebellum (vermis)	-	6.67		0, -76, -28
R inferior temporal gyrus	37	8.28	362	44, -54, -12
L inferior frontal gyrus	44	7.96	204	-50, 8, 34
R inferior occipital gyrus	18	7.48	208	28, -92, -8
L middle frontal gyrus	6	7.35	332	-28, -4, 54
R medial frontal gyrus	6	7.09	193	8, 20, 40
L medial frontal gyrus	6	5.29		-4, 10, 50
R insula	13	6.41	57	40, 18, 0
L orbitofrontal gyrus	46	4.71**	66	-44, 52, -4
R orbitofrontal gyrus	11	4.52**	10	30, 44, -14
Cerebral regions showing decreasing activation	**Brodmann area**	***t* values***	**Cluster extent (no. of voxels)**	**MNI coordinates (X, Y, Z)**
L calcarine cortex	18	10.65	3564	-8, -86, -6
L lingual gyrus	18	9.99		-16, -78, .10
L middle occipital gyrus	18	9.52		-18, -92, 14

R cingulum	23	6.79		4, -56, 14
L cingulum	23	6.79		-2, -60, 16
R lingual gyrus	18	6.01		12, -80, -2
R middle temporal gyrus	21	8.81	619	56, 0, -22
R middle temporal gyrus	39	8.14	297	46, -66, 30
R superior frontal gyrus	9	8.01	141	22, 36, 42
L angular gyrus	39	7.88	397	-44, -70, 32
R orbitofrontal cortex	11	7.80	482	4, 56, -6
L cingulum	10	7.37		0, 44, 0
L orbitofrontal cortex	10	7.27		-4, 52, -4
L middle temporal gyrus	22	7.10	129	-54, -8, -12
L superior frontal gyrus	9	6.59	29	-12, 56, 32
R middle temporal gyrus	21	6.47	41	54, -34, 0
R superior temporal gyrus	48	6.45	21	42, -30, 14
R medial frontal gyrus	10	6.37	115	10, 60, 26
R inferior frontal gyrus	48	6.16	50	54, -10, 10
L superior frontal gyrus	9	5.98	15	-22, 28, 40
Controls				
Cerebral regions showing increasing activation	**Brodmann area**	***t* values***	**Cluster extent (no. of voxels)**	**MNI coordinates (X, Y, Z)**
L middle frontal gyrus	6	8.28		-26, -12, 58
L inferior parietal lobule	40	8.11		-40, -44, 54
L postcentral gyrus	3	7.39	1357	-52, -24, 44
R inferior occipital gyrus	18	7.64	91	26, -92, -10
R superior parietal lobule	7	7.23	287	22, -66, 52
R inferior frontal gyrus	44	6.75	57	48, 8, 28
R cerebellum (culmen)	-	6.41	222	34, -48, -26
R cerebellum(vermis)	-	6.28		2, -58, -26
L middle frontal gyrus	6	6.40	22	-52, 8, 38

L thalamus	-	6.04	22	-16, -10, 16
Cerebral regions showing decreasing activation	**Brodmann area**	***t* values***	**Cluster extent (no. of voxels)**	**MNI coordinates (X, Y, Z)**
L orbitofrontal cortex	10	9.47	1453	-4, 50, -2
R orbitofrontal cortex	10	8.94		10, 52, -6
L cingulum	24	7.69		-4, 34, 18
R middle temporal gyrus	22	7.82	562	58, -8, -12
L superior occipital gyrus	18	7.57	204	-12, -86, 22
R lingual gyrus	18	6.93	103	10, -78, -4
R middle temporal gyrus	21	6.69	101	60, -56, 18
R middle frontal gyrus	9	6.68	66	24, 34, 38
R posterior cingulate cortex	31	6.62	72	10, -64, 28
L calcarine cortex	18	6.52	37	-6, -88, -8
L middle frontal gyrus	8	6.44	25	-30, 30, 50
L lingual gyrus	18	6.26	41	-16, -76, -10
R medial frontal gyrus	9	6.19	24	10, 52, 44
R angular gyrus	39	6.06	34	48, -66, 30
L superior frontal gyrus	9	6.05	11	-14, 56, 30
L angular gyrus	39	5.93	19	-42, -78, 32
L temporal pole	38	5.91	22	-36, 6, -18

*Age- and sex-adjusted linear model (p<0.05, voxelwise FWE-corrected for multiple comparisons).
**Age- and sex-adjusted linear model (p<0.001, uncorrected).

Abbreviations: L=left, R=right.

Supplementary Table 3.1.3. Regions showing significant increasing or decreasing activation associated to the colour discrimination task in migraine patients and controls.

Migraine patients				
Cerebral regions showing increasing activation	**Brodmann area**	***t* values***	**Cluster extent (no. of voxels)**	**MNI coordinates (X, Y, Z)**
L postcentral gyrus	3	9.68	1937	-56, -20, 46
L precentral gyrus	6	8.82		-32, -12, 60
L inferior occipital gyrus	18	9.17	195	-30, -90, -12
L supplementary motor area	6	9.04	339	-6, 6, 48
R cerebellum (culmen)	-	8.52	416	32, -52, -28
R fusiform gyrus	18	8.51	219	28, -92, -10
L postcentral gyrus	48	8.40	118	-52, -20, 18
L inferior frontal gyrus	48	6.77	63	-44, -4, 10
Cerebellar vermis	-	6.68	148	2, -66, -16
L middle temporal gyrus	37	6.10	18	-40, -64, 0
Cerebral regions showing decreasing activation	**Brodmann area**	***t* values***	**Cluster extent (no. of voxels)**	**MNI coordinates (X, Y, Z)**
R calcarine cortex	17	10.38	2258	12, -88, 6
R superior occipital gyrus	18	9.82		20, -90, 18
L middle occipital gyrus	18	9.87		-18, -92, 14
L calcarine cortex	17	9.23		-8, -86, -6
L cuneus	19	6.93		-16, -80, 40
R lingual gyrus	18	6.47		18, -74, -10
L lingual gyrus	18	5.90		-16, -78, -10
L posterior cingulate cortex	7	6.06	14	0, -42, 48
R middle frontal gyrus	9	6.03	26	28, 32, 46

Controls				
Cerebral regions showing increasing activation	**Brodmann area**	***t* values***	**Cluster extent (no. of voxels)**	**MNI coordinates (X, Y, Z)**
L precentral gyrus	6	9.59	2215	-28, -14, 58
L postcentral gyrus	3	9.34		-56, -20, 46
R supplementary motor area	6	9.35	417	10, 10, 50
L supplementary motor area	6	8.54		-6, 6, 48
R fusiform gyrus	18	8.95	204	28, -92, -10
L thalamus	-	7.55	222	-20, -16, 16
L precentral gyrus	6	7.53	123	-52, 6, 38
R cerebellum (culmen)	-	6.58	120	6, -62, -30
L postcentral gyrus	48	6.57	23	-54, -18, 18
R precentral gyrus	6	6.55	78	42, -2, 56
L inferior temporal gyrus	37	6.40	47	-40, -62, -2
Cerebral regions showing decreasing activation	**Brodmann area**	***t* values***	**Cluster extent (no. of voxels)**	**MNI coordinates (X, Y, Z)**
L posterior cingulate cortex	7	7.79	142	0, -42, 48
L middle occipital gyrus	19	6.91	62	-32, -82, 34
R lingual gyrus	18	6.69	131	8, -80, -6
R calcarine cortex	17	6.52		12, -88, 6
R angular gyrus	39	6.55	53	44, -70, 32
L cuneus	19	6.25	110	-10, -88, 24
L calcarine cortex	17	6.13	34	-8, -92, 0
R middle temporal gyrus	21	6.11	21	54, -6, -16

*Age- and sex-adjusted linear model (p<0.05, voxelwise FWE-corrected for multiple comparisons).

Abbreviations: L=left, R=right.

4. INTERICTAL FUNCTIONAL MRI ALTERATIONS: A TRAIT OR A STATE OF MIGRAINE?

4.1. Dysregulation of multisensory processing stands out from an early stage of migraine: a study in pediatric patients. Messina *et al.*, J Neurol 2019.

This chapter describes the work published in Journal of Neurology (PMID: 31745724, DOI: 10.1007/s00415-019-09639-9).

Journal of Neurology
https://doi.org/10.1007/s00415-019-09639-9

ORIGINAL COMMUNICATION

Check for updates

Dysregulation of multisensory processing stands out from an early stage of migraine: a study in pediatric patients

Roberta Messina[1,4] · Maria A. Rocca[1,2] · Bruno Colombo[2] · Paola Valsasina[1] · Alessandro Meani[1] · Andrea Falini[3,4] · Massimo Filippi[1,2,4]

Received: 27 May 2019 / Revised: 13 November 2019 / Accepted: 14 November 2019

Abstract
Resting state (RS) functional connectivity (FC) abnormalities of brain networks involved in pain- and multisensory processing have been disclosed in adult-migraine patients. We explored RS FC of large-scale brain networks in pediatric-migraine patients and their correlation with patients' clinical characteristics. RS functional MRI data was acquired from 13 pediatric-migraine patients and 14 age- and sex-matched controls. Intra- and inter-network RS FC differences between patients and controls were evaluated. Correlations between RS FC abnormalities and patients' clinical characteristics were also assessed. Compared to controls, pediatric-migraine patients had a decreased RS FC of the left parieto-occipital junction of the default mode network (DMN) and left-dorsolateral prefrontal cortex of the executive control network (ECN). They also experienced an increased RS FC of the right frontopolar cortex of the right frontoparietal network (FPN) and the right-middle occipital gyrus of the secondary visual network. A significant stronger connectivity between the ECN and primary visual network and between the right FPN and primary sensorimotor, primary visual and auditory networks were found in migraine patients compared to controls. A significant weaker connectivity between the DMN and right FPN was revealed in migraineurs compared to controls. No correlation was found between intra- and inter-network RS FC abnormalities and patients' clinical characteristics. Pediatric-migraine patients harbor significant RS FC abnormalities in brain networks involved in multisensory processing and in the cognitive control of pain. An early dysregulation of multisensory processing, including pain, might represent a phenotypic biomarker of the disease.

Introduction

Over the last decades, an increasing recognition of migraine as one of the most disabling neurological diseases worldwide (208) has led to a growing interest in understanding its pathophysiology and developing new treatments. Migraine is now widely accepted as a complex brain network disorder that involves the interaction of multiple neuronal systems (30). Widespread brain structural and functional MRI alterations in pain and multisensory processing areas have been shown in migraine patients during the ictal and interictal phase (99). Although the clinical phenotype of migraine differs between adult and pediatric patients, similar patterns of brain structural (140, 209-211) and CBF (212) have been revealed in the two populations of patients.

RS FC MRI studies provide information about the functional interplay between different brain areas. Their application in studying adult migraine patients has shed light on the mechanisms responsible for the onset of the migraine attacks and has disclosed functional abnormalities of different brain networks, including the DMN, salience, ECN and visual networks, that might account for the pain and the wide constellation of symptoms usually experienced by migraine patients during and outside the attacks (149). So far, only one study has investigated RS FC abnormalities of the precuneus and amygdala in pediatric patients with migraine using a seed-based approach (210).

Whether brain functional alterations represent a predisposing trait to migraine or are the consequence of the recurrence of headache attacks or a combination of both is still a matter of debate. Many studies have demonstrated that the RS FC of different brain networks might be influenced by migraine disease activity (148, 213). Patterns of RS FC of the insula, amygdala, temporal and frontal lobes classified migraine patients from controls with an accuracy of 86% (214), supporting the use of these measures as a biomarker of this condition. Another unanswered question is whether it is possible to identify a RS FC MRI pattern that is specific for migraine.

In this study, we wished to investigate whether RS FC abnormalities of brain networks involved in pain, multisensory processing and high-order cognitive functions are already present in pediatric patients with migraine. Given the evidence (215, 216) that dysfunctional brain networks, rather than single brain areas, contribute to migraine pathophysiology, we also explored the functional interaction among the studied RS networks, by performing an analysis of functional network connectivity (217). The study

of patients at an early stage of the disease is a worthwhile strategy to elucidate the mechanisms underlying brain functional abnormalities in migraine and improve our understanding of migraine pathophysiology.

Methods

Participants. We prospectively examined 18 right-handed pediatric (age at study enrolment < 18 years) patients with episodic migraine and 18 right-handed, sex and age-matched pediatric controls, without a history of neurological dysfunction (including migraine and other headache disorders except from low-frequency tension-type headache (179)) and a normal neurological exam. Patients with more than 18 and less than 6 years old were excluded from the study. The exclusion criteria for both patients and controls were the use of regular medications, except from migraine treatments, perinatal or pediatric diseases, hypertension, hypercholesteremia, diabetes mellitus, vascular/heart diseases and other major systemic, neurological or psychiatric conditions. Four patients and three controls withdrew from the study prior to the MRI exam. Images of one patient and one control were excluded due to MRI artefacts. Thirteen migraine patients and 14 controls were included in the final analysis. To minimize the risk of measuring functional abnormalities related to an acute attack (116, 118), patients were studied attack-free, including aura, for at least 72 hours before the MRI exam.

Patients were recruited consecutively from the migraine population attending the Outpatient Clinic, Department of Neurology of the Scientific Institute and University Hospital San Raffaele (Milan, Italy). Prior to the MRI exam, all patients were assessed clinically by a single neurologist, who was unaware of the MRI results. All patients met the criteria of the International Classification of Headache Disorders for the diagnosis of migraine (179).

During the MRI visit, all patients were interrogated regarding their disease duration and attack frequency. Seven patients had a diagnosis of migraine with aura (5 visual, 1 visual and sensory, 1 sensory and speech) and six had migraine without aura. Apart from two patients who suffered from a right-sided migraine, all remaining patients had bilateral migraine. Ten patients had a positive familial history of migraine. At the time of MRI, one patient was taking flunarizine and four patients were having the non-pharmacological treatment ginkgolide B for migraine prevention.

Ethics approval and consent to participate. This study was approved by the Local Ethical Committes on human studies and all subjects' parents provided written informed consent prior to study participation.

MRI acquisition. Using a 3.0 Tesla Intera scanner (Philips Medical Systems, Best, The Netherlands), the following sequences of the brain were obtained from all subjects: 1) RS fMRI scans, using a T2*-weighted echo-planar imaging sequence (TR/TE=3000/35 ms; FlA=90°, FOV=240 mm^2, 200 sets of 30 contiguous axial slices, slice thickness=4 mm; matrix size=128x128); 2) T2-weighted turbo-spin echo (TR/TE=3000/120 ms, FlA=90º, matrix size=512x512, FOV=230 mm^2, 28, 4 mm thick, contiguous slices); 3) FLAIR (TR/TE=11000/120 ms, inversion time=2800 ms, FlA=90°, matrix size=256x256, FOV=230 mm^2, 28, 4 mm thick, contiguous slices); and 4) 3D T1-weighted fast field echo (TR/TE= 25/4.6 ms; FlA=30°; matrix size= 256x256; FOV= 230x230 mm^2; 220 contiguous slices with voxel size= 0.89x0.89x0.8 mm). During the RS acquisition, subjects were instructed to keep their eyes closed and not to fall asleep.

MRI analysis

T2-weighted scans were pre-processed for the presence of WMHs and FLAIR scans were always used to increase confidence in their identification. T2-hyperintense LV (T2 LV) were measured using a local thresholding segmentation technique (Jim 7; Xinapse Systems Ltd., Colchester, UK).

RS fMRI data were analyzed using Statistical Parametric Mapping (SPM) 12 (http://www.fil.ion.ucl.ac.uk/spm/) and REST software (http://resting-fmri.sourceforge.net). First, each subject's images were rigid-body realigned to the mean of each session to correct for minor head movements. After rigid registration of realigned images to the 3D T1-weighted scan, RS fMRI images were normalized to the Montreal Neurological Institute (MNI) template using a standard affine transformation followed by non-linear warping. Linear detrending and band-pass filtering (0.01-0.08 Hz) were performed to partially remove low-frequency drifts and physiological high-frequency noise. Finally, normalized images were smoothed using a 3D 6-mm Gaussian kernel.

After pre-processing, RS FC was assessed using independent component analysis (ICA) and the GIFT software (http://mialab.mrn.org/software/gift/) following four main steps: (i) concatenation of all subjects scans, (ii) data reduction, (iii) group ICA, and (iv) back reconstruction (218). Group independent components (IC) were estimated within a brain mask (automatically generated by the GIFT software) retaining only brain voxels included in all subjects scans. The number of IC was 40, a dimension determined using the minimum description length criterion (218). The statistical reliability of the IC decomposition was tested by using the ICASSO toolbox (219). After back reconstruction, IC images and time courses of each study subject were converted to Z-scores, as implemented by default in the GIFT software (218), to standardize intensity distribution within and across subjects and to improve gaussianity of data. Visual inspection of the spatial patterns as initial screening, a frequency analysis of the spectra of the estimated IC and a template-matching procedure allowed removing components clearly related to motion-related artifacts and physiological noise, and to select components related to the RS networks of interest (220). Mean RS FC values, expressed as Z-scores, of each network were extracted using the REX toolbox.

To investigate functional interactions between the studied RS networks, the temporal functional connectivity among the RS networks generated by ICA was estimated as Pearson's correlation coefficients between pairs of component time courses, using the Mancovan toolbox implemented in GIFT (221). ICA time courses were detrended (linear, quadratic and cubic) and band-pass filtered between 0.01-0.15 Hz prior to computing pairwise correlation coefficients. This analysis produced sets of pair-wise correlations between networks for each study subject, which were transformed to Z-scores using Fisher's transformation and then entered into statistical comparisons (217).

Statistical analysis

Given the challenges of recruiting pediatric patients and the number of participants needed for estimating fMRI changes in headache disorders reported in the literature (193), we estimated that a sample size of 10-14 participants would have been acceptable.

The qq-plots and Kolmogorov-Smirnov and Shapiro-Wilk tests were used to assess whether continuous data were normally distributed. Since the distribution of the

data was not normal, demographic and clinical characteristics were compared between groups using the Mann-Whitney test. The Fisher exact test was used for categorical variables (SAS software, version 9.4, SAS Institute Inc., Cary, NC).

For each RS network of interest, intra-network voxel-wise RS FC in the two study groups was assessed and compared using an age- and sex-adjusted linear model, as implemented in SPM12. All the analyses were masked with FWE-corrected effects of interest to retain only those brain regions showing significant positive RS FC *Z*-scores in each network. This approach restricted our analysis to the brain regions showing coherent RS FC within each network and avoided the inclusion of voxels not significantly belonging to a given network, or voxels showing anti-correlated RS FC, the interpretation of which is still debated (222).

In patients with migraine, voxel-wise correlation analyses between RS FC maps and clinical characteristics (disease duration and attack frequency) were performed with a multiple regression model, using SPM12. Age and sex were included as covariates in all analyses. All the voxel-wise analyses were tested at a threshold of $p < 0.05$, clusterwise FWE-corrected for multiple comparisons.

Age- and sex-adjusted linear models were performed to assess and compare global mean RS FC values of each network and between networks pairwise correlation coefficients, both expressed as Z-scores, in the two study groups. The association between patients' clinical features and global RS FC measures were investigated using partial correlations analyses. Results were tested at a threshold of $p<0.05$ (SAS software, version 9.4, SAS Institute Inc., Cary, NC).

Results

The main demographic and clinical characteristics of patients with migraine and controls are summarized in **Table 4.1.1**. Age (p=0.8) and sex (p=0.7) did not differ between migraine patients and controls. No WMHs were found in controls and 10 (77%) of the 13 migraine patients. Three patients with migraine without aura had few small, punctate T2 hyperintensities in deep and subcortical WM. Mean T2 LV in these patients was 0.017 ml (SD=0.03 ml).

RS fMRI analysis

Ten RS networks were selected among the 40 resulting from the ICA, including the DMN (R^2 with the DMN template=0.40), ECN (R^2 with the ECN template=0.47), left and right frontoparietal networks (FPN) (R^2 with the left and right FPN template=0.30 and 0.26, respectively), salience network (R^2 with the salience network template=0.14), primary and secondary SMN (R^2 with the templates of the primary and secondary SMN=0.36 and 0.24, respectively), primary and secondary visual networks (R^2 with the templates of the primary and secondary visual networks=0.58 and 0.33, respectively) and auditory network (R^2 with the auditory network template=0.62) (**Fig. 4.1.1**). All these components were stable across multiple runs of IC decomposition (stability index assessed by ICASSO ranged from 0.83 to 0.98).

Intra-network RS FC analyses

Patients with migraine showed decreased mean RS FC values of the DMN compared to controls (p=0.05) (**Table 4.1.2**).

Fig. 4.1.2 and **Table 4.1.3** show the regional differences of RS FC in each network of interest between migraine patients and controls. Compared to controls, patients with migraine had reduced RS FC in the left parieto-occipital junction of the DMN and in the left dorsolateral prefrontal cortex (DLPFC) of the ECN. Patients with migraine experienced also increased RS FC in the right frontopolar cortex of the right FPN and in the right middle occipital gyrus of the secondary visual network.

Between-network RS FC analyses

Table 4.1.4 and **Fig. 4.1.3** show RS networks with a significantly different pair-wise connectivity between migraine patients and controls. Compared to controls, migraine patients had a stronger connectivity between the ECN and primary visual network and between the right FPN and primary SMN, primary visual and auditory networks. A weaker connectivity between the DMN and right FPN was found in migraineurs compared to controls.

Correlations analyses

In patients with migraine, no correlation was found between RS FC abnormalities and disease duration and attack frequency.

Discussion

The main finding of this study is that significant RS FC abnormalities of brain networks involved in multisensory processing and in the cognitive control of pain are already present in pediatric patients with migraine.

Although the activation of single brain areas is related to specific symptoms reported by migraine patients during the different phases of the migraine cycle, the idea that brain regions can play a solo in the complex pathophysiology of migraine attacks seems to be an oversimplification. Some evidence suggests that the altered activity of specific brain areas involved in migraine pathophysiology, like the hypothalamus, pons and STN, may result from the interaction with other brain regions. Numerous RS fMRI studies have demonstrated abnormal FC of large-scale brain networks in adult migraine patients during both the ictal and interictal phase (149). So far, only one study (210) has demonstrated an altered RS FC of the amygdala and precuneus with brain regions involved in sensory, motor and affective functions in a cohort of female pediatric migraine patients. Here, we investigated the functional coupling of several large-scale brain networks in pediatric patients with migraine.

Migraine is now widely accepted as a disorder of brain sensory processing. Currently available evidence suggests that a dysfunctional regulation of the cortical excitatory-inhibitory balance alters the perception of sensory inputs in migraineurs, thus leading to the neurological symptoms commonly experienced by patients, like photophobia, phonophobia and cutaneous allodynia (13). Hypersensitivity to light is one of the key non-head pain symptoms described by patients during and between migraine attacks. Several fMRI studies have demonstrated a higher activation in primary and extrastriate visual areas in adult migraine patients during visual stimulation (223). Widespread RS FC abnormalities in brain regions involved in visual processing have been shown in patients with migraine with aura compared to controls and migraine patients without aura (224). Similarly to what has been observed in adults, young patients with migraine exhibited an increased RS FC of the extrastriate visual cortex. These fMRI results are in agreement with morphometric studies showing diffusion tensor MRI abnormalities of the optic radiations (140) and altered GM volume of the fusiform gyrus (160) in pediatric migraine patients. Functional and structural processes may render the

visual cortex more excitable and prone to elicit the copious visual phenomena associated with migraine from the early stage of the disease.

Consistent with results from adult migraine patients (158), we found a disrupted RS FC within the DMN in young migraine patients. Specifically, compared to controls, patients with migraine showed a weaker RS FC of the left parieto-occipital junction, a multisensory processing area where somesthetic and visual stimuli converge (225). The DMN is one of the most studied brain RS networks. Numerous studies have reported significant changes in DMN function in adult migraine patients, both interictally and during the migraine attack (149). It comprises different fronto-parietal and temporal regions and has a critical role in cognition, attention, interoception and self-monitoring. The DMN is also involved in monitoring the external environment and facilitating the retrieval and integration of relevant stimuli (226). The altered RS FC of the parieto-occipital junction we have found within the DMN in young migraine patients might be associated to an increased patients' attention to sensory and visual stimuli.

Cognitive symptoms, particularly deficits in attention and memory, are frequently reported by adult and pediatric migraine patients during the premonitory and the headache phase of the migraine attack (54). On the other hand, the study of inter-ictal cognitive abilities in migraine has produced inconsistent results (227). While some authors found cognitive deficits involving the executive, memory and attentive functions in migraine patients, others were unable to find any difference between controls and migraineurs. The ECN, which encompasses the anterior cingulate cortex, superior and medial frontal gyrus, is involved in executive functions, such as control processes, attention sustention, working memory, decision-making and goal-oriented planning. The FPN is a lateralized network which includes the medial and inferior frontal gyrus, precuneus, inferior parietal and angular gyrus. This network has been associated with different functions such as memory, attention, language and visual processing (228). A weaker FC of fronto-parietal regions in the ECN has been found in adult patients with migraine with and without aura, in the absence of deficits of executive functions (157, 229). Similarly, we found a decreased RS FC of the left DLPFC in the ECN and an increased RS FC of the right frontopolar cortex in the right FPN in pediatric migraine patients. The experience of recurrent painful attacks can be modulated by emotions, attention or cognitive control (230). The DLPFC and frontopolar cortex are highly interconnected with each other and

have extensive anatomical and functional connections with other cortical and subcortical regions of the pain network. They both play a role in attention to sensory input and pain modulation with goal-directed behaviour. Together with the anterior cingulate cortex, hypothalamus and PAG, the DLPFC and frontopolar cortex are part of a descending pathway that is responsible for the top-down cognitive modulation of pain (231, 232). The lateral frontopolar cortex is also involved in episodic memory and future retrievals. During painful stimulation, the activation of the frontopolar cortex may guide the selection of specific goal-directed behaviours, like pain avoidance and protection, according to what has been memorized in the past (233). The functional alterations we have observed in the ECN and right FPN suggest that the cognitive control of pain is dysfunctional in pediatric patients with migraine. Unfortunately, due to the lack of a neuropsychological evaluation, we could not exclude that these functional alterations are associated with broader cognitive deficits.

To further characterize the large-scale organization of brain networks in young patients with migraine, we have also explored the interaction between distinct brain networks. Similar to adult migraine patients (234), our findings demonstrated a decreased FC between the DMN and the right FPN in young migraine patients compared to controls. Internally-directed thought processes and mind-wandering are driven by the interaction between the DMN and FPN (235, 236). The altered coupling between these two networks we have found in pediatric migraine patients might reflect an abnormal mind wandering and self-oriented attention away from pain.

Remarkably, the between-network RS FC analysis also disclosed an increased connectivity between sensory processing and attentive neural networks in patients with migraine. When compared to controls, migraine patients had an increased connectivity between the ECN and primary visual network and between the right FPN and primary visual, SMN and auditory networks. The ECN and right FPN serve as alerting systems that detect behaviourally relevant sensory stimuli in the environment and reorient the attention to these stimuli (198, 229). Most regions involved in attention control are multimodal and combine information arising from the different senses and hence mediate multisensory attention control (225). Previous neurophysiological studies have demonstrated an altered top-down attentional control of visual and auditory stimuli in adult and pediatric migraine patients (237). Moreover, contrary to controls, adult migraine

patients do not habituate to sensory, visual and auditory stimuli (238). Our findings further support an early state of heightened alertness and sensitivity to sensory stimuli in migraineurs.

The presence of functional reorganization in the main sensory and cognitive brain networks from an early stage of the disease and the lack of a significant correlation between RS FC abnormalities and patients' clinical characteristics suggest that these functional patterns might represent a phenotypic biomarker of migraine. However, further studies in larger cohort of patients and with a longitudinal design are warranted to confirm our findings and to clarify their role in the pathophysiology of migraine.

Our study is not without limitations. First, the sample size was relatively small and the migraine sample was heterogeneous, including both patients with and without aura, males and females. Second, we did not have reliable pieces of information concerning the time elapsed between the MRI and the subsequent migraine attack (to avoid functional changes due to preictal states of an attack), nor severity of pain or cognitive deficits. Moreover, one patient was on pharmacological and four patients were on non-pharmacological preventive treatments. As a consequence, the possible influence of such therapies on the RS FC of brain networks cannot be excluded.

Overall, our results support the notion that migraine is a network-based disorder of sensory processing. Abnormalities of cognitive modulation of pain and an enhanced attention to visual, sensory and auditory stimuli occur in migraine patients from an early stage of the disease. An early dysregulation of multisensory processing, including pain, might represent a phenotypic biomarker of the disease and might account for the wide constellation of symptoms usually experienced by migraine patients during and outside the attacks.

Table 4.1.1. Main demographic and clinical characteristics of the subjects enrolled in the study.

	Controls	**Migraine patients**			***p* values patients *vs* controls**
		All patients	**Migraine with aura**	**Migraine without aura**	
Girls/Boys	6/8	7/6	3/4	4/2	0.7
Mean age (range) [years]	13.6 (8-18)	13.8 (9-17)	14.3 (12-17)	13.3 (9-16)	0.8
Mean attack frequency per year (range)	-	24 (0.5-48)	18 (0.5-48)	31 (12-48)	-
Mean disease duration (range) [years]	-	3.3 (0.25-10)	2.3 (0.25-5)	4.5 (0.5-10)	-

Table 4.1.2. Global mean values and standard deviation of RS FC values of brain resting-state networks in controls and patients with migraine, expressed as Z-scores.

RS network	Controls	Migraine patients	*p* values patients vs controls*
Default mode network	1.28 (0.19)	1.16 (0.17)	0.05
Executive control	1.39 (0.29)	1.32 (0.23)	0.3
Right frontoparietal	1.31 (0.21)	1.23 (0.19)	0.2
Left frontoparietal	1.14 (0.20)	1.18 (0.14)	0.7
Salience	1.30 (0.17)	1.23 (0.15)	0.1
Primary sensorimotor	1.94 (0.34)	1.90 (0.43)	0.7
Secondary sensorimotor	1.27 (0.16)	1.18 (0.25)	0.3
Primary visual	1.42 (0.45)	1.53 (0.37)	0.5
Secondary visual	1.33 (0.42)	1.39 (0.36)	0.7
Auditory	1.56 (0.32)	1.50 (0.22)	0.4

*Age- and sex-adjusted linear model ($p<0.05$).

T**able 4.1.3.** Regions showing significant RS FC differences between patients with migraine and controls in the RS networks of interest.

RS network	**Findings**	**Region**	**Brodmann area**	***t* values***	**Cluster extent (no. of voxels)**	**MNI coordinates (X, Y, Z)**
Default mode network	Decreased RS FC	L parieto-occipital junction	39	5.98	77	-38, -78, 24
Executive control	Decreased RS FC	L dorsolateral prefrontal cortex	46	5.15	40	-24, 36, 28
Right frontoparietal	Increased RS FC	R frontopolar cortex	10	6.66	71	24, 62, 16
Secondary visual	Increased RS FC	R middle occipital gyrus	19	4.76	54	38, -84, 14

*Age- and sex-adjusted linear model ($p<0.05$, clusterwise FWE-corrected for multiple comparisons).

Abbreviations: FC=functional connectivity, L=left, R=right, RS=resting state.

Table 4.1.4. Within-group and between-group correlation coefficients (*r*) among the RS networks of interest in migraine patients and controls.

RS network pairs		**Controls**		**Migraine patients**		***p* values patients *vs* controls***
Between	*and*	*r*	*p values**	*r*	*p values**	
Default mode network	Executive	0.009	0.9	0.13	0.07	0.2
	Right frontoparietal	0.43	<0.0001	0.27	<0.0001	**0.04**
	Left frontoparietal	0.23	0.0002	0.19	0.001	0.6
	Salience	-0.21	0.01	-0.30	0.001	0.5
	Primary sensorimotor	0.02	0.7	0.002	0.9	0.8
	Secondary sensorimotor	0.16	0.01	0.15	0.01	0.9
	Primary visual	-0.02	0.7	0.10	0.07	0.1
	Secondary visual	0.05	0.5	0.03	0.6	0.9
	Auditory	0.07	0.2	0.08	0.07	0.2
Executive control	Right frontoparietal	0.24	<0.0001	0.19	0.0005	0.6
	Left frontoparietal	0.07	0.6	0.14	0.1	0.5
	Salience	0.35	<0.0001	0.27	0.0005	0.3
	Primary sensorimotor	-0.02	0.5	0.02	0.6	0.4
	Secondary sensorimotor	0.06	0.3	0.04	0.6	0.7
	Primary visual	0.02	0.7	0.19	0.001	**0.03**
	Secondary visual	0.11	0.06	0.23	0.0002	0.08
	Auditory	0.05	0.3	0.17	0.008	0.2
Right frontoparietal	Left frontoparietal	0.38	<0.0001	0.29	<0.0001	0.3
	Salience	-0.15	0.003	-0.19	0.002	0.8

	Primary sensorimotor	-0.09	0.01	0.004	0.9	**0.05**
	Secondary sensorimotor	-0.04	0.3	0.01	0.8	0.4
	Primary visual	-0.13	0.007	0.007	0.9	**0.04**
	Secondary visual	-0.04	0.2	-0.03	0.6	0.6
	Auditory	-0.07	0.05	0.03	0.4	**0.05**
Left frontoparietal	Salience	-0.22	0.002	-0.23	0.007	0.8
	Primary sensorimotor	-0.005	0.9	0.05	0.2	0.4
	Secondary sensorimotor	-0.08	0.06	-0.02	0.7	0.3
	Primary visual	-0.11	0.03	-0.04	0.4	0.3
	Secondary visual	-0.06	0.1	0.001	0.9	0.3
	Auditory	-0.13	0.006	-0.07	0.2	0.3
Salience	Primary sensorimotor	0.28	<0.0001	0.27	<0.0001	0.7
	Secondary sensorimotor	0.33	<0.0001	0.21	0.001	0.1
	Primary visual	0.24	0.0004	0.13	0.03	0.2
	Secondary visual	0.16	0.003	0.12	0.02	0.6
	Auditory	0.53	<0.0001	0.46	<0.0001	0.2
Primary sensorimotor	Secondary sensorimotor	0.35	<0.0001	0.38	<0.0001	0.6
	Primary visual	0.23	0.01	0.26	0.003	0.7
	Secondary visual	0.16	0.03	0.28	0.0003	0.2
	Auditory	0.35	<0.0001	0.38	<0.0001	0.4
Secondary sensorimotor	Primary visual	0.36	0.0003	0.29	0.003	0.6
	Secondary visual	0.29	0.0007	0.28	0.001	0.9

	Auditory	0.48	<0.0001	0.44	<0.0001	0.7
Primary visual	Secondary visual	0.51	<0.0001	0.53	<0.0001	0.8
	Auditory	0.45	<0.0001	0.38	<0.0001	0.5
Secondary visual	Auditory	0.35	<0.0001	0.28	<0.0001	0.4

*Age- and gender-adjusted linear model ($p<0.05$).

Significant between-group differences are highlighted in bold.

Fig. 4.1.1. Resting state networks of interest. Spatial maps of resting state networks of interest from patients with migraine and controls ($p < 0.05$ FWE corrected).

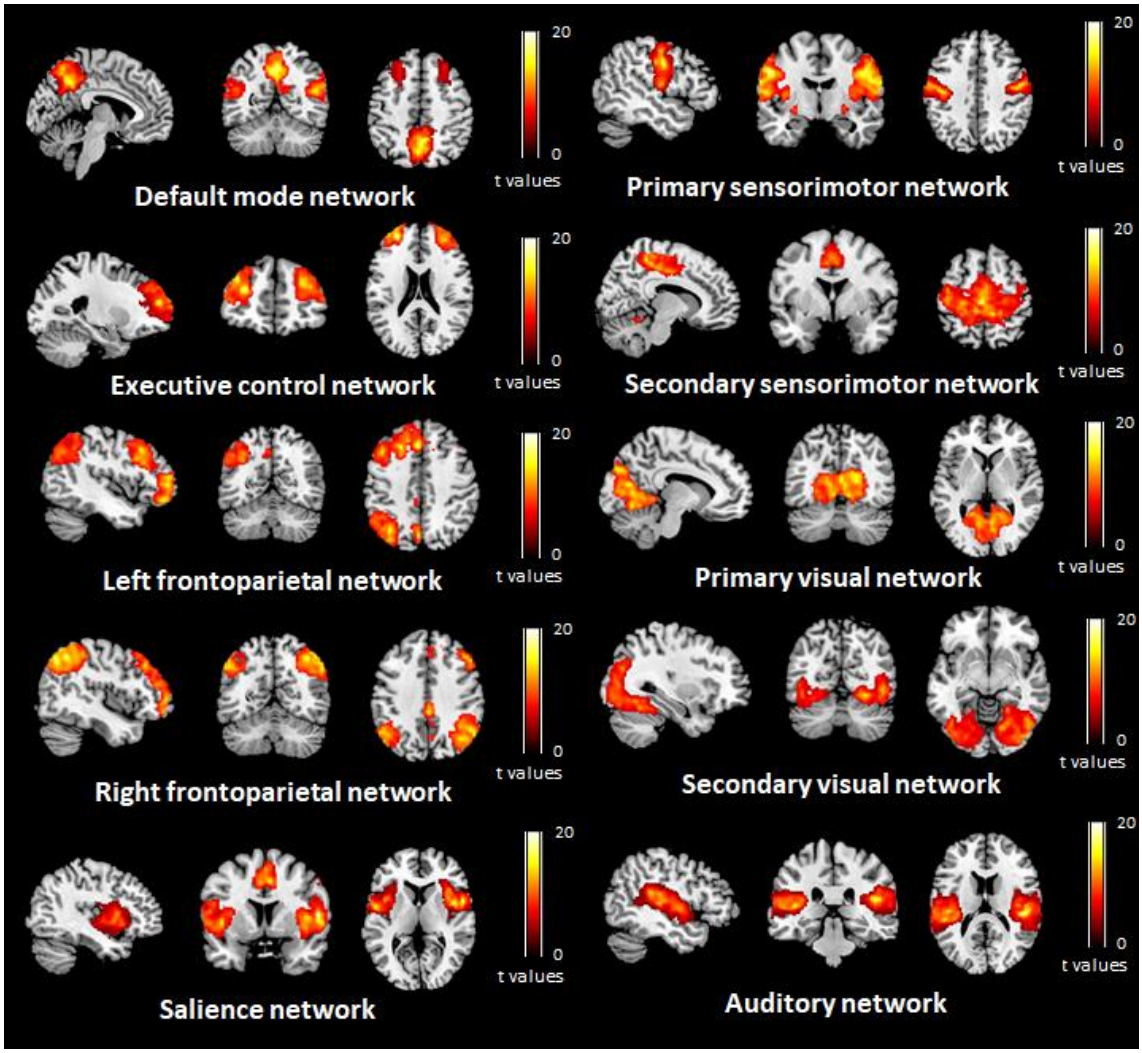

Fig. 4.1.2. Intra-network resting state functional connectivity differences between migraine patients and controls. Areas showing significant resting state (RS) functional connectivity (FC) differences between patients with migraine and controls ($p<0.001$, uncorrected for display), represented on a high resolution T1-weighted template. Regions of decreased RS FC are shown in cyan (color-coded for their t values) (A), and regions of increased RS FC are represented in yellow (color-coded for their t values) (B). Regions of increased and decreased RS FC are overlaid on spatial maps of the corresponding RS network.
Abbreviations: L=left, R=right.

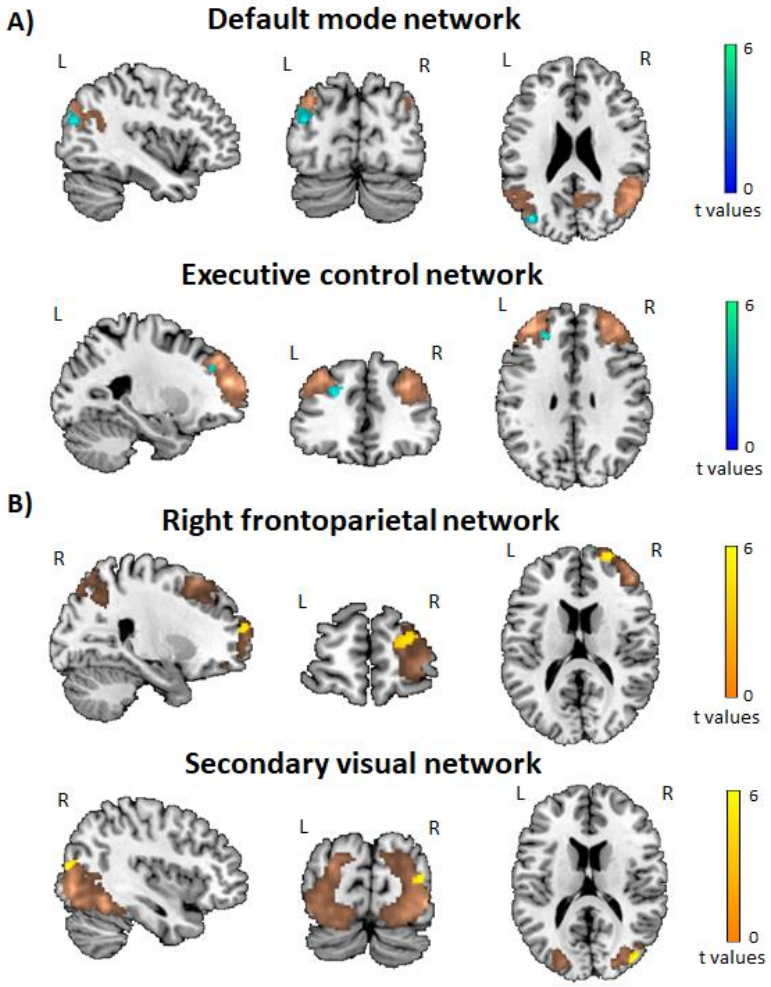

Fig. 4.1.3. Between-network resting state functional connectivity differences between migraine patients and controls. A diagram showing resting state networks with a significantly different pair-wise connectivity between migraine patients and controls. Red arrows indicate stronger connectivity in patients with migraine compared to controls and the blue arrow indicates weaker connectivity in migraine patients compared to controls.

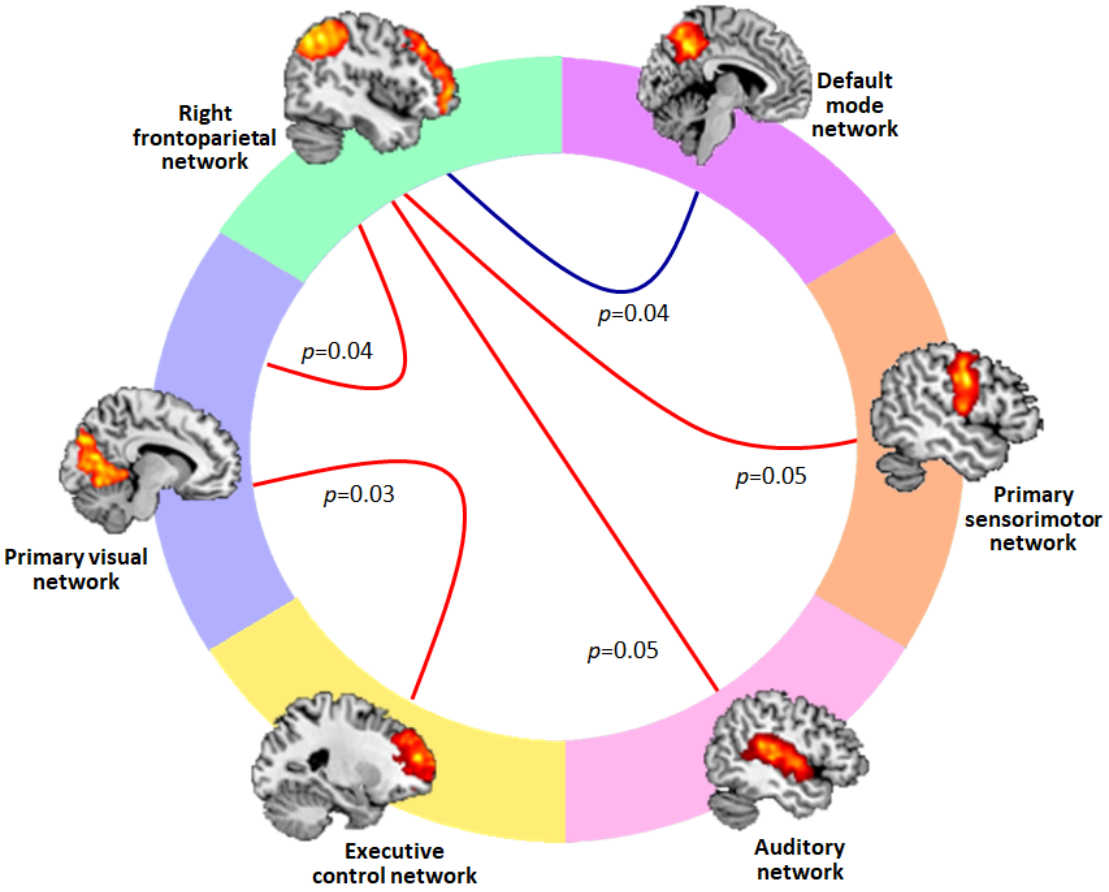

5. CROSS-SECTIONAL AND LONGITUDINAL RESTING STATE FUNCTIONAL CONNECTIVITY CHANGES OF THE HYPOTHALAMUS IN MIGRAINE PATIENTS

5.1. Clinical correlates of hypothalamic functional changes in migraine patients. Messina *et al.*, Cephalalgia 2021.

This chapter describes the work published in Cephalalgia (PMID: 34644197, DOI: 10.1177/03331024211046618).

Abstract

Objective. To elucidate the hypothalamic involvement in episodic migraine and investigate the association between hypothalamic RS FC changes and migraine patients' clinical characteristics and disease progression over the years.

Methods. Ninety-one patients with episodic migraine and seventy-three controls underwent interictal RS functional MRI. Twenty-three patients and controls were re-examined after a median of 4.5 years. Hypothalamic RS FC changes were investigated using a seed-based correlation approach.

Results. At baseline, a decreased functional interaction between the hypothalamus and the parahippocampus, cerebellum, temporal, lingual and orbitofrontal gyrus (OFG) was found in migraine patients *vs* controls. Increased RS FC between the hypothalamus and bilateral OFG was demonstrated in migraine patients at follow-up *vs* baseline. Migraine patients experienced also decreased right hypothalamic RS FC with ipsilateral lingual gyrus. A higher migraine attack frequency was associated with decreased hypothalamic-lingual gyrus RS FC at baseline, while greater headache impact at follow-up correlated with decreased hypothalamic-OFG RS FC at baseline. At follow-up, a lower frequency of migraine attacks was associated with higher hypothalamic-OFG RS FC.

Conclusions. During the interictal phase, the hypothalamus modulates the activity of pain and visual processing areas in episodic migraine patients. The hypothalamic-cortical interplay changes dynamically over time according to patients' clinical features.

Introduction

Migraine is widely recognized as an intricate neurological disease that comprises the interaction of different brain networks (13). Neuroimaging studies have widened the understanding of migraine physiopathology, showing that the activation of specific brain regions can explain the broad clinical spectrum of migraine (99).

The hypothalamus is one of the key actors in the manifestation of migraine. PET and fMRI studies (100, 102) demonstrated an early hypothalamic activation in the premonitory phase of migraine, suggesting that the hypothalamus could mediate symptoms like yawning, food craving, thirst and fatigue. An increased hypothalamic activation has also been demonstrated in the pain phase of migraine (100, 102, 107). During trigeminal nociceptive stimulation, the functional connection between the hypothalamus and brain regions implicated in the generation of migraine headache, such as the STN and dorsal pons, changes throughout the preictal and pain phase. These findings point to a hypothalamic involvement in the onset of the migraine attack and highlight dynamic functional changes of the hypothalamic connectivity during the migraine cycle (102).

Although many studies have investigated the role of the hypothalamus in the acute phases of the migraine attack in episodic migraine patients, only one small study has explored its involvement in the interictal phase. It has been shown that the functional connectivity (FC) between the hypothalamus and cortical regions implicated in pain processing, sympathetic and parasympathetic functions is altered in episodic migraine patients without aura studied during the interictal phase (156). Whether the interictal functional alterations of the hypothalamus could evolve over the years is unknown.

There is evidence supporting a role of the hypothalamus in migraine chronification (108). The hypothalamic interaction with pain processing brain areas is stronger in chronic migraine patients in comparison with patients with an episodic form of the disease (239). A recent study showed that a decreased RS FC between the hypothalamus and medial prefrontal cortex, an area that is involved in pain perception, could modulate the pain severity perceived by chronic migraine patients during their attack (240). Even though the role of the hypothalamus in determining the severity of migraine is well established in patients with a chronic form of the disease (239, 240), the

association between hypothalamic functional alterations and clinical features of episodic migraine patients has not been investigated so far.

In this study, we hypothesized that episodic migraine patients experience hypothalamic RS FC alterations that are influenced by patients' clinical features (e.g., disease duration, migraine attack frequency, presence of aura). We also assumed that the functional interplay between the hypothalamus and other brain regions implicated in migraine pathophysiology might change over time, thus affecting the disease activity. To test our hypotheses, we explored cross-sectional hypothalamic RS FC alterations in a large cohort of episodic migraine patients and assessed the correlation between hypothalamic functional abnormalities and patients' clinical features. We also followed the clinical evolution of patients over 4 years and explored longitudinal hypothalamic RS FC changes and their association with clinical data and disease progression, as measured by changes in migraine frequency. Finally, we investigated whether baseline hypothalamic RS FC alterations could influence migraine severity over time.

Methods

Participants. Between October 2006 and May 2016, we prospectively studied 91 right-handed, episodic migraine patients (42 patients with migraine with aura (MWA) and 49 without aura (MWoA)) and 73 right-handed controls. All participants were asked to participate in a clinical and MRI follow-up evaluation. Both baseline and follow-up visits included a detailed clinical evaluation and an MRI session, including RS fMRI and structural MRI sequences. Results obtained from the structural MRI analysis performed on part of patients included in the present study were previously published (164). To avoid measuring imaging changes associated to acute migraine symptoms, all patients had to be attack-free, including aura, in the 48 hours before the MRI and during the exam.

Exclusion criteria for patients and controls included the presence of vascular risk factors (e.g., vascular disease, heart disease, hypercholesteremia, hypertension, diabetes mellitus), abnormal neurological exam, systemic conditions, other psychiatric, or neurologic diseases. Controls were excluded from the study if they suffered from any headaches with the exception of infrequent tension-type headache (<1 headache day/month). Patients who attended the Headache Outpatient Clinic of the IRCCS San Raffaele Scientific Institute (Milan, Italy) were enrolled in the study. Migraine was

diagnosed applying the standard diagnostic criteria of the International Classification of Headache Disorders (241, 242). Controls were recruited among hospital workers, university students and consented friends. The clinical assessment of all participants was performed by a single neurologist, before the MRI evaluation.

At baseline and follow-up, we obtained an accurate clinical history of patients, comprising their frequency of migraine attacks and disease duration. At follow-up, the median headache pain severity of the 3 months preceding the visit was evaluated using the NRS (180), and patients' disability was quantified using the HIT-6 (182) and MIDAS questionnaire (181).

At baseline, 25 patients were taking preventive therapies for migraine, comprising topiramate, β-blockers, pizotifen, amitriptyline and flunarizine. During the follow-up, 4 patients never stopped taking preventive medications, 8 patients stopped taking preventive treatments and 1 patient started a new preventive drug.

To explore whether hypothalamic functional changes might be related to disease progression and migraine phenotype, patients were divided into subgroups according to changes in migraine frequency over the follow-up (IoS = patients with decreased or stable attack frequency at follow-up, Wo = patients with increased attack frequency at follow-up) and presence/absence of aura. Patients' improvement or worsening was evaluated taking note of the number of migraine days reported by patients in their headache diaries at the baseline and follow-up visit.

Patient consents and protocol approvals. The Local Ethical Committee on human studies approved this study. Written informed consent was obtained from all participants before study entry.

Image acquisition. Using a 3.0 Tesla Intera scanner (Philips Medical Systems, Best, The Netherlands), the following brain sequences were obtained from all participants at baseline and follow-up: 1) RS fMRI scans (T2*-weighted echo planar imaging sequence with 200 sets of 30 contiguous axial slices, slice thickness = 4 mm, matrix size = 96 x 96, reconstructed to 128 × 128, TR/TE = 3000/35 ms, FlA = 90°, FOV = 240 mm^2); 2) T2-weighted turbo-spin echo (28 contiguous axial slices, 4 mm thick, TR/TE = 3000/120 ms, FlA = 90º, matrix size = 512 × 512, FOV = 230 mm^2); 3) fluid attenuated inversion

recovery (28 axial contiguous slices, 4 mm thick, TR/TE = 11000/120 ms, inversion time = 2800 ms, FlA = 90°, matrix size = 256 × 256, FOV = 230 mm^2); and 4) 3D T1-weighted fast field echo (220 contiguous axial slices with voxel size = 0.89 × 0.89 x 0.8 mm, TR/TE = 25/4.6 ms; FlA = 30°; matrix size = 256 × 256; FOV = 230 × 230 mm^2). During the RS fMRI acquisition, participants were instructed to stay awake with their eyes closed. The same patient positioning procedure was used at the two study time points and baseline MRI localizer images were used as reference to achieve the same slice positioning on baseline and follow-up MRI exams.

MRI analysis. Statistical Parametric Mapping (SPM) 12 (https://www.fil.ion.ucl.ac.uk/spm/) and REST software (https://resting-fmri.sourceforge.net) were used to analyse baseline and follow-up RS fMRI images. The pre-processing of RS fMRI images comprised the following steps: 1) rigid-body realignment of raw RS fMRI images to the mean of each session, to correct for minor head movements; 2) rigid registration of realigned images to the 3D T1-weighted image; 3) normalization of RS fMRI data to the MNI template using a standard affine transformation followed by nonlinear warping; 4) linear detrending and band-pass filtering (0.01–0.08 Hz), performed to partially remove low frequency drifts and physiological high-frequency noise; 5) removal of non-neuronal sources of synchrony between RS fMRI time series by regressing out the six motion parameters estimated by SPM12 and the average signals of the ventricular cerebro-spinal fluid and WM; 6) smoothing of normalized images using a 3D 6-mm Gaussian kernel.

After pre-processing, a seed-based correlation approach was applied to study voxel-wise baseline and follow-up RS FC between the left and right hypothalamus, separately, and the remaining voxels of the brain (243). Based on previous studies (100, 108), we used a 6-mm sphere around the peak MNI coordinates of hypothalamic activation (X=±6, Y=-6, Z=-10). Briefly, the correlation coefficients between the average time series extracted from the left and right hypothalamus and any other brain voxels were calculated. The Gaussianity of the obtained correlation coefficients was improved using a Fisher's z transform (244).

Statistical analysis. Given the challenges of retaining a big sample of patients and controls throughout the entire follow-up period in a 4-year study, based on previous literature (193), we estimated that a sample size of at least 20 patients would have been acceptable to assess fMRI abnormalities in headache disorders. The distribution of the data was assessed using the Q-Q plots, Kolmogorov-Smirnov and Shapiro-Wilk tests. Since the data were not normally distributed, between-group differences in demographic and clinical variables were assessed using the Mann-Whitney test for continuous variables and the Fisher exact test for categorical variables (version 26.0; SPSS software, IBM, Armonk, NY). Using SPM12, the following linear models were performed on hypothalamic RS FC maps: 1) average baseline hypothalamic RS FC within the group of migraine patients and controls, separately (age- and sex-adjusted one sample t-tests); 2) between-group comparisons (patients *vs* controls, MWA *vs* MWoA) of hypothalamic RS FC at baseline (age- and sex-adjusted two-sample t-tests and conjunction analyses); 3) changes over time of hypothalamic RS FC in the entire group of patients with migraine, each subgroup of patients and controls, separately (age-adjusted paired sample t-tests); and 4) time-by-group interactions tested comparing the RS FC delta at follow-up *vs* baseline between migraine patients and controls and between the different subgroups of patients (age- and sex-adjusted two-sample t-tests). To exclude a possible effect of migraine preventive treatments, we performed a between-group comparison of hypothalamic RS FC at baseline considering the use of preventive drugs (age- and sex-adjusted two-sample t-tests and conjunction analyses) and explored longitudinal hypothalamic RS FC changes in the subgroup of patients who were not taking any preventive drugs at baseline and follow-up. The use of preventive therapies was included as an additional covariate in the analysis investigating the longitudinal effect of disease progression. To prevent misinterpretations associated with anticorrelated connections, only brain regions showing positive RS FC with the hypothalamus in both patients and controls were included in the between-group comparison analyses (245). In migraine patients, multiple linear regression models, adjusted for age and sex, were performed using SPM12 to investigate the association between abnormal hypothalamic RS FC and clinical characteristics at baseline and follow-up (frequency of migraine attacks, disease duration, NRS, MIDAS and HIT-6 scores). A statistical threshold of $p < 0.05$, FWE corrected, and $p < 0.001$, uncorrected was used to test the results. Exploratory analyses in

the subgroups of migraine patients were also tested at a $p < 0.05$, uncorrected for multiple comparisons.

Data availability. Data supporting the results of this study are available from the corresponding author, upon reasonable request.

Results

Clinical and demographic findings. The main clinical and demographic characteristics of participants are summarized in **Table 5.1.1**. Twenty-three migraine patients (11 MWA and 12 MWoA) and 23 controls agreed to participate to the clinical and MRI follow-up evaluation after a median of 4.5 years (interquartile range = 2-5 years; patients: mean follow-up years: 4.5, range: 3-6; controls: mean follow-up years: 3.9, range: 2-6). Sixty-eight patients and 50 controls withdrew from the follow-up evaluation because they moved to another city, due to familial or work commitments, pregnancy or interest loss.

During the follow-up, 11 patients (48%) reported a reduction of migraine attack frequency, 8 patients (35%) had an increased number of migraine attacks and in the remaining 4 patients (17%) the migraine attack frequency did not change. We found no association between patients' disease progression during the follow-up and the use of migraine preventive drugs at baseline ($p = 0.2$) and follow-up ($p = 1.0$).

We did not find any sex differences in migraine patients *vs* controls (baseline: $p = 0.4$, follow-up: $p = 0.1$). At the two time points, patients with migraine were older than controls (baseline: $p = 0.02$, follow-up: $p = 0.02$). At baseline, patients with MWoA were older than patients with MWA ($p = 0.04$). Compared to MWA, patients with MWoA had a higher attack frequency at baseline ($p=0.0009$) and follow-up ($p = 0.03$). At follow-up, except from migraine attack frequency, we did not find any significant demographic and clinical differences among migraine patients with improved or stable migraine and those with worsening migraine (**Table 5.1.1**).

Baseline demographic and clinical characteristics did not differ between the entire group of participants and the subgroup of patients and controls who underwent longitudinal assessment (**Supplementary Table 5.1.1**).

Baseline hypothalamic RS FC. **Supplementary Table 5.1.2** summarizes the brain areas with positive hypothalamic RS FC in patients with migraine and controls at baseline. Both patients and controls showed positive left and right hypothalamic RS FC with cerebellar, occipital, frontal and temporal regions.

Decreased RS FC between the right and left hypothalamus and left parahippocampus and bilateral orbitofrontal gyrus (OFG) was found in migraine patients *vs* controls (**Figure 5.1.1** and **Table 5.1.2**). Compared to controls, migraine patients experienced also decreased RS FC between the left hypothalamus and right cerebellar crus II, as well as decreased RS FC between the right hypothalamus and the right lingual gyrus, cerebellar lobule VI and inferior temporal gyrus (**Figure 5.1.1** and **Table 5.1.2**). Similar findings were obtained when the subgroup of patients who were on preventive drugs for migraine and those who were not taking any treatments were separately compared to controls (**Supplementary Table 5.1.3**). We found no difference of hypothalamic RS FC in patients who were on preventive drugs for migraine compared to those who were not taking medications.

Compared with MWA patients and controls, MWoA patients showed decreased RS FC between the left hypothalamus and the right temporal pole (**Table 5.1.2**).

Similar findings were found when analysing the subgroup of controls and patients that were studied longitudinally (**Supplementary Table 5.1.4**).

Longitudinal hypothalamic RS FC changes. No significant longitudinal hypothalamic RS FC changes were found in controls. At follow-up *vs* baseline, the left and right hypothalamus showed increased RS FC with bilateral OFG in migraine patients (**Figure 5.1.2** and **Table 5.1.3)**. Migraine patients also experienced decreased right hypothalamic RS FC with the ipsilateral lingual gyrus (**Figure 5.1.2** and **Table 5.1.3)**. We found no significant time-by-group interaction in migraine patients compared to controls.

Similar results were detected in the exploratory analysis investigating longitudinal hypothalamic RS FC changes in the subgroup of patients who were not taking any preventive treatments at the two time points (**Supplementary Table 5.1.5**).

Effect of disease progression and aura over time. The exploratory subgroup analysis showed an increased left hypothalamic RS FC with the ipsilateral OFG in patients with

an improved or stable migraine at follow-up, while patients with worsening migraine experienced decreased RS FC between bilateral hypothalamus and left OFG (**Figure 5.1.3** and **Table 5.1.3**). We found no significant longitudinal changes in the subgroups of patients with and without aura. No significant time-by-group interactions were observed in patients with improved or stable migraine *vs* patients with worsening migraine, as well as in MWA *vs* MWoA patients.

Correlation analysis. At baseline, in migraine patients the lower the right hypothalamic RS FC with the right lingual gyrus, the higher the migraine attack frequency was ($r=-0.39$, $p<0.05$, voxelwise FWE-corrected for multiple comparisons). Moreover, the decreased hypothalamic RS FC with the right OFG observed in migraine patients at baseline correlated with greater headache impact at follow-up (left hypothalamus: $r=-0.82$, $p<0.001$, uncorrected; right hypothalamus: $r=-0.87$, voxelwise FWE-corrected for multiple comparisons). At follow-up, the increased RS FC between the right hypothalamus and the ipsilateral OFG was associated with lower migraine attack frequency ($r=-0.73$, $p < 0.001$ uncorrected).

Discussion

The main finding of this study is that episodic migraine patients experience hypothalamic RS FC alterations during the interictal phase according to their clinical features. Using a longitudinal fMRI study design, we showed that the hypothalamic-cortical interplay changes dynamically over time in episodic migraine patients. Changes in the functional coupling between the hypothalamus and pain and visual processing brain regions can influence the course of migraine.

Recent evidence highlighted an important hypothalamic involvement in migraine physiopathology, showing an altered activity of the hypothalamus during all phases of the migraine attack. The hypothalamus is involved in numerous functions including pain modulation, sleep, cognition, autonomic and homeostatic regulation (13). An early activation of the hypothalamus can mediate migraine premonitory symptoms and facilitate the onset of the migraine headache (100, 102). It has been shown that the hypothalamus can contribute to migraine chronification and influence the severity of migraine attacks in chronic migraine patients (108, 240). Only one study (156) has

investigated interictal hypothalamic RS FC alterations in 12 patients with episodic migraine, showing an altered functional coupling between the hypothalamus and brain structures involved in pain and autonomic functions. Consistent with the previous cross-sectional study (156), we found an altered hypothalamic RS FC with brain regions implicated in nociception and migraine pathophysiology, including the cerebellum, parahippocampal, lingual and OFG, in a large sample of interictal episodic migraine patients. The parahippocampus, cerebellar crus II and lobule VI are associated with sympathetic and parasympathetic regulation (156). The altered connection we have found between the hypothalamus and these brain areas at baseline may contribute to explain autonomic nervous system dysfunctions accompanying the migraine attack (246). Our cross-sectional analysis showed only a decreased hypothalamic RS FC, while both decreased and increased hypothalamic RS FC have been previously described in migraine patients (156). This variability among studies could relate to different study designs, statistical approaches and sample size of patients.

A valuable strategy to elucidate the hypothalamic involvement in the course of migraine is to study patients longitudinally. Previous fMRI studies have investigated migraine-phase dependent hypothalamic changes (100, 102). Here, we explored longitudinal changes of the hypothalamic connectivity showing that migraine patients studied interictally developed increased hypothalamic RS FC with frontal nociceptive regions, as well as decreased RS FC between the hypothalamus and visual areas after 4 years.

Numerous imaging studies reported a specific hypothalamic activation during the pain phase of primary headache disorders, such as cluster headache and migraine, and showed that the hypothalamus can modulate the activity of brain areas usually implicated in pain transmission and perception (99, 107). The hypothalamus is highly connected with the trigeminal cervical complex, as well as brainstem, thalamic and cortical structures involved in nociception (13). Nociceptive inputs originating from the trigeminal cervical complex can converge into the hypothalamus, which mediates autonomic, neuroendocrine, cognitive and behavioural responses to pain through reciprocal connections with cortical and subcortical areas (247). Similar to previous studies (156, 240, 248) supporting reciprocal connections between the hypothalamus and frontal areas, we found a weak RS FC between the hypothalamus and OFG at baseline, which was

strengthened after 4 years. The OFG is part of the descending pain-inhibitory pathway and is involved in the modulation of pain threshold and emotional aspects of pain (249). This frontal area is innervated by hypothalamic orexinergic neurons (240, 250, 251). The neuropeptides orexins A and B are exclusively produced by the hypothalamus and are involved in autonomic functions, pain modulation, arousal, feeding and sleep regulation (13). The orexinergic neurons seem to modulate patients' susceptibility to the onset of a migraine attack and the duration of migraine pain (247). In line with previous data in chronic migraine (240), the decreased hypothalamic RS FC with the OFG we have detected in our cross-sectional analysis may lead to an impairment of the antinociceptive system in patients with episodic migraine. Notably, an adaptive coping response that lower the migraine attack frequency over the years occurred in migraine patients. We showed that the interaction between the hypothalamus and OFG was reinforced after 4 years, and the increased RS FC was associated to a lower migraine attack frequency at follow-up. In support of this hypothesis, we found that the hypothalamic-orbitofrontal connection was strengthened over time in those patients who reported fewer migraine attacks or remained stable, whereas it decreased in patients with worsening migraine.

It also interesting to note that, at baseline, a lower hypothalamic functional interaction with the OFG was related to greater headache impact at follow-up, suggesting that weakened hypothalamic-frontal connections may be a prognostic marker for migraine disability. This finding is in agreement with the notion that functional and structural abnormalities of the OFG may predispose to a more severe form of migraine (248, 252).

Visual pathways have been widely studied in MWA and MWoA patients (177, 253). It has been suggested that neural mechanisms associated to visual manifestations commonly described by patients with migraine during and between attacks, like light hypersensitivity, can involve a complex brain network including retinal afferents, trigeminal nuclei, hypothalamus, thalamus, and visual processing cortical areas (13, 254). Recent studies demonstrated direct connections of the hypothalamus with visual cortical areas, with possible implications in visuospatial processing, regulating the circadian rhythm and encoding the salience of multisensory information (240, 255). Both the hypothalamus and visual cortex show an abnormal activation across all phases of the migraine attack (100, 102, 177). Previous research (240, 248) has found abnormal

hypothalamic functional and structural connectivity with occipital brain regions in patients with episodic and chronic migraine, highlighting the role of visual areas in migraine pathophysiology and its chronification via direct and indirect connections between the visual, thalamic, hypothalamic and trigeminovascular pathways. Here, we showed a reduced RS FC between the right hypothalamus and ipsilateral lingual gyrus that further decreased over time. Functional and structural alterations of the lingual gyrus, an extrastriate visual area involved in higher order visual functions, such as visual memory and perception of colour, have been widely described in migraine patients (136, 177). Interestingly, in our cohort of patients a lower functional interaction between the hypothalamus and lingual gyrus was related to higher migraine attack frequency at baseline, suggesting that an aberrant interaction between these two regions during the interictal phase might facilitate the onset of a migraine attack. These findings further corroborate the interplay between the hypothalamus, visual and trigeminovascular systems.

It is also worth noting that we found functional alterations between the hypothalamus and visual areas regardless of the presence of migraine with aura. The only difference we have observed between patients with and without aura was a lower hypothalamic connectivity with the right temporal pole, a nociceptive processing brain area involved in migraine pathophysiology (256), in patients without aura. The cortical spreading depression (CSD) is the most widely accepted neurophysiological mechanism underlying migraine aura. It is characterized by a wave of neuronal depolarization followed by prolonged inhibition that originates from striate and extrastriate visual areas (31). Recent experimental studies showed that the CSD can also activate the thalamus and trigeminovascular system, suggesting an involvement of the CSD also in migraine without aura (38). Which is the role of CSD in the onset of migraine pain and whether "silent CSD attacks" originating from the visual cortex can activate the trigeminovascular system or vice versa is still unclear (177, 253). Consistent to previous studies showing functional and structural alterations in visual processing areas regardless of the presence of migraine aura, our results support the notion that migraine patients with and without aura may share common pathogenic mechanisms (99, 257).

It is noteworthy that cross-sectional and longitudinal hypothalamic RS FC changes we have observed here were not influenced by the use of migraine preventive

medications at baseline and follow-up. Based on these findings we could suppose that changes in the hypothalamic connectivity we have observed here and their clinical correlates reflect the natural history of the disease. Future studies including drug-naïve patients are necessary to support this conclusion.

A few limitations of the study should be noted. The sample size of the migraine subgroups was quite small and the lack of a strict control of false positives using an uncorrected statistical threshold in the comparison between subgroups should be considered. Moreover, information regarding the time elapsed between the MRI and the following migraine attack was missing, as well as data concerning the headache pain severity and patients' disability at baseline. Although all statistical models were controlled for age, the group of patients was older than that of controls. In addition, we did not have reliable pieces of information concerning female hormonal changes over the years that could have influenced the hypothalamic function. At last, the duration of follow-up was shorter compared to the migraine disease duration. Further larger studies with a longer follow-up are needed to confirm our results. In addition, future studies should investigate longitudinal hypothalamic connectivity changes in patients at an early onset of the disease, like pediatric patients, as well as in chronic migraine patients.

Overall, our results showed that the hypothalamus modulates the activity of key brain areas implicated in migraine physiopathology, thus affecting the course of the disease. As such, we highlighted a possible target for novel pharmacological and neuromodulation approaches.

Table 5.1.1. Main demographic and clinical characteristics of migraine patients and controls enrolled in the study.

Baseline									
	Controls	**Migraine patients**	**MWA patients**	**MWoA patients**	***p* values patients *vs* controls**			***p* values MWA *vs* MWoA patients**	
Women/Men	47/26	65/26	29/13	36/13	0.4			0.6	
Age (years)	27 (25-41)	34 (27-42)	33 (26-39)	37 (28-47)	0.02*			0.04*	
Attack frequency per month	-	3.5 (1-6)	2.3 (1-5)	4 (2-8)	-			0.009*	
Disease duration (years)	-	15 (10-21)	14 (4-21)	16 (10-22)	-			0.3	
Use of preventive medications	-	25	9	16	-			0.3	
Follow-up									
	Controls	**Migraine patients**	**MWA patients**	**MWoA patients**	**IoS patients**	**Wo patients**	***p* values patients *vs* controls**	***p* values MWA *vs* MWoA patients**	***p* values IoS *vs* Wo patients**
Women/Men	9/14	15/8	9/2	6/6	10/5	5/3	0.1	0.06	1

Age (years)	36 (26-45)	45 (36-48)	37 (31-48)	45 (41-50)	46 (37-50)	44 (33-48)	0.02*	0.06	0.6
Attack frequency per month	-	3 (1-5)	1.5 (0.1-4)	4 (2-7)	1.5 (0.4-4)	4.5 (2-9)	-	0.03*	0.01*
Duration of follow-up (years)	4.5 (2-5)	4.7 (4-5)	4.8 (4-5)	4.5 (4-5)	4.7 (4-5)	4.5 (4-5)	0.3	0.4	0.8
Use of preventive medications	-	5	1	4	3	2	-	0.4	1.0
MIDAS score	-	11 (6-30)	15 (8-28)	9 (2-46)	11 (4-30)	17 (6-41)	-	0.5	0.9
HIT-6 score	-	60 (55-67)	59 (55-67)	60 (58-68)	58 (55-68)	64 (59-67)	-	0.5	0.3
NRS score	-	7 (6-8)	7 (5-8)	7 (6-8)	6.5 (5-8)	8 (7-9)	-	0.9	0.5

Abbreviations: HIT-6 = 6-item Headache Impact Test; IoS = Improved or stable migraine; MIDAS = Migraine Disability Assessment; MWA = migraine with aura; MWoA = migraine without aura; NRS = Numerical Rating Scale; Wo = worsening migraine.

Measures are reported as medians and interquartile ranges (25th–75th percentiles). Sex and the use of preventive medications are reported as frequencies.
*Mann-Whitney test, $p<0.05$

Table 5.1.2. Regions showing significant decrease of hypothalamic resting state functional connectivity in patients with migraine compared to controls at baseline, as well as among subgroups of patients.

Migraine patients *vs* controls				
Left hypothalamus				
Connected regions	**Brodmann area**	***t* values***	**Cluster extent (no. of voxels)**	**MNI coordinates (X, Y, Z)**
R cerebellum (crus II)	-	5.31	141	50, -62, -46
L orbitofrontal gyrus	11	4.62		-16, 10, -16
L parahippocampal gyrus	28	4.10	167	-12, -4, -24
R orbitofrontal gyrus	11	4.62	185	16, 26, -18
Right hypothalamus				
Connected regions	**Brodmann area**	***t* values***	**Cluster extent (no. of voxels)**	**MNI coordinates (X, Y, Z)**
L parahippocampal gyrus	28	4.43	480	-12, -4, -24
L orbitofrontal gyrus	11	3.85		-18, 10, -16
R orbitofrontal gyrus	11	4.13		18, 18, -20
R inferior temporal gyrus	37	4.32	228	60, -50, -22
R lingual gyrus	18	4.27	244	20, -74, 2
R cerebellum (lobule VI)	-	3.79		6, -64, -10
MWoA *vs* MWA				
Left hypothalamus				
Connected regions	**Brodmann area**	***t* values***	**Cluster extent (no. of voxels)**	**MNI coordinates (X, Y, Z)**
R temporal pole	48	3.76	131	66, 4, -2
MWoA *vs* controls				

Left hypothalamus				
Connected regions	**Brodmann area**	***t* values****	**Cluster extent (no. of voxels)**	**MNI coordinates (X, Y, Z)**
R temporal pole	48	4.32	77	64, 6, -4

*Age- and sex-adjusted linear model (p<0.05, clusterwise FWE-corrected for multiple comparisons).
**Age- and sex-adjusted linear model (p<0.001, uncorrected).

Abbreviations: L = left, MWA = migraine with aura, MWoA = migraine without aura, R = right.

Table 5.1.3. Regions showing significant hypothalamic resting state functional connectivity changes in the whole group of migraine patients over time, as well as in subgroups of patients.

Whole migraine patient group				
Increased hypothalamic RS FC at follow-up *vs* baseline				
Left hypothalamus				
Connected regions	**Brodmann area**	***t* values**	**Cluster extent (no. of voxels)**	**MNI coordinates (X, Y, Z)**
L orbitofrontal gyrus	11	5.46*	108	-22, 28, -8
R orbitofrontal gyrus	11	4.56**	35	24, 36, -10
Right hypothalamus				
Connected regions	**Brodmann area**	***t* values****	**Cluster extent (no. of voxels)**	**MNI coordinates (X, Y, Z)**
L orbitofrontal gyrus	11	4.17	33	-22, 28, -12
R orbitofrontal gyrus	11	3.51	23	24, 32, -10
Decreased hypothalamic RS FC at follow-up *vs* baseline				
Right hypothalamus				
Connected regions	**Brodmann area**	***t* values****	**Cluster extent (no. of voxels)**	**MNI coordinates (X, Y, Z)**
R lingual gyrus	17	4.84	15	4, -72, 4
Patients with improved or stable migraine at follow-up§				
Increased hypothalamic RS FC at follow-up *vs* baseline				
Left hypothalamus				
Connected regions	**Brodmann area**	***t* values****	**Cluster extent (no. of voxels)**	**MNI coordinates (X, Y, Z)**
L orbitofrontal gyrus	11	4.75	7	-24, 24, -6
Patients with worsening migraine at follow-up				

Decreased hypothalamic RS FC at follow-up *vs* baseline				
Left hypothalamus				
Connected regions	**Brodmann area**	***t* values***	**Cluster extent (no. of voxels)**	**MNI coordinates (X, Y, Z)**
L orbitofrontal gyrus	11	16.65	77	-12, 16, -24
Right hypothalamus				
Connected regions	**Brodmann area**	***t* values***	**Cluster extent (no. of voxels)**	**MNI coordinates (X, Y, Z)**
L orbitofrontal gyrus	11	12.67	61	-14, 16, -24

*Age- and sex-adjusted linear model (p<0.05, clusterwise FWE-corrected for multiple comparisons).
**Age- and sex-adjusted linear model (p<0.001, uncorrected).
§ The use of preventive therapies was included as an additional covariate

Abbreviations: L=left, R=right.

Figure 5.1.1. Hypothalamic resting state functional connectivity alterations in migraine patients at baseline. Areas of decreased hypothalamic resting state (RS) functional connectivity (FC) in migraine patients compared to controls (two sample t-test, $p<0.05$, clusterwise FWE-corrected for multiple comparisons), color-coded in blue based on their t values. A) RS FC alterations of the left hypothalamus; B) RS FC alterations of the right hypothalamus.
Abbreviations: A = anterior; L = left, OFG = orbitofrontal gyrus; P = posterior; R = right.

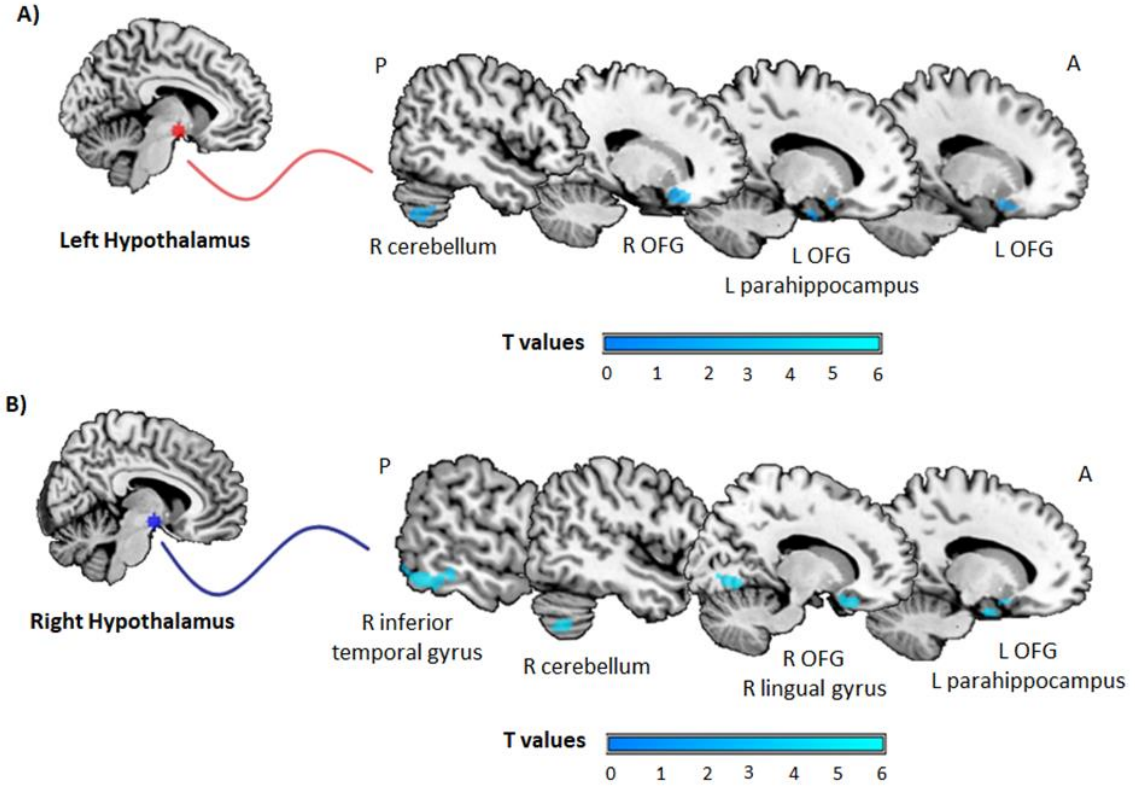

Figure 5.1.2. Longitudinal hypothalamic resting state functional connectivity changes in patients with migraine. Areas of increased hypothalamic RS FC are represented in red and areas of decreased hypothalamic RS FC are shown in blue, color-coded for their t values (paired sample t-test, $p<0.001$, uncorrected for display). A) Left hypothalamic RS FC changes; B) Right hypothalamic RS FC changes. Abbreviations: A = anterior; L = left, OFG = orbitofrontal gyrus; P = posterior; R = right.

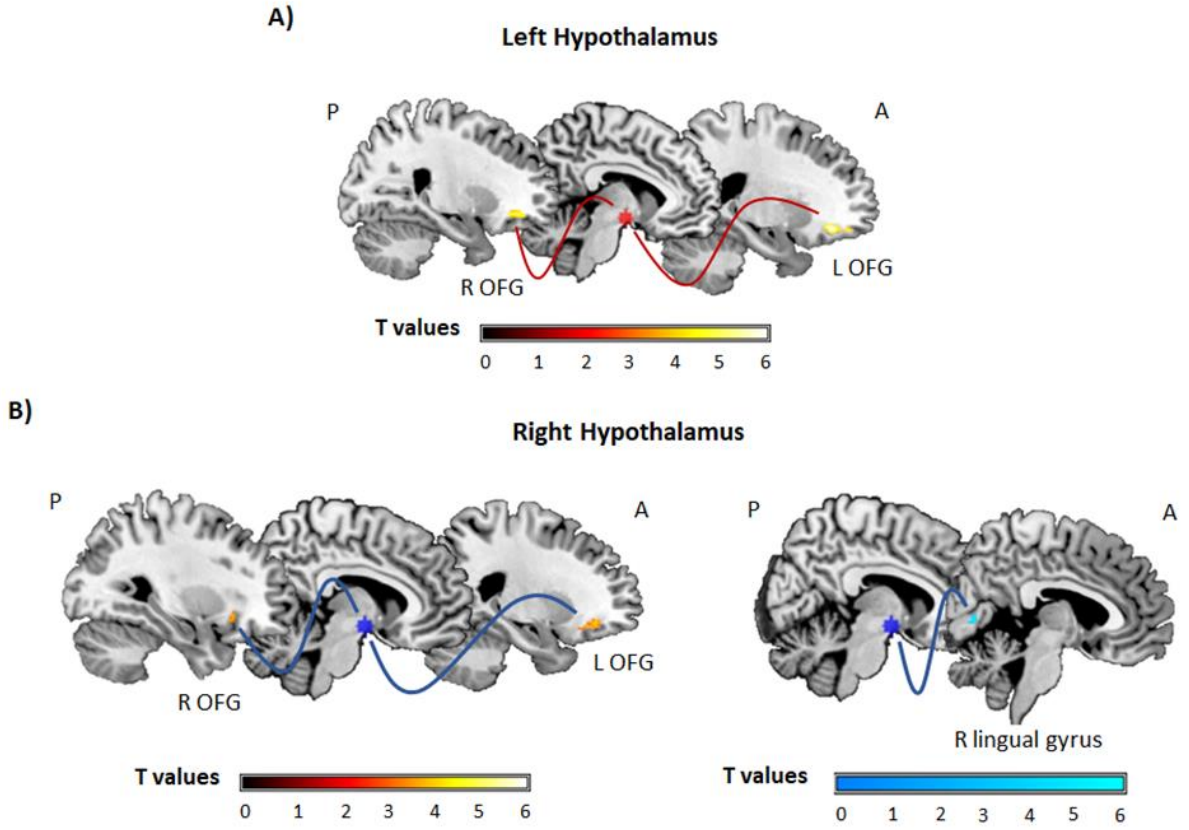

Figure 5.1.3. Longitudinal hypothalamic resting state functional connectivity changes and disease progression in patients with migraine. Longitudinal hypothalamic resting state functional connectivity changes in patients with an improved or stable migraine (A) and patients with worsening migraine (B) (paired sample t-test, $p<0.001$, uncorrected for display). Areas of increased hypothalamic RS FC are represented in red and areas of decreased hypothalamic RS FC are shown in blue, color-coded for their t values.
Abbreviations: A = anterior; L = left, OFG = orbitofrontal gyrus; P = posterior; R = right.

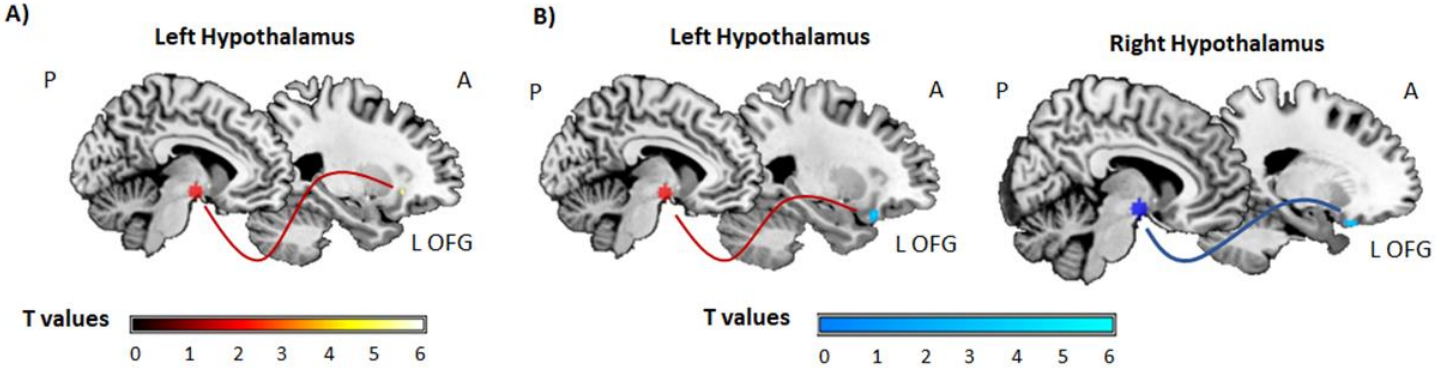

Supplementary materials

Supplementary Table 5.1.1. Main baseline demographic and clinical characteristics of the subgroups of patients and controls that were studied longitudinally and those who were studied only at baseline.

Patients and controls studied longitudinally			
	Controls	**Migraine patients**	***p* values patients *vs* controls**
Women/Men	9/14	15/8	0.1
Age (years)	28 (23-41)	41 (32-45)	0.03*
Attack frequency per month	-	4.5 (1-7.5)	-
Disease duration (years)	-	17 (10-27)	-
Use of preventive medications	-	12	-
Patients and controls studied only at baseline			
	Controls	**Migraine patients**	***p* values patients *vs* controls**
Women/Men	38/12	50/18	0.8
Age (years)	27 (24-41)	33 (26-42)	0.2
Attack frequency per month	-	3.5 (1.5-5)	-
Disease duration (years)	-	15 (9-21)	-
Use of preventive medications	-	13	-

Measures are reported as medians and interquartile ranges (25th–75th percentiles). Sex and the use of preventive medications are reported as frequencies.
*Mann-Whitney test, $p<0.05$.

Supplementary Table 5.1.2. Regions showing positive resting state functional connectivity with the hypothalamus in migraine patients and controls at baseline.

Left hypothalamus									
Migraine patients					**Controls**				
Connected regions	**Brodmann area**	***t* values***	**Cluster extent (no. of voxels)**	**MNI coordinates (X, Y, Z)**	**Connected regions**	**Brodmann area**	***t* values***	**Cluster extent (no. of voxels)**	**MNI coordinates (X, Y, Z)**
L parahippocampal gyrus	27	15.82		-16, -38, -4	R orbitofrontal gyrus	11	46.82	22746	14, 14, -16
L orbitofrontal gyrus	11	14.68	21521	-18, 16, -14	L parahippocampal gyrus	28	17.84		-22, 4, -14
R middle temporal gyrus	21	9.73	979	56, -30, -4	R superior frontal gyrus	9	7.46	84	18, 34, 48
R superior frontal gyrus	9	9.10	327	22, 34, 42	L calcarine cortex	17	6.88	134	2, -82, 4
R middle temporal gyrus	37	6.54	41	52, -54, 6	L cerebellum (crus II)	-	6.84	120	-40, -68, -44
L lingual gyrus	17	6.29	87	-6, -76, 6			6.22	43	-18, -76, -40
R orbitofrontal gyrus	11	5.92	24	18, 62, -12	L middle temporal gyrus	21	6.55	29	-52, -50, 0
R cerebellum (lobule IX)	-	5.92	11	8, -60, -54	L orbitofrontal gyrus	11	6.53	147	-10, 54, -16

L calcarine cortex	17	5.55	5	2, -84, 0	R cerebellum (crus II)	-	5.69	5	48, -62, -46
Right hypothalamus									
Migraine patients					**Controls**				
Connected regions	**Brodmann area**	***t* values***	**Cluster extent (no. of voxels)**	**MNI coordinates (X, Y, Z)**	**Connected regions**	**Brodmann area**	***t* values***	**Cluster extent (no. of voxels)**	**MNI coordinates (X, Y, Z)**
R lingual gyrus	18	19.84	22470	8, -32, -6	L orbitofrontal gyrus	11	16.92	22505	-14, 10, -14
R orbitofrontal gyrus	11	19.32		2, 12, -8	R orbitofrontal gyrus	11	16.05		16, 18, -14
L parahippocampal gyrus	27	15.63		-18, -36, -4	L parahippocampal gyrus	28	15.61		-24, -2, -10
L cerebellum (lobule IX)	-	7.88	55	-6, -60, -50	R lingual gyrus		15.18		24, -28, -6
L lingual gyrus	17	7.54	289	-6, -78, 4	L middle temporal gyrus	21	10.27	1089	-52, -34, -6
R superior frontal gyrus	9	7.11	123	20, 36, 44	R superior frontal gyrus	9	7.13	30	18, 34, 48
L orbitofrontal gyrus	11	7.08	47	-24, 54, -4	R cerebellum (crus II)	-	6.73	57	42, -64, -44
L superior frontal gyrus	9	6.74	161	-18, 36, 46	R cerebellum (lobule VI)	-	3.94**		32, -46, -36
R cerebellum (lobule IX)	-	6.53	34	8, -60, -50	R cerebellum (lobule IX)	-	6.49	14	8, -58, -52
R cerebellum (crus II)	-	4.20**	42	16, -82, -40					
R inferior temporal gyrus	20	3.38**	35	46, 0, -31					

Abbreviations: L = Left; R = Right.

*Age- and sex-adjusted linear model ($p<0.05$, voxelwise FWE-corrected for multiple comparisons).

**Age- and sex-adjusted linear model ($p<0.001$, uncorrected)

Supplementary Table 5.1.3. Regions showing significant decrease of hypothalamic resting state functional connectivity at baseline between migraine patients on and not on preventive treatments considered separately and controls.

Left hypothalamus									
Migraine patients on preventive drugs *vs* controls					**Migraine patients not taking preventive drugs *vs* controls**				
Connected regions	**Brodmann area**	***t* values**	**Cluster extent (no. of voxels)**	**MNI coordinates (X, Y, Z)**	**Connected regions**	**Brodmann area**	***t* values**	**Cluster extent (no. of voxels)**	**MNI coordinates (X, Y, Z)**
L precentral gyrus	6	4.96	217	-38, -2, 62	R cerebellum (crus II)	-	4.78	105	52, -60, -46
R inferior temporal gyrus	37	4.78	276	60, -50, -20	L orbitofrontal gyrus	11	4.26	39	-14, 10, -16
L inferior temporal gyrus	20	4.44	107	-54, -42, -16	L cerebellum (crus II)	-	4.04	48	-50, -62, -50
R cerebellum (crus II)	-	4.40	74	48, -62, -46	R orbitofrontal gyrus	11	3.94	65	16, 26, -18
R orbitofrontal gyrus	11	4.20	82	18, 26, -20	L parahippocampal gyrus	27	3.90	32	-12, -4, -24
L cerebellum (crus I)	-	4.14	72	-44, -46, -36					
R middle frontal gyrus	46	4.01	67	38, 52, 30					
R middle temporal gyrus	38	3.94	52	46, 18, -30					

L orbitofrontal gyrus	11	3.91	130	-22, 18, -20					
L parahippocampal gyrus	27	3.91	11	-14, 0, -28					
Right hypothalamus									
Migraine patients on preventive drugs *vs* controls					**Migraine patients not taking preventive drugs *vs* controls**				
Connected regions	**Brodmann area**	***t* values**	**Cluster extent (no. of voxels)**	**MNI coordinates (X, Y, Z)**	**Connected regions**	**Brodmann area**	***t* values**	**Cluster extent (no. of voxels)**	**MNI coordinates (X, Y, Z)**
R cerebellum (crus I)	-	5.25	498	-40, -44, -36	R lingual gyrus	18	4.55	277	22, -74, 2
R inferior temporal gyrus	20	4.56	335	68, -42, -20	R cerebellum (crus II)	-	4.41	66	50, -62, -46
R middle frontal gyrus	46	4.71	116	38, 52, 28	L parahippocampal gyrus	28	4.03	63	-12, -4, -24
R orbitofrontal gyrus	11	4.71	433	20, 26, -24	L calcarine cortex	17	3.95	52	-4, -96, 2
R middle temporal gyrus	21	4.61	91	54, -36, -4	R inferior temporal gyrus	37	3.93	45	60, -52, -20
L precentral gyrus	6	4.42	182	-42, -4, 56	R cerebellum (lobule V)	-	3.82	13	10, -48, -4
L orbitofrontal gyrus	11	3.57	135	-22, 16, -18	R lingual gyrus	18	3.68	65	-8, -80, -4
R cerebellum (crus II)	-	4.38	49	48, -60, -46	L orbitofrontal gyrus	11	3.45	40	-16, 8, -16
L middle temporal gyrus	20	4.17	88	-50, -36, -14	R orbitofrontal gyrus	11	3.38	9	16, 18, -20
L parahippocampal gyrus	27	4.09	40	-14, -2, -28					

L superior occipital gyrus	18	3.77	56	-20, -86, 8					
R cerebellum (lobule VIII)	-	3.68	13	26, -42, -50					

Abbreviations: L = left; R = right.

*Age- and sex-adjusted linear model ($p<0.001$, uncorrected).

Supplementary Table 5.1.4. Regions showing significant decrease of hypothalamic resting state functional connectivity at baseline between the subgroups of migraine patients and controls that were studied at the two study time points, as well as among different subgroups of migraine patients.

Migraine patients *vs* controls				
Left hypothalamus				
Connected regions	**Brodmann area**	***t* values****	**Cluster extent (no. of voxels)**	**MNI coordinates (X, Y, Z)**
L orbitofrontal gyrus	11	4.35	24	-16, 10, -16
L parahippocampal gyrus	28	3.06	20	-14, -4, -26
R cerebellum (crus II)	-	2.72	5	56, -58, -46
R orbitofrontal gyrus	11	2.67	10	20, 16, -20
Right hypothalamus				
Connected regions	**Brodmann area**	***t* values*****	**Cluster extent (no. of voxels)**	**MNI coordinates (X, Y, Z)**
R inferior temporal gyrus	37	3.69	78	66, -52, -20
R lingual gyrus	18	3.60	25	24, -40, 6
L parahippocampal gyrus	28	3.20	128	-8, 2, -24
L orbitofrontal gyrus	11	2.52	11	-16, 10, -14
R orbitofrontal gyrus	11	2.15	46	20, 16, -20
R cerebellum (lobule VI)	-	2.02	7	6, -66, -12
MWoA *vs* MWA				
Left hypothalamus				
Connected regions	**Brodmann area**	***t* values**	**Cluster extent (no. of voxels)**	**MNI coordinates (X, Y, Z)**
L putamen	-	5.24*	160	-30, 0, -4
R temporal pole	38	2.57***	3	64, 10, -4

MWoA *vs* controls				
Left hypothalamus				
Connected regions	**Brodmann area**	***t* values*** **	**Cluster extent (no. of voxels)**	**MNI coordinates (X, Y, Z)**
R temporal pole	38	2.27	23	62, 6, -4

Abbreviations: L = left; MWA = migraine with aura; MWoA = migraine without aura; R = right.

*Age- and sex-adjusted linear model ($p<0.05$, clusterwise FWE-corrected for multiple comparisons).
**Age- and sex-adjusted linear model ($p<0.01$, uncorrected).
***Age- and sex-adjusted linear model ($p<0.05$, uncorrected).

Supplementary Table 5.1.5. Regions showing significant longitudinal hypothalamic resting state functional connectivity changes in the subgroup of patients who were not taking preventive treatments at baseline and follow-up.

Increased hypothalamic RS FC at follow-up *vs* baseline				
Left hypothalamus				
Connected regions	**Brodmann area**	***t* values***	**Cluster extent (no. of voxels)**	**MNI coordinates (X, Y, Z)**
L orbitofrontal gyrus	11	4.53	101	-2, 28, -30
R orbitofrontal gyrus	11	2.51		12, 30, -22
Right hypothalamus				
Connected regions	**Brodmann area**	***t* values***	**Cluster extent (no. of voxels)**	**MNI coordinates (X, Y, Z)**
L orbitofrontal gyrus	11	3.79	60	-2, 28, -30
R orbitofrontal gyrus	11	2.76	18	20, 20, -24
Decreased hypothalamic RS FC at follow-up *vs* baseline				
Right hypothalamus				
Connected regions	**Brodmann area**	***t* values***	**Cluster extent (no. of voxels)**	**MNI coordinates (X, Y, Z)**
R lingual gyrus	17	3.16	12	16, -38, -2

*Age- and sex-adjusted linear model ($p<0.05$, uncorrected).

Abbreviations: L=left, R=right.

6. IDENTIFICATION OF BIOMARKERS OF MIGRAINE AND CLUSTER HEADACHE

6.1. BIOMARKERS OF MIGRAINE AND CLUSTER HEADACHE: DIFFERENCES AND SIMILARITIES

Abstract

Background. Although migraine and cluster headache have different clinical phenotypes, they share some pathophysiological mechanisms. Both migraine and cluster headache patients showed functional and structural abnormalities in multisensory processing brain areas. This study aimed to identify MRI biomarkers that differentiate migraine from cluster headache patients and disclose imaging features shared by patients.

Methods. Clinical, functional and structural MRI data were obtained from 20 migraine patients, 20 cluster headache patients and 15 controls. An independent component analysis was performed to transform MRI data into a set of features. Support vector machine algorithms and a stepwise removal process were used to obtain the best accuracy rates of MRI models for discrimination between patients and controls, and between subgroups of patients. The accuracy of models combining clinical and MRI data was also assessed. Voxel-wise *t tests* were performed to investigate brain regional between-group differences within the most discriminative MRI features. The association between imaging features and patients' clinical characteristics was assessed using correlation analysis.

Results. The accuracy for classifying the entire group of headache patients from controls was 80%. The classification accuracy for discrimination between migraine and controls was 89%, and for cluster headache patients and controls it was 98%. The MRI classifier yielded an accuracy of 78% in distinguishing cluster headache from migraine patients. Adding patients' clinical features to the MRI measures improved the classification accuracy to 99%. Distinct patterns of brain activation and morphometry contributed to the classification models. Bilateral hypothalamic and PAG functional networks were the most important MRI features in classifying migraine and cluster headache patients from controls. The activity of the PAG networks was significantly

associated to patients' clinical features. The left thalamic network was the most discriminative MRI feature in classifying migraine from cluster headache patients. Compared to migraine, cluster headache patients showed a decreased functional interaction between the left thalamus and cortical areas mediating interoception and sensory integration. The presence of restlessness was the most important clinical feature in discriminating the two groups of patients.

Conclusion. Although clinical history remains the mainstay for migraine and cluster headache diagnosis, our results highlight the value of machine learning techniques and multimodal MRI data in understanding migraine and cluster headache pathophysiology. Functional biomarkers, including the hypothalamic and PAG networks, are shared by migraine and cluster headache patients. The thalamo-cortical pathway might be the neural substrates that differentiate migraine from cluster headache attacks with their distinct clinical features.

Introduction

Primary headache disorders, like migraine and cluster headache, are one of the most common and debilitating neurological diseases worldwide (208). Diagnosis of migraine and cluster headache is mainly based on taking a good clinical history. Migraine attacks are characterized by unilateral or bilateral, throbbing pain that might last from 4 to 72 hours, and might be associated with nausea, vomiting, increased sensitivity to sounds, light and movements (40). Core features of cluster headache attacks are the excruciating unilateral pain, lasting from 15 to 180 minutes, cranial autonomic symptoms, like conjunctival injection and lacrimation, and a sense of restlessness and agitation (2). Cluster headache attacks often recurs in bouts of daily headache attacks, which may last from 7 days to 1 year. Between one bout and another one patients are pain-free, this period is called "out of bout" phase (258).

Although the clinical phenotype of these two primary headaches can be different, they share some pathophysiological mechanisms. Both migraine and cluster headache are now commonly recognized as brain disorders that involve the activation of different cortical, diencephalic and brainstem regions and the subsequent release of key neuropeptides, such as the CGRP. Recent works suggest that the brainstem and hypothalamus might be putative drivers of migraine and cluster headache attacks (259). A series of advanced MRI techniques have been applied to the study of migraine and cluster headache patients, both in the course of an acute attack and during the interictal phase, revealing widespread structural and functional abnormalities in brain areas involved in multisensory processing, including pain (99). Only a few MRI studies (248, 260, 261) have directly compared migraine and cluster headache patients, showing bilateral enlargement of the hypothalamus, reduced GM volume of frontal and occipital areas and increased functional activity of brain cognitive networks in patients with cluster headache compared to patients with migraine.

In the last years, machine learning techniques have obtained promising results in the medical field, providing biomarkers for diagnosis, disease classification, prognosis, personalized treatments and shedding lights on disease pathophysiology. One of the main advantages of using machine learning approaches is that they allow inference at the single-subject level, and they are sensitive to subtle and spatially distributed differences in the brain that might be undetectable at group level comparisons (173, 262). Supervised

and unsupervised algorithms of machine learning have been applied to clinical and MRI data to identify distinct phenotypes of migraine, predict disease progression and discriminate migraine patients from controls, as well as from other chronic pain disorders (170-173, 263). A recent study provided some insights into predictors of treatment response in cluster headache patients using a supervised machine learning model combining clinical and volumetric imaging data (264). Which could be the potential of machine learning techniques in discriminating migraine from cluster headache patients has not been investigated so far.

In this study, we applied a supervised machine learning approach and multimodal MRI modalities to identify MRI biomarkers that accurately differentiate migraine from cluster headache patients and disclose imaging features shared by these two types of primary headaches. Our working hypothesis is that patients with migraine and cluster headache might share some structural and functional abnormalities in cortical and subcortical regions involved in the onset of both types of headache attacks and in pain processing. However, different MRI alterations might explain those clinical features that differ between these conditions. A secondary analysis identified the best clinical predictors of migraine and cluster headache diagnosis and investigated whether a more accurate classification of patients could be achieved combining MRI and clinical data.

Materials and methods

Subjects. Between April 2017 and March 2018, we prospectively enrolled 60 migraine patients, 45 cluster headache patients and 30 controls. Patients were recruited consecutively from the migraine and cluster headache population attending the headache clinics at King's College Hospital. The recruitment of patients and controls was also extended through King's College London staff and students advertising. Inclusion criteria for patients were as follows: *(a)* diagnosis of an episodic form of headache; *(b)* no headache at the time of the MRI; *(c)* not using pharmacological preventive treatments for migraine or cluster headache or drugs affecting the central nervous system for at least one month before the MRI. Exclusion criteria for headache patients and controls were any other chronic pain syndrome, neurological, psychiatric, or other major systemic conditions, use of painkillers for more than 8 days a month, use of illicit drugs and MRI showing any brain pathology. Only controls who had infrequent tension type headaches

were included in the study. Forty migraine patients, 25 patients with cluster headache and 15 controls were excluded due to chronic headache, the presence of headache the day of the MRI exam, MRI artefacts, concurrent psychiatric conditions, use of illicit drugs, use of antidepressants or because they were on preventive treatments for headaches.

Clinical assessment. Before the MRI exam, the clinical history, neurological examination, weight, height, sitting blood pressure and pulse rate of all participants were obtained. All patients met the criteria of the International Classification of Headache Disorders for the diagnosis of episodic migraine and episodic cluster headache (2). Both patients and controls were asked to fill in a headache diary in order to control whether they had any kind of headaches the days preceding and following the MRI visit. The average headache pain intensity was assessed using the NRS (180).

Ethical approval. The Local Ethical Committee on human studies approved the study and all subjects provided written informed consent prior to study participation, according to the Declaration of Helsinki.

MRI acquisition. A detailed description of the imaging protocol is provided in the Supplementary material. Using a General Electric Discovery MR750 3.0 Tesla scanner (General Electric, Chicago, IL), the following sequences of the brain were acquired from all subjects in a single session: *(a)* FLAIR sequence, *(b)* 3D T1-weighted inversion recovery prepared gradient echo sequence, *(c)* pulsed-gradient spin-echo, echo-planar sequence, with diffusion gradients applied in 60 non-collinear directions, *(d)* RS fMRI using a T2*-weighted multi-echo echoplanar imaging, and *(e)* 3D pCASL sequence. To reduce the inter-subjects variability of the fMRI measurements, participants were asked to abstain from taking nonsteroidal anti-inflammatory drugs or paracetamol (265, 266), having alcohol or caffeine-containing products and using tobacco- or nicotine-containing products (267) the day before the MRI.

MRI data analysis. FLAIR scans were analysed for the presence of WMHs. The volume of FLAIR hyperintensities was measured using a local thresholding segmentation technique (Jim 8, Xinapse Systems Ltd., Colchester, United Kingdom, UK). All images

were preprocessed and analysed in order to obtain brain volumetric, WM FA, WM MD, CBF and RS FC maps of each subject (**Fig. 6.1.1A**), as described in detail in the Supplementary material. The RS fMRI analysis was focused on subcortical brain areas playing a pivotal role in migraine and cluster headache pathophysiology, including the hypothalamus, dorsal pons, STN, thalamus and PAG (99). A dual regression analysis (268) was used to study voxel-wise FC within different regions of interested (ROI). Based on previous studies, we used a 6-mm sphere around the peak MNI coordinates of the hypothalamus (X=±6, Y=-6, Z=-10 from (100) and (108)), a 3-mm sphere around the peak MNI coordinates of the dorsal pons (X=±6, Y=-36, Z=-27 from (100)), STN (X=±3, Y=-36, Z=-45 from (112)) and PAG (X=±6, Y=-30, Z=-9 from (269) and (104)). A thalamic ROI was also defined using the Harvard-Oxford probabilistic anatomical atlas within FSL (thresholded at >20%).

Brain volumetric, WM FA, WM MD, CBF and RS FC maps of each subject were temporal concatenated using FSL (https://fsl.fmrib.ox.ac.uk/fsl) and analyzed using MELODIC group temporal concatenation ICA (270) (**Fig. 6.1.1B and Fig. 6.1.1C**). The ICA outputs are spatial component maps, showing patterns of covariant MRI metric changes across subjects, associated to subject courses, which indicate the degree to which each subject contributes to the MRI measure variance. Each IC spatial map was transformed to thresholded voxel-wise Z-statistics map in order to infer voxels that were significantly modulated by each subjects' contribute (271). This approach allowed us to transform the original MRI data into a set of features which could be included in the following classification analysis. Five independent components (IC) were obtained for each MRI modality (272, 273). Only those components showing patterns of temporally coherent signal confined to the brain parenchyma were used as features to classify the different groups of study participants (**Fig. 6.1.1C**).

Classification analysis. A linear kernel support vector machine (SVM) model, implemented in the LIBSVM library (274) running under MATLAB, was used to assess the most accurate classification of patients and controls. The relative importance of each feature in classifying patients and controls, as well as subgroups of patients was ranked based on the weight vector provided by the classification model. After each round of SVM training, the least informative metric was removed and a new SVM trained with the

remaining metrics. This process was repeated until only one single feature remained. The accuracy of the classifier was recorded at each stepwise removal. The classifier with the highest accuracy was considered the best performing (275). Sensitivity and specificity were estimated based on true positives, true negatives, false positives, and false negatives provided by the classification model. Features whose weight vector lied >1 SD above that of the next highest metric were considered having the highest importance in the classification (275). In addition, a 10-fold cross-validation model was performed to assess generalizability. Briefly, the original dataset was partitioned into k equally sized samples. Data from k-1 folds were used to train the model and data from the k^{th} fold were used as a test set for assessing the performance of the model. The process was then iterated until each fold has been used as test (276).

First, to investigate which MRI metrics produce the best discrimination of patients and controls and subgroups of patients, we performed a classification analysis including the MRI features obtained from the ICA, which encoded the patterns of brain activation (RS FC and CBF maps) and morphometry (brain volumetric, WM FA and MD maps) (**Fig. 6.1.1D**). Estimation of the classification accuracy was adjusted for age and gender effects. Secondly, to test the accuracy of clinical features currently used in the diagnosis of migraine and cluster headache, we run a secondary classification analysis including those clinical characteristics the are specific for migraine (photophobia, phonophobia, nausea/vomiting, movement sensitivity, severity and laterality of pain) and cluster headache (cranial autonomic symptoms, a sense of restlessness, severity and laterality of pain) (2). Age, gender, disease duration and headache attack frequency were also included in the clinical classification analysis. At last, to investigate whether combined MRI and clinical data would be more accurate in classifying migraine and cluster headache patients, we performed a classification analysis including the MRI and clinical features of the best classification models.

Statistical analysis. The p-plots, Kolmogorov-Smirnov and Shapiro-Wilk tests were used to assess whether continuous data were normally distributed. Since the distribution of the data was not normal, demographic and clinical characteristics were compared between groups using the Mann-Whitney test for continuous variables and the Chi-squared or Fisher exact test for categorical variables (SPSS software, version 22.0).

Five thousand random permutations were calculated to create the null distribution for assessing the test statistics of the dual regression analyses (268) during the RS fMRI pre-processing. For the ICA, results were thresholded at a p>0.5 level under an alternative hypothesis test based on a Gaussian/Gamma mixture model fitted to the intensity histogram of the component (277, 278).

To establish whether the observed classification accuracy was statistically significant, a repeated random subsampling validation, with a random selection of *n* subjects removed from both the patient and control group, repeated 1000 times for each *n* from 1 to 10, was performed. The association between MRI features with the highest contribution in the classification model and patients' clinical characteristics was assessed using partial correlation analysis (SPSS software, version 22.0).

Voxel-wise *t tests* were performed to investigate regional between-group differences (patients *vs* controls, migraine *vs* cluster headache) within the most discriminative MRI features, using SPM12 (**Fig. 6.1.1E**). The correlations between such regional differences and patients' clinical features were assessed using multiple linear regression models as implemented in SPM12. Age and sex were included as covariates in all regional analyses.

Data availability. Data supporting the findings of this study are available from the corresponding author, upon reasonable request.

Results

Demographic, clinical and conventional MRI data. Twenty migraine patients (10 without aura and 10 with aura: 7 visual, 3 visual and sensory), 20 cluster headache patients and 15 controls were included in the final analysis. A patient with migraine reported a migraine attack the day before the MRI, while all other patients were headache-free for at least two days before the exam. Most of the patients with migraine also denied having headaches the days following the MRI (data not available for 5 patients). All cluster headache patients were scanned when they were out of bout and none of them had any headache attacks for at least 48 hours before the MRI. Beyond cluster headache attacks, three patients had also migraine without aura attacks (patient 1: two attacks in six years; patients 2: four attacks per year; patient 3: four attacks per month), two patients used to

suffer from migraine without aura during their adolescence and other four patients had also a diagnosis of probable migraine. Eight controls suffered from infrequent tension type headache. None of the controls reported any headaches before the MRI.

The main demographic and clinical characteristics of controls, migraine and cluster headache patients are summarized in **Table 6.1.1**. Headache patients were older than controls (headache patients: median age 34 years, interquartile range 27-45; controls: median age 24 years, interquartile range 23-28; $p<0.001$). Compared to controls ($p<0.001$) and migraine patients ($p<0.001$), cluster headache patients were the oldest, while age did not differ between migraine patients and controls ($p=0.07$). Gender did not differ between the entire group of headache patients and controls ($p=0.6$). As expected considering the gender prevalence of the two diseases, migraine patients were predominantly females, while most of the cluster headache patients were males ($p<0.001$). The median number of headache attacks per month in migraine patients was 3.7 (interquartile range: 1.5-5.6). Cluster headache patients had a median of 0.8 bouts per year (interquartile range: 0.5-1), lasting a median of 45 days (interquartile range: 30-71), and 2.5 attacks per day (interquartile range: 1.1-3.4). Photophobia, phonophobia, movement sensitivity and nausea/vomiting were more prevalent in migraine patients, while a sense of restlessness and unilateral pain were more frequent in cluster headache patients. Compared to migraine patients, patients with cluster headache experienced more severe headache attacks (**Table 6.1.1**).

Two migraine patients, four patients with cluster headache and two controls had small, aspecific, punctate WMHs (migraine patients: mean lesion volume=0.054 ml, SD 0.23; cluster headache patients: mean lesion volume=0.122 ml, SD 0.39; controls: mean lesion volume=0.027 ml, SD 0.08). The volume of WMHs did not differ between headache patients and controls (headache patients *vs* controls: $p=0.9$, migraine patients *vs* controls: $p=0.8$, cluster headache patients *vs* controls: $p=0.6$, migraine patients *vs* cluster headache: $p=0.4$).

Feature selection. Different structural (**Supplementary Fig. 6.1.1**) and functional (**Supplementary Fig. 6.1.2** and **Supplementary Fig. 6.1.3**) MRI patterns including the brainstem, cerebellum, thalamus, basal ganglia, frontal, parietal, temporal and occipital areas, were selected from the ICA and included as features in the MRI classification

analyses. Clinical and demographic features included in the clinical classification analysis were: age, sex, disease duration, headache attack frequency, presence of photophobia, phonophobia, nausea/vomiting, movement sensitivity, cranial autonomic symptoms and restlessness, severity and laterality of pain.

Classification analysis.

Headache patients and controls. The MRI model yielding the highest classification accuracy in discriminating controls from the entire group of headache patients (overall accuracy 80%, p=0.006) included the volume IC1, IC3 and IC4, WM FA IC1, WM MD IC3, CBF IC5, right and left hypothalamic RS FC IC3 and IC5, left hypothalamic RS FC IC4, RS FC IC4 of the right and left PAG, RS FC IC1 and IC4 of the right and left pons, right pontine RS FC IC 5, RS FC IC1 of the left STN, and RS FC IC3 and IC5 of the left thalamus (**Fig. 6.1.2A** and **Table 6.1.2**).

Although there were no MRI features whose weight vector exceeded one standard deviation of the next highest metric, the right hypothalamic RS FC IC3, left hypothalamic RS FC IC5 and left RS FC IC4 of the PAG had the highest feature importance in the prediction. In the RS FC IC3, the right hypothalamus had an increase FC with the insula, precuneus, supplementary motor area, calcarine cortex, superior temporal, middle occipital, fusiform, lingual and parietal gyrus (**Fig. 6.1.2B**). While, the left hypothalamus showed a decrease functional coupling with the insula, precuneus, supplementary motor area, calcarine cortex, superior temporal, middle occipital, fusiform, lingual and parietal gyrus in the RS FC IC5 (**Fig. 6.1.2B**). In the RS FC IC4, the left PAG had a decrease RS FC with the pons, medial and superior frontal gyrus, as well as an increase RS FC with the precuneus, calcarine cortex, fusiform, lingual, middle temporal and orbitofrontal gyrus (**Fig. 6.1.2B**).

We found a positive correlation between the RS FC IC4 of the left PAG and the presence of movement sensitivity (r=0.4, p=0.009), phonophobia (r=0.3, p=0.05) and nausea/vomiting (r=0.3, p=0.03). While the RS FC IC4 of the left PAG was negatively correlated with the presence of cranial autonomic symptoms (r=-0.3, p=0.04) and pain severity (r=-0.3, p=0.04).

Migraine patients and controls. The best MRI classifier in discriminating migraine patients and controls (overall accuracy 89%, p=0.008) included the WM FA IC1, left hypothalamic RS FC IC4, RS FC IC1 of the right PAG, RS FC IC4 of the right and left PAG, right and left pontine RS FC IC1 and RS FC IC5 of the left pons (**Fig. 6.1.3A** and **Table 6.1.2**).

The RS FC IC4 of the right PAG had the highest feature importance in the classification, with the value of its weight vector lying >1 SD above that of the next highest metric. In this RS network, the right PAG had an increase RS FC with the insula, anterior cingulate cortex, medial and superior frontal gyrus, and a decrease RS FC with the cerebellum, inferior occipital and orbitofrontal gyrus (**Fig. 6.1.3C**).

In migraine patients, a positive correlation was observed between the RS FC IC4 of the right PAG and the presence of cranial autonomic symptoms (r=0.5, p=0.02).

Cluster headache patients and controls. The combination of MRI features that showed the best performance in distinguishing cluster headache patients from controls (overall accuracy 98%, p<0.001) included the volume IC1 and IC5, WM FA IC2, WM MD IC2, CBF IC2 and IC5, RS FC IC1 of the right PAG, RS FC IC2 of the right and left PAG, RS FC IC4 of the right PAG, RS FC IC2 of the right pons, RS FC IC3 of the left pons, right and left pontine RS FC IC5, RS FC IC3 of the right STN, right thalamic RS FC IC2 and left thalamic RS FC IC5 (**Fig. 6.1.3B** and **Table 6.1.2**).

The right RS FC IC4 of the PAG was the MRI feature with the highest importance in the prediction. No significant correlations were found between the RS FC IC4 of the right PAG and cluster headache patients' clinical characteristics.

Migraine and cluster headache patients. The MRI model yielding the highest classification accuracy (overall accuracy 78%, p=0.01) in discriminating cluster headache from migraine patients included the CBF IC4, RS FC IC3 of the right PAG, RS FC IC2 and IC4 of the left PAG, left pontine RS FC IC1, right thalamic RS FC IC2, left thalamic RS FC IC4 and IC5 (**Fig. 6.1.4A** and **Table 6.1.2**).

The left thalamic RS FC IC4 had the highest feature importance in the classification with the value of its weight vector lying >1 SD above that of the next highest metric. In this network, the left thalamus showed a decrease RS FC with the precuneus,

angular, middle temporal and medial frontal gyrus, and an increase RS FC with the cerebellum, cingulum, calcarine cortex, lingual, middle occipital and frontal gyrus (**Fig. 6.1.4B**). We did not find any significant association between the left thalamic RS FC IC4 and patients' clinical features.

The best classification accuracy for correctly classifying individual patients as having migraine or cluster headache based on all demographic and clinical features was 99% (p<0.001) (**Fig. 6.1.4C** and **Table 6.1.2**). Although there were no clinical features whose weight vector exceeded one standard deviation of the next highest metric, the presence of restlessness and the severity of pain had the highest feature importance in the prediction.

The best MRI-clinical combined classification model achieved an accuracy of 99% (p<0.001) (**Fig. 6.1.4D** and **Table 6.1.2**). The presence of restlessness was the feature with the highest importance in the prediction.

Voxel-vise analyses.

Headache patients and controls. There were no significant brain regional differences between headache patients and controls in the left hypothalamic RS FC IC5, right hypothalamic RS FC IC3 and the RS FC IC4 of the left PAG.

Migraine patients and controls. Within the RS FC IC4 of the right PAG, an increased RS FC between the right PAG and ipsilateral cerebellum was found in migraine patients compared to controls (**Fig. 6.1.3C** and **Table 6.1.3**). No significant correlations were found between such functional alterations and migraine patients' clinical characteristics.

Cluster headache patients and controls. The brain areas included in the RS FC IC4 of the right PAG did not show any significant differences between cluster headache patients and controls.

Migraine and cluster headache patients. Within the left thalamic RS FC IC4, compared to patients with migraine, cluster headache patients showed decreased RS FC between the left thalamus and left precuneus, angular and middle temporal gyrus (**Fig. 6.1.4B,**

Table 6.1.3 and **Supplementary Table 6.1.1**). We did not find any significant association between the left thalamic RS FC alterations and patients' clinical features.

Discussion

In this study, using a supervised machine learning approach and multimodal imaging data we identified the most discriminative MRI patterns that distinguish migraine from cluster headache patients, as well as imaging features shared by these two primary headache disorders.

Our results showed a robust and accurate classification of patients with primary headaches and controls. A classification accuracy of 80% was achieved for classifying the entire group of headache patients from controls. When we trained the model to discriminate migraine and cluster headache patients from controls separately, an overall accuracy of 89% and 98%, respectively, was obtained. The first interesting result of our study is that the combination of different patterns of brain activation and morphometry yielded the best classification performance in distinguishing migraine and cluster headache patients from controls.

Previously, a lower accuracy rate ranging from 67 to 86% was obtained by classifiers based only upon brain cortical morphometric or functional measures, for distinguishing migraine patients from controls (169, 171, 256). Our findings are in line with a previous study that demonstrated the advantage of combining GM volume and RS fMRI data over the single imaging feature in the discrimination between patients with migraine and controls (83% *vs* 71% of accuracy) (263). Previous MRI studies using standard univariate analysis have shown widespread structural and functional abnormalities in brain areas involved in multisensory processing, including pain, in both migraine and cluster headache patients (99). However, only a few studies have explored the presence of concurrent morphometric and functional brain changes in headache patients (279-281). The integration of multiple functional and structural imaging metrics discloses complementary information regarding the underlying biological processes. Our results support the value of combining multimodal MRI data providing insights into the function, macro- and micro- structure of the brain. This approach might help us to achieve a better understanding of headache pathophysiology.

It is interesting to note that the model discriminating cluster headache patients from controls achieved a classification accuracy of 98% with a specificity of 100%. These results suggest that being sure a control does not harbor cluster headache biology is not as challenging as for migraine (13).

The most discriminative MRI patterns in classifying migraine and cluster headache patients from controls included brain RS FC networks of the PAG and hypothalamus. The prominent role of the hypothalamus in migraine and cluster headache pathophysiology is well established. There is ample evidence supporting a key role of the hypothalamus in the acute phase of the migraine and cluster headache attacks (100, 107, 282, 283). Recent fMRI studies during trigeminal nociceptive stimulation, highlighted dynamic functional changes of hypothalamic activity during the migraine and cluster headache cycle supporting its pivotal involvement in driving the onset of the headache attacks (102, 284). Similar to previous interictal studies (156, 248, 285-288), here we showed a significant functional interaction between the hypothalamus and brain areas implicated in pain control and visual processing in both migraine and cluster headache patients studied outside their headache attacks.

The PAG is a key area of the endogenous pain inhibitory system. It is highly connected to brain regions involved in pain modulation, like the trigeminal cervical complex, nucleus cuneiforms, rostral ventral medulla, hypothalamus, thalamus, cerebellum, frontal and parietal areas (289). There is evidence revealing an altered functional interaction between nociceptive brain areas and the PAG that might contribute to the development of allodynia in migraine patients (151, 269). It has also been showed that PAG stimulation could provoke the onset of headache pain (290). Here, we have found a specific involvement of the networks connecting the left and right PAG to the cerebellum, insula, frontal, temporal and occipital areas in the whole group of headache patients, as well as in migraine and cluster headache patients separately. It is worth noting that although the left and right PAG were connected with similar brain areas, they showed an opposite direction of their functional coupling. The significant association we have found in headache patients between the left RS FC network of the PAG and pain severity reinforce its crucial role in modulating pain perception. Interestingly, in our sample of patients the global functional activity of the PAG networks was also significantly associated to the presence of cranial autonomic symptoms and migraine-specific

symptomatology, like movement sensitivity, phonophobia and nausea/vomiting. These findings are in line with a previous PET study (104) suggesting a possible contribution of the PAG to the presence of nausea in migraine patients and preclinical studies showing an involvement of the PAG in the control of sensory, autonomic and motor processes (291). PAG activity can be modulated by various neuropeptides and neurotransmitters involved in migraine and cluster headache pathophysiology, such as serotonin, orexin, and CGRP, suggesting the PAG as a possible site of actions of acute and preventive headache treatments, like triptans and anti-CGRP monoclonal antibodies (291-293). Our findings highlighted the PAG as one of the mediators of symptoms accompanying the migraine and cluster headache pain, supporting its potential as a therapeutic target.

The MRI model discriminating cluster headache and migraine patients achieved the lowest accuracy rate (78%). Interestingly, beyond cluster headache attacks, nine patients had also a history of definite or probable migraine without aura. These data are in line with previous findings demonstrating a higher prevalence of migraine and family history of migraine in cluster headache patients (294). The coexistence of the two types of headaches on 45% of cluster headache patients might explain the lower accuracy rate we obtained and support common genetic predisposition and pathophysiological mechanisms between migraine and cluster headache.

Adding patients' clinical features to the MRI measures improved the classification accuracy of the model distinguishing migraine from cluster headache patients a lot, reaching an overall accuracy of 99%. Clinical characteristics of patients provided the highest accuracy in identifying individuals as having migraine or cluster headache. Thus, reinforcing the importance of clinical criteria for the differential diagnosis of these two forms of primary headaches. Interestingly, both clinical and MRI-clinical combined models revealed that the most important feature in discriminating migraine and cluster headache patients was the presence of restlessness. Behavioral disturbances, such as restlessness and agitation, are cluster headache-specific symptoms often described by patients (258). In our sample, all patients with cluster headache reported the experience of restlessness during their attacks.

The identification of the most discriminative MRI features revealed a central role of the thalamus in classifying migraine from cluster headache patients. We found a lower functional interaction between the left thalamus and parietal brain regions, including the

precuneus and angular gyrus, in cluster headache compared to migraine patients. The thalamus is a key area for the processing and integration of nociceptive stimuli. Thalamocortical projections to limbic, visual, somatosensory, auditory, motor and olfactory regions can explain part of the complexity of headache features (295). The precuneus and angular gyrus are components of the default mode network, a brain network known to be involved in cognition, self-monitoring, sensory integration and interoception (226). Based on our results, we could speculate that an abnormal processing of the inner-generated sensory stimuli may lead to the sense of agitation and the compulsion to move described by patients with cluster headache. This hypothesis is in line with previous evidence showing an association between abnormal thalamo-cortical activity and the presence of agitation in patients with restless leg syndrome or psychiatric disorders (296, 297).

Our study is not without limitations. Its main limit is the small sample size. Moreover, future studies should include cluster headache patients who do not have also a migraine biology. Further studies to classify migraine and cluster headache patients in the ictal and interictal phase are also warranted.

Although a detailed clinical history remains the mainstay for migraine and cluster headache diagnosis, our data highlight the value of machine learning techniques and multimodal MRI data in understanding the neurobiological basis of migraine and cluster headache. MRI classifiers including functional and structural MRI measures of distinct brain networks accurately classified individuals as having migraine or cluster headache, supporting the view of these primary headaches as complex brain disorders. We identified brain functional biomarkers, including the hypothalamic and PAG networks, shared by migraine and cluster headache that could mediate the pain and associated symptoms experienced by patients. We also proposed the thalamo-cortical pathway as the neural substrates that could differentiate migraine from cluster headache attacks with their distinct clinical features. As newer acute and preventive therapies are licensed, the application of machine learning techniques and multimodal MRI data may cast further lights on primary headaches physiopathology, reveal new therapeutic targets and guide the development of new drugs tailored to each form of primary headache.

Table 6.1.1. Demographic and clinical characteristics of controls and patients.

	Controls	**Migraine**	**Cluster Headache**	***p* values Migraine *vs* Controls**	***p* values Cluster Headache *vs* Controls**	***p* values Migraine *vs* Cluster Headache**
Women/Men	8/7	18/2	4/16	0.02	0.07	<0.001
Age (years)	24 (23-28)	29 (24-31)	41 (26-56)	0.1	<0.001	<0.001
Disease duration (years)	-	14 (8-17)	16 (10-25)	-	-	0.2
Headache attack frequency per year	-	45 (18-68)	68 (32-127)	-	-	0.06
Presence of movement sensitivity	-	20	3	-	-	<0.001
Presence of photophobia	-	19	9	-	-	0.001
Presence of phonophobia	-	17	6	-	-	0.001
Presence of nausea/vomiting	-	19	12	-	-	0.02
Presence of cranial autonomic symptoms	-	17	20	-	-	0.2
Presence of restlessness	-	3	20	-	-	<0.001

Presence of unilateral pain	-	9	20	-	-	<0.001
NRS score	-	7.2 (6.6-8.4)	10 (8.6-10)	-	-	<0.001

Measures are reported as medians and interquartile ranges (25th–75th percentiles). Gender and patients' clinical features are reported as frequencies. Abbreviation: NRS = Numerical rating scale.

Table 6.1.2. Classification performance of the most discriminative models differentiating headache patients from controls, as well as migraine from cluster headache patients.

Headache *vs* controls			**Migraine *vs* controls**			**Cluster headache *vs* controls**		
MRI Classifier performance			**MRI Classifier performance**			**MRI Classifier performance**		
Accuracy (%)	**Sensitivity (%)**	**Specificity (%)**	**Accuracy (%)**	**Sensitivity (%)**	**Specificity (%)**	**Accuracy (%)**	**Sensitivity (%)**	**Specificity (%)**
80	87	66	89	95	80	98	80	100
	Headache	*Controls*		*Migraine*	*Controls*		*Cluster headache*	*Controls*
Headache	35	5	*Migraine*	19	1	*Cluster headache*	16	4
Controls	5	10	*Controls*	3	12	*Controls*	0	15
Migraine vs cluster headache								
MRI classifier performance			**Clinical classifier performance**			**MRI-clinical combined classifier performance**		
Accuracy (%)	**Sensitivity (%)**	**Specificity (%)**	**Accuracy (%)**	**Sensitivity (%)**	**Specificity (%)**	**Accuracy (%)**	**Sensitivity (%)**	**Specificity (%)**
78	65	70	99	95	100	99	95	100
	Migraine	Cluster headache		*Migraine*	*Cluster headache*		*Migraine*	*Cluster headache*
Migraine	13	7	*Migraine*	19	1	*Migraine*	19	1

Cluster headache	6	14	*Cluster headache*	0	20	*Cluster headache*	0	20

Table 6.1.3. Regional resting state functional connectivity differences between migraine patients and controls, as well as between cluster headache and migraine patients.

Migraine vs controls				
Cerebral regions showing increased RS FC with the right PAG in migraine patients	**Brodmann area**	***t* values***	**Cluster extent (no. of voxels)**	**MNI coordinates (X, Y, Z)**
Right cerebellum (crus I)	-	6.04	655	-9, -85, -19
Migraine vs cluster headache				
Cerebral regions showing decreased RS FC with the left thalamus in cluster headache patients	**Brodmann area**	***t* values***	**Cluster extent (no. of voxels)**	**MNI coordinates (X, Y, Z)**
Left angular gyrus	39	4.90	662	-46, -72, 32
Left middle temple gyrus	39	4.24		-48, -63, 20
Left precuneus	7	4.08	457	-10, -55, 44

* $p<0.05$, clusterwise FWE-corrected for multiple comparisons

Fig. 6.1.1. Overview of MRI data analysis. A) Images were preprocessed and analysed to obtain brain volumetric, white matter (WM) fractional anisotropy (FA), white matter (WM) mean diffusivity (MD), cerebral blood flow (CBF) and resting state (RS) functional connectivity (FC) maps of each subject. B) Brain volumetric, WM FA, WM MD, CBF and RS FC maps of each subject were temporal concatenated. C) An independent component analysis was performed to obtain spatial component maps, showing patterns of covariant MRI metric changes across subjects. Five independent components were obtained for each MRI modality and included in the following classification analysis as MRI features. D) A support vector machine (SVM) model was used to identify the best performing classifier and most informative MRI features in discrimination of patients and controls, as well as subgroups of patients. The accuracy, sensitivity and specificity of the model were estimated, and the relative importance of each feature in classifying patients and controls was ranked based on the weight vector provided by the classification model. After each round of SVM training, the least informative metric was removed and a new SVM trained with the remaining metrics. The accuracy of the classifier was recorded at each stepwise of removal. E) Voxel-wise *t tests* were performed to investigate regional between-group differences within the most discriminative MRI features.
Abbreviations: A=anterior, DTI= diffusion tensor imaging, fMRI=functional magnetic resonance imaging, P=posterior, R=right, RS=resting state.

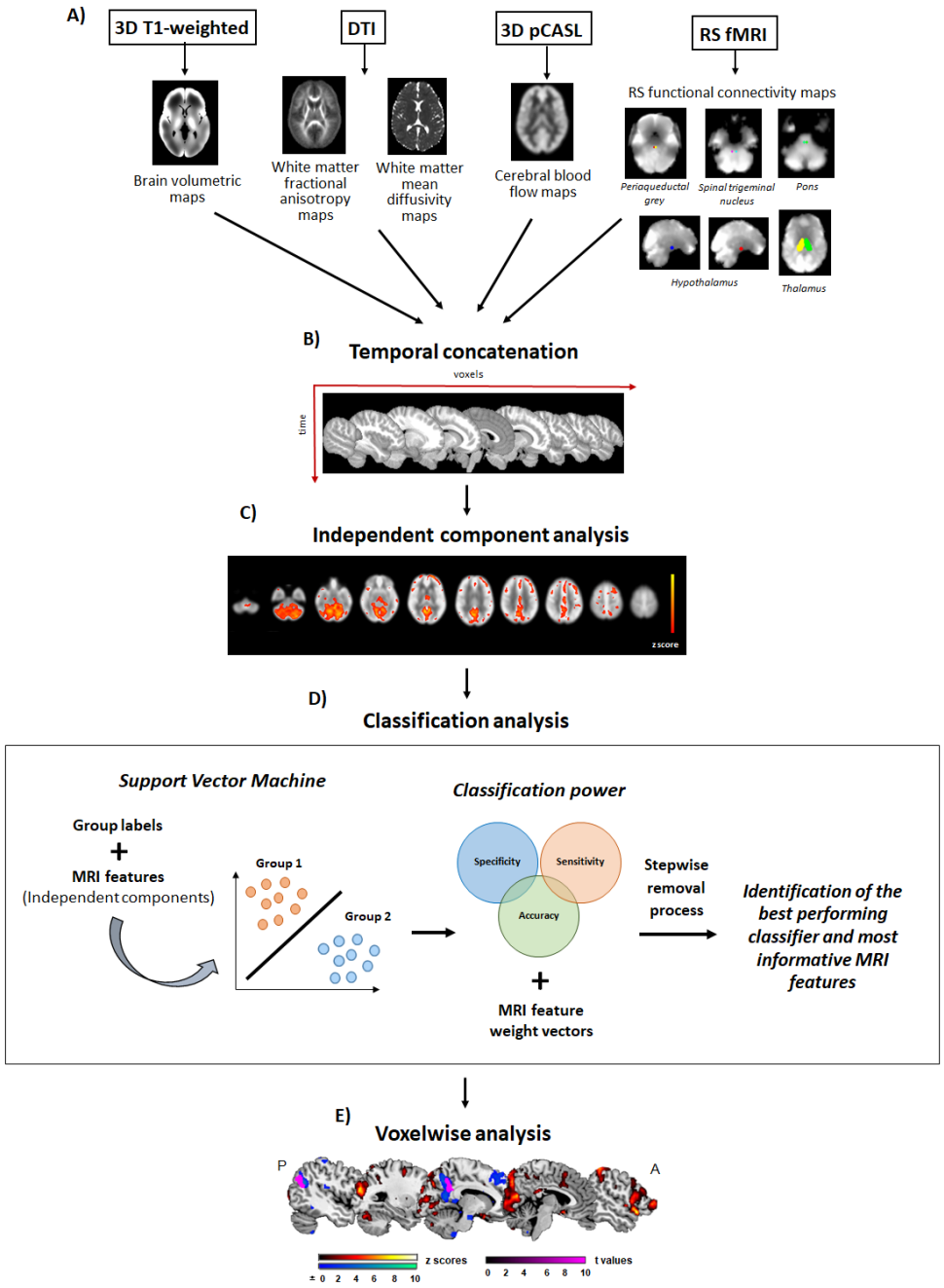
A)
3D T1-weighted
DTI
3D pCASL
RS fMRI
Brain volumetric maps
White matter fractional anisotropy maps
White matter mean diffusivity maps
Cerebral blood flow maps
RS functional connectivity maps
Periaqueductal grey
Spinal trigeminal nucleus
Pons
Hypothalamus
Thalamus
B)
Temporal concatenation
voxels
time
C)
Independent component analysis
z score
D)
Classification analysis
Support Vector Machine
Group labels
+
MRI features
(Independent components)
Group 1
Group 2
Classification power
Specificity
Sensitivity
Accuracy
+
MRI feature weight vectors
Stepwise removal process
Identification of the best performing classifier and most informative MRI features
E)
Voxelwise analysis
P
A
z scores
± 0 2 4 6 8 10
t values
0 2 4 6 8 10

Fig. 6.1.2. Classification model discriminating headache patients from controls. A) The bar graph represents normalized weights of MRI features included in the model yielding the highest classification accuracy in discriminating controls from the entire group of headache patients. B) Spatial maps of the MRI features with the highest importance in the prediction. Maps were thresholded at a p>0.5 level under an alternative hypothesis. High z-scores are represented in red-yellow and low z scores are represents in blue.
Abbreviations: A=anterior, CBF= cerebral blood flow, IC=independent component, FA=fractional anisotropy, FC=functional connectivity, L=left, MD=mean diffusivity, PAG= periaqueductal gray, P=posterior, R=right, RS=resting state, STN=spinal trigeminal nucleus, WM=white matter.

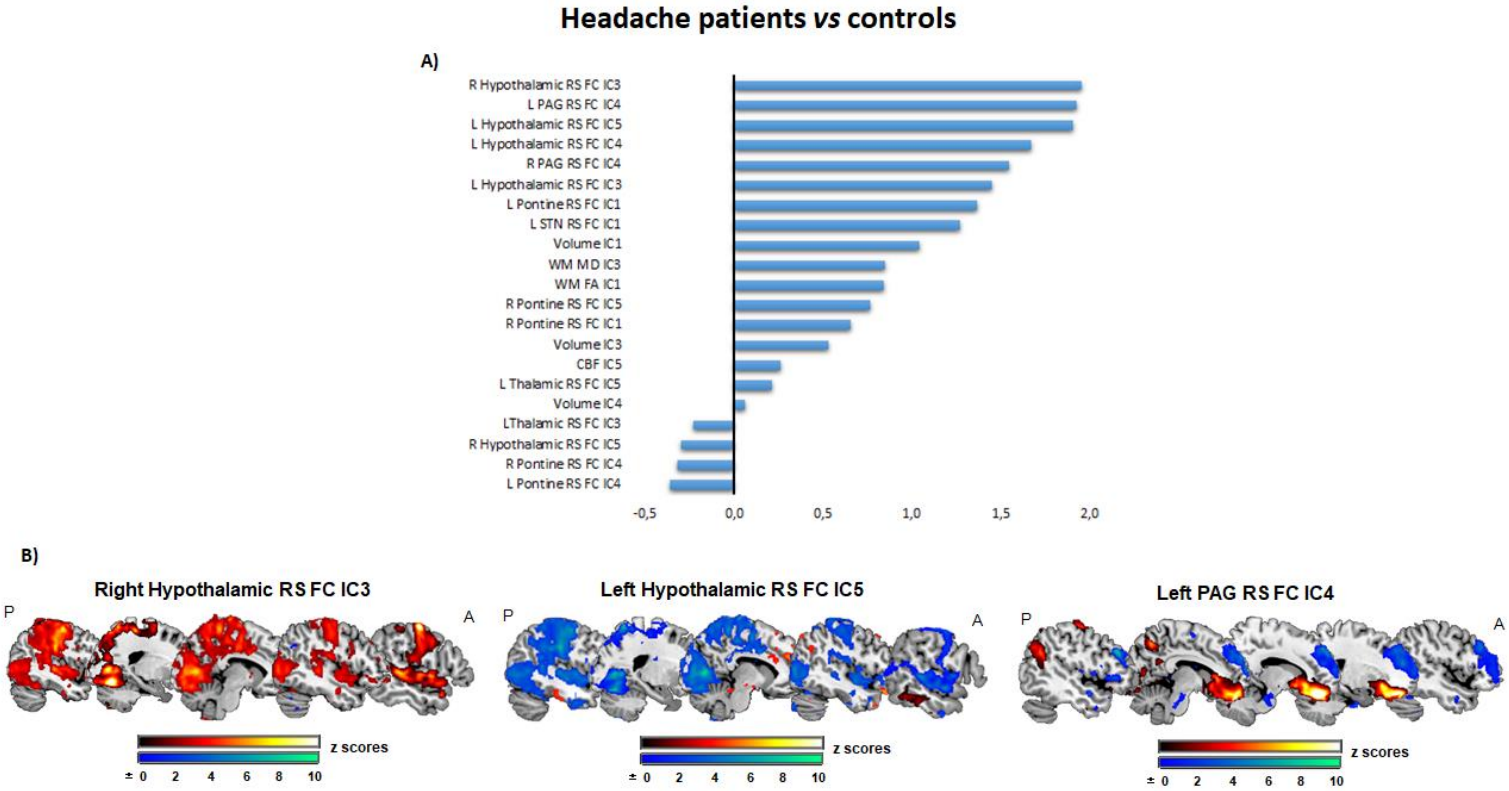

Fig. 6.1.3. Classification model discriminating migraine patients and cluster headache patients from controls. A) The bar graph represents normalized weights of MRI features included in the model yielding the highest classification accuracy in discriminating migraine patients from controls. B) The bar graph represents normalized weights of MRI features included in the model yielding the highest classification accuracy in discriminating cluster headache patients from controls. C) Spatial map of the RS FC IC4 of the right PAG thresholded at a p>0.5 level under an alternative hypothesis. High z-scores are represented in red-yellow and low z scores are represents in blue. Brain regions showing increased RS FC with the right PAG in migraine patients compared to controls are shown in green (colour-coded for their t values) (p<0.05, clusterlwise FWE-corrected for multiple comparisons). Abbreviations: A=anterior, CBF= cerebral blood flow, IC=independent component, FA=fractional anisotropy, FC=functional connectivity, L=left, MD=mean diffusivity, PAG= periaqueductal gray, P=posterior, R=right, RS=resting state, STN=spinal trigeminal nucleus, WM=white matter.

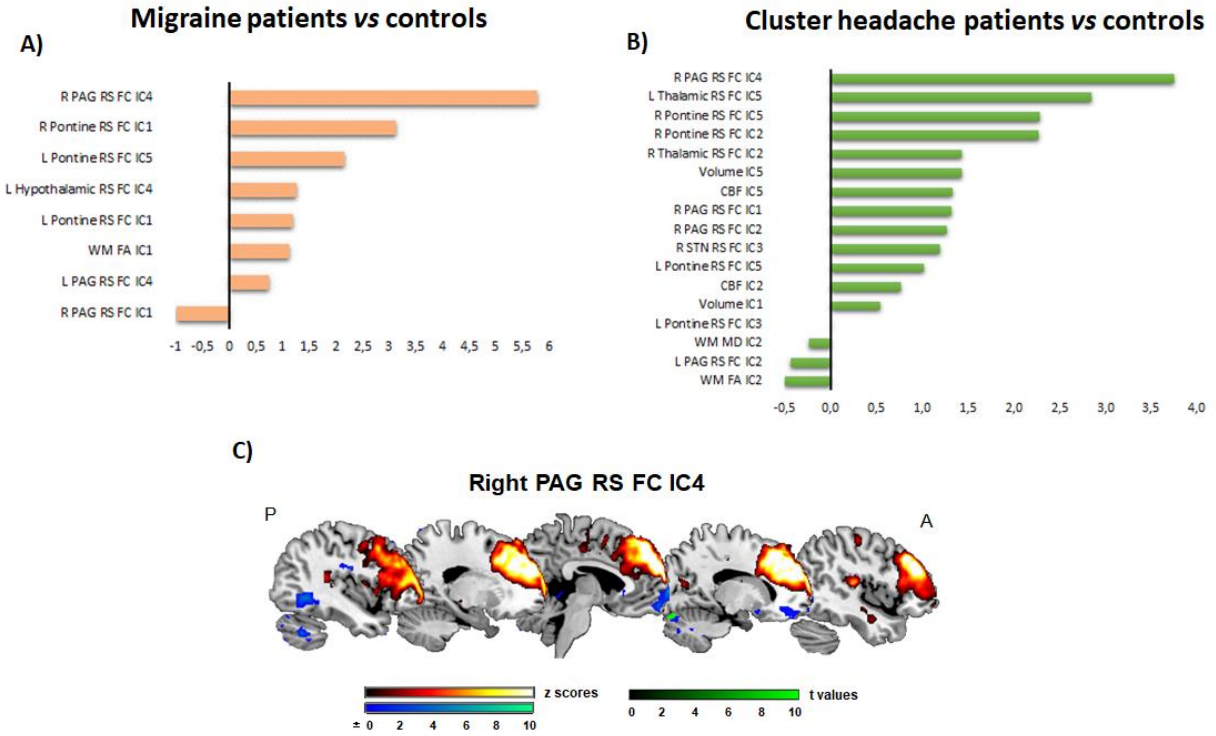

Fig. 6.1.4. Classification models discriminating migraine from cluster headache patients. A) The bar graph represents normalized weights of MRI features included in the model yielding the highest classification accuracy in discriminating migraine from cluster headache patients. B) Spatial map of the RS FC IC4 of the left thalamus thresholded at a p>0.5 level under an alternative hypothesis. High z-scores are represented in red-yellow and low z scores are represents in blue. Brain regions showing decreased RS FC with the left thalamus in cluster headache patients compared to migraine patients are shown in violet (colour-coded for their t values) (p<0.05, clusterlwise FWE-corrected for multiple comparisons). C) The bar graph represents normalized weights of clinical and demographic features included in the clinical model yielding the highest classification accuracy in discriminating migraine from cluster headache patients. D) The bar graph represents normalized weights of clinical, demographic and MRI features included in the MRI-clinical combined model yielding the highest classification accuracy in discriminating migraine from cluster headache patients. Abbreviations: A=anterior, CBF= cerebral blood flow, IC=independent component, FA=fractional anisotropy, FC=functional connectivity, L=left, MD=mean diffusivity, PAG= periaqueductal gray, P=posterior, R=right, RS=resting state, STN=spinal trigeminal nucleus, WM=white matter.

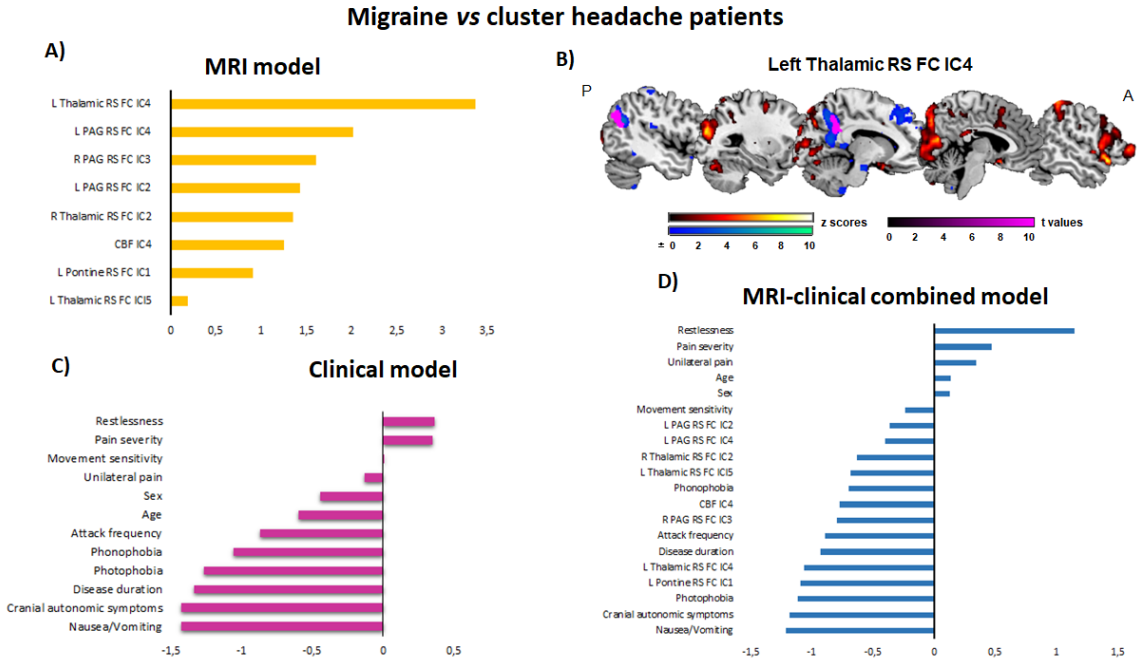

Supplementary material

Materials and methods

MRI acquisition. Using a General Electric Discovery MR750 3.0 Tesla scanner (General Electric, Chicago, IL), the following sequences of the brain were acquired from all subjects in a single session:

- Axial FLAIR sequence (TR/TE=8000/125 ms, inversion time [IT]=2000 ms; FlA=111º, matrix size=256×128, FOV=240×240 mm^2, 4 mm-thick, 36 contiguous axial slices);
- 3D T1-weighted inversion recovery prepared gradient echo sequence (TR/TE=7.3/3.0 ms; IT=400 ms; FlA=11°; matrix size=256×256×196; FOV=270×270 mm^2; 1.2 mm-thick, 196 contiguous sagittal slices);
- Pulsed-gradient spin-echo, echo-planar sequence (TE/TR=74/11250 ms; FlA=90°; matrix size=128x128; FOV=256x256 mm^2; 2 mm-thick, 72 contiguous axial slices), consisting of two different scans of 30 diffusion-weighted directions (b-value 1500 mm^2/s) combined together for a total of 60 directions and six non-diffusion weighted volumes.
- RS fMRI using a T2*-weighted multi-echo echoplanar imaging (TR/TE=2500/44 ms; FlA=80°; matrix size=64×64; FOV=240×240 mm^2; 3mm-thick, 32 contiguous axial slices);
- 3D-pCASL sequence (TE/TR=11/5180 ms, FOV=240×240 mm^2, 56 slice-partitions of 3mm thickness). Labelling of arterial blood was achieved with a 1525ms train of Hanning shaped radio frequency pulses in the presence of a net magnetic field gradient along the flow direction (the z-axis of the magnet). After a post-labelling delay of 2025ms, a whole brain volume was read using a 3D inter-leaved “stack-of-spirals” Fast Spin Echo readout consisting of 8 interleaved spiral arms in the in-plane direction, with 512 points per spiral interleave. The spiral sampling of k-space was re-gridded to a rectangular matrix with an approximate in-plane resolution of 3.6mm. The sequence used 4 control-label pairs. CBF maps were computed from the mean perfusion weighted difference image derived from the four control-label pairs, by scaling the difference image against a proton density image acquired at the end of the sequence, using identical readout parameters. This computation was done according to the formula suggested in the ASL

consensus article (298). The sequence uses four background suppression pulses to minimize static tissue signal at the time of image acquisition (299).

MRI data analysis.

Morphometric analysis. FLAIR scans were analysed for the presence of WMHs. The volume of FLAIR hyperintensities was measured using a local thresholding segmentation technique (Jim 8, Xinapse Systems Ltd., Colchester, United Kingdom, UK).

Three-dimensional T1-weighted images were processed using the Geodesic Information Flows (300) for an initial tissue segmentation. After extraction of the possible WMHs (301), T1 images were inpainted at the location of hyperintensity (302). The tissue segmentation was then reprocessed on the corrected image generating 3D maps of GM and WM. The corrected T1 images were then non-linearly registered to the MNI Template 1.5 mm using NiftyReg (303) and the obtained jacobian volumetric maps of deformation further masked and used for ICA.

Diffusion tensor imaging analysis. For each subject, DTI data were visually inspected to exclude those having corrupted images on more than two diffusion-weighted imaging volumes. DTI data were pre-processed using the ExploreDTI (304) software package, including the robust estimation of tensors by outlier rejection algorithm (305), and corrected for eddy current, motion artefacts and EPI geometric distortion. FA and MD maps were then calculated from the diffusion-tensor.

Arterial spin labeling analysis. The ASL image was acquired twice to increase statistical power. This approach was preferred against the option of doubling the number of control-label pairs, because it reduces motion induced artefacts. During the acquisition, participants were instructed to lie still with their eyes open. ASL data were preprocessed using the following steps: 1) the two ASL scans were co-registered and realigned to the T1 space; 2) 3D T1-weighted and PD images were realigned; 3) the extra cerebral signal was removed from the CBF map masking the brain segmentation obtained from the T1 segmentation processing; 4) skull-stripped CBF maps were spatially normalized to the MNI standard space $1.5mm^3$. For each subject, a mean CBF map was obtained from the two pre-processed CBF maps. Finally, CBF maps were spatially smoothed using a 8-mm Gaussian smoothing kernel using NiftySeg (299).

RS fMRI analysis. During the acquisition, participants were instructed to lie still with their eyes open. The RS fMRI dataset was pre-processed using AFNI (306). Pre-

processing steps included volume re-alignment, time-series de-spiking and slice time correction. After the pre-processing, functional data were optimally combined by taking a weighted summation of the three echoes using an exponential T2* weighting approach (307). The optimally combined data were then de-noised with the Multi-Echo ICA approach implemented by the tool meica.py (Version v2.5 beta9) (308, 309), given its proven effectiveness in removing physiological and motion-related noise and increasing temporal signal-to-noise ratio (310-312). Then, data were spatially smoothed with an 8-mm FWHM Gaussian kernel; WM and cerebrospinal fluid signals were regressed out using the maps from the T1 segmentation processing step and a high-pass temporal filter with a cut-off frequency of 0.005 Hz was applied. Each participant's dataset was registered to standard MNI152 space using the combination of known transformation from fMRI to T1 and from T1 to MNI152 space using NiftyReg.

Supplementary tables

Supplementary table 6.1.1. Regional thalamic resting state functional connectivity differences between patients with cluster headache and controls within the left thalamic RS FC IC4.

Cluster headache patients vs controls				
Cerebral regions showing decreased RS FC with the left thalamus in cluster headache patients	**Brodmann area**	***t* values****	**Cluster extent (no. of voxels)**	**MNI coordinates (X, Y, Z)**
Left precuneus	7	2.97	91	-10, -45, 26
Left angular gyrus	39	2.60	3	-46, -66, 27

** Age- and sex-adjusted linear model ($p<0.01$, uncorrected).

Supplementary figures

Supplementary Figure 6.1.1. Independent components of brain morphometric measures. Independent component spatial maps showing the cross-subject co-variance of brain volume (A), white matter fractional anisotropy (B) and white matter mean diffusivity (C). Maps are thresholded at a p>0.5 level under an alternative hypothesis. High z-scores are represented in red-yellow and low z scores are represents in blue. Abbreviations: IC=independent component.

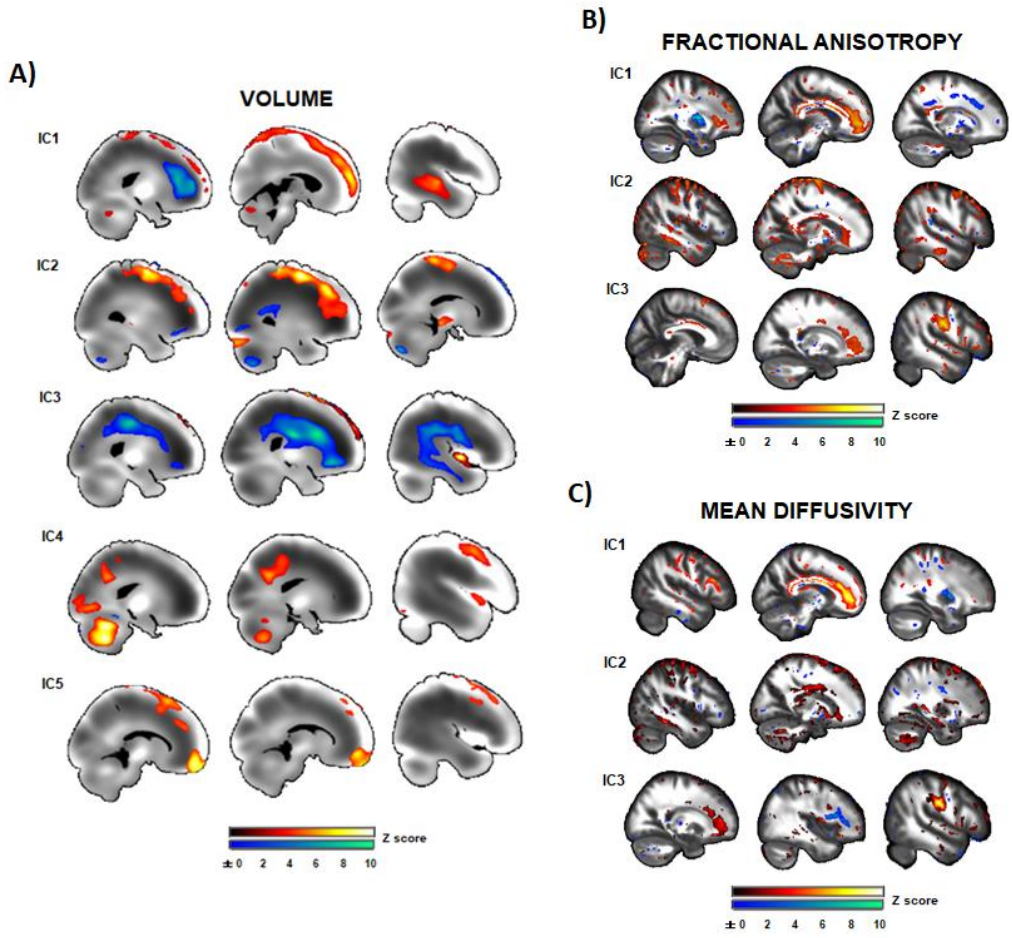

Supplementary Figure 6.1.2. Cerebral blood flow independent components. Independent component spatial maps showing the cross-subject co-variance of cerebral blood flow. Maps are thresholded at a p>0.5 level under an alternative hypothesis. High z-scores are represented in red-yellow and low z scores are represents in blue. Abbreviations: IC=independent component.

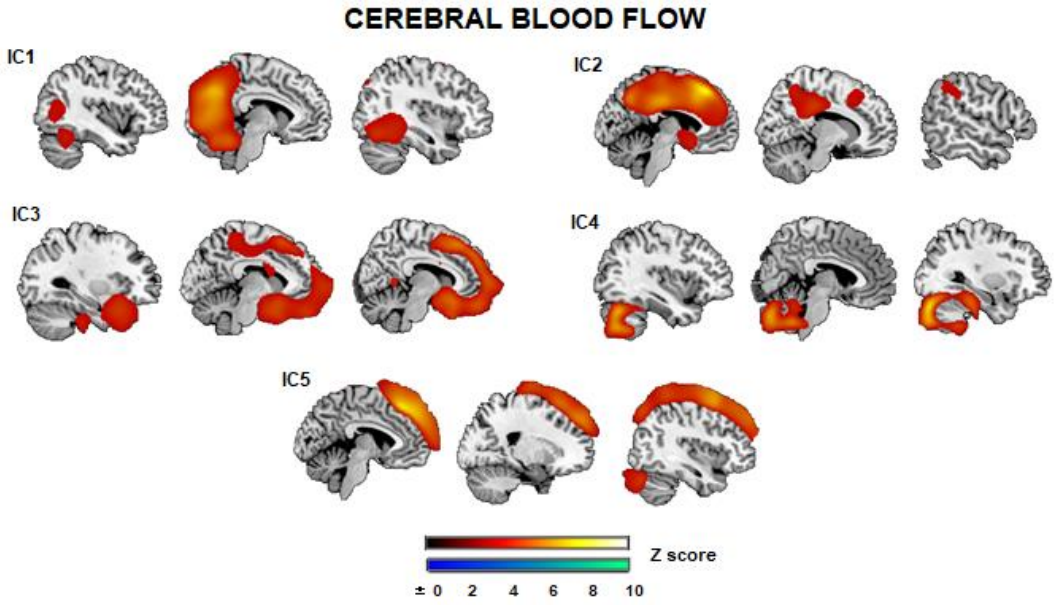

Supplementary Figure 6.1.3. Resting state functional connectivity independent components. Independent component spatial maps showing the cross-subject co-variance of resting state functional connectivity of the left and right hypothalamus (A), PAG (B), pons (C), spinal trigeminal nucleus (D) and thalamus (E). Abbreviations: IC=independent component, L=left, PAG= periaqueductal gray, R=right.

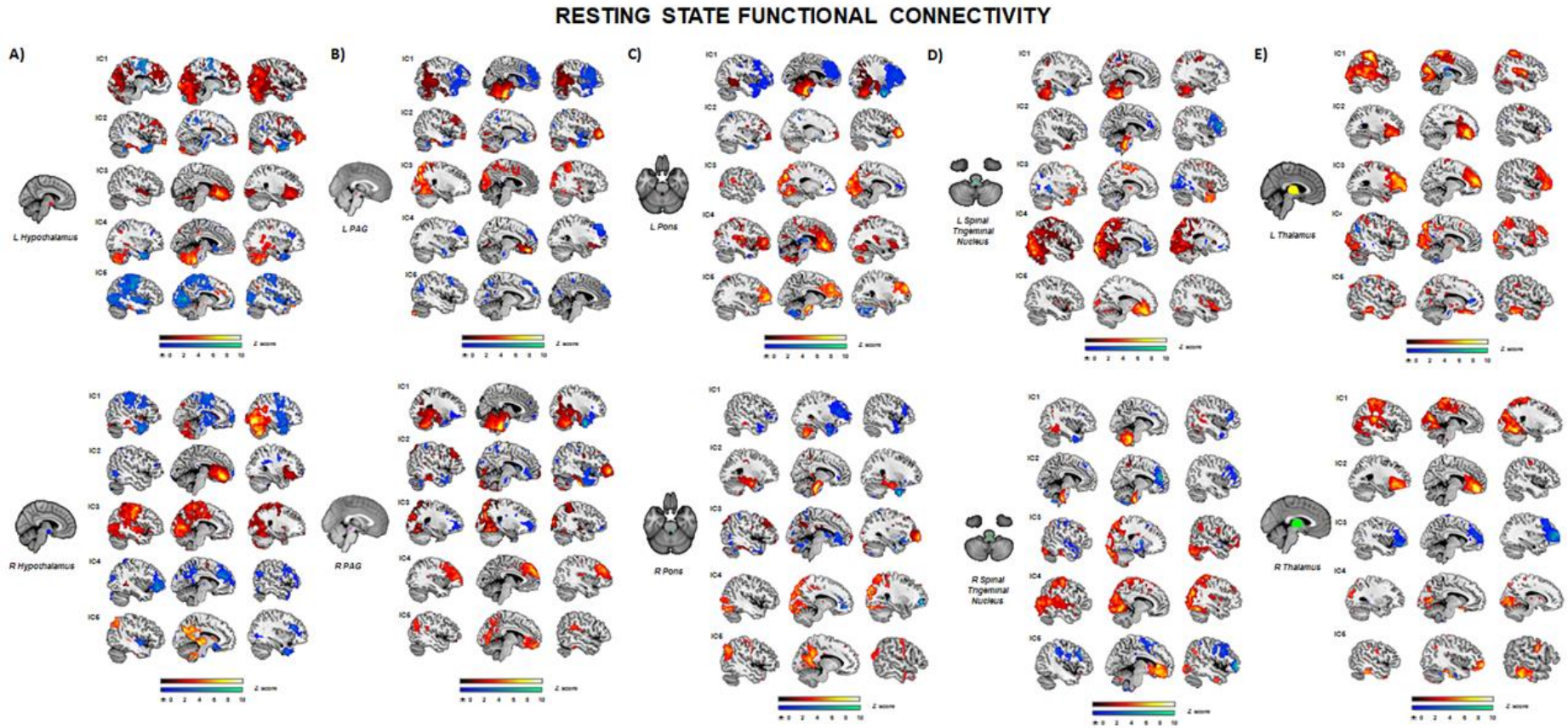

7. DISCUSSION

In recent years, we have seen great progress in migraine research as a result of the advancement of brain imaging techniques. Although the pathogenesis of migraine is not yet entirely understood, it is increasingly accepted that migraine is a complex neurological disease involving the interplay of the trigeminovascular system, signalling molecules, and cortical and subcortical brain areas (4). Imaging studies and human provocation models have shed light on brain areas mediating the wide spectrum of symptoms characterizing the acute phases of the migraine attack (13). There is ample evidence demonstrating alterations in WM tracts, cortical and subcortical areas that contribute to atypical pain, sensory and cognitive processing in interictal migraine patients (99).

By performing an fMRI study including an angle and a colour discrimination task, during my PhD, I have explored cerebral mechanisms underlying visuospatial processing in migraine patients (**Chapter 3**). In line with previous evidence (69, 70), approximately 20% of migraine patients enrolled in the study showed selective deficits in visuospatial cognition. During the performance of a visuospatial task, migraine patients experienced higher activation of frontal and limbic areas and deactivation of the posterior cingulate cortex, an area of the DMN. These functional alterations may represent compensatory mechanisms that could help migraine patients to overcome impaired visuospatial skills and to maintain an adequate level of performance during a visuospatial task. Interestingly, the same brain regions activated by patients during the visuospatial task are usually involved in nociception, suggesting that the adaptive mechanisms observed in the study may be strengthen by the recurrent involvement of these regions in the attentional modulation of migraine pain. These findings do not only offer a new insight into the mechanisms underlying cognitive processing in migraine patients but may pave the way to novel treatments. The identification of a common brain network for visuospatial and pain processing could open the way to psychological approaches that could help patients to cope with the pain.

A crucial question that remains unresolved is whether interictal functional and structural brain alterations represent a brain trait that predisposes to the development of migraine or a brain state secondary to the recurrence of migraine attacks (159). This PhD project aimed to shed light on this issue studying migraine patients at an early stage of

the disease (**Chapter 4**). Using RS fMRI, I explored the intra- and inter-network functional activity of large-scale brain networks in pediatric migraine patients and investigated the correlation between functional alterations and patients' clinical characteristics. Similar to adult migraine patients, pediatric patients experienced RS FC alterations of brain networks involved in pain, visual, auditory, sensorimotor and cognitive processing. Interestingly, patients showed also an altered functional interaction between sensory and attentive brain networks, reflecting an abnormal attentional control of pain and multisensory stimuli. Taken together these findings reinforce the concept of migraine as a network-based disorder of sensory processing and highlight the presence of an early state of heightened alertness and sensitivity to sensory stimuli and a dysfunctional cognitive control of pain. The early dysregulation of the main sensory and cognitive brain networks along with the lack of a significant association between RS FC abnormalities and patients' clinical characteristics suggest that these functional patterns could be a phenotypic biomarker of migraine.

The idea that the complex pathophysiology of migraine could be mediated by distinct networks of neuronal structures has gained increasing support in the last years (13).There is evidence showing that the altered activity of key brain areas involved in the generation of the migraine attack, like the hypothalamus, pons and STN, may result from the interaction with other brain regions. In this PhD project, I have focused the attention on the hypothalamus investigating its interaction with other brain areas during the migraine interictal phase and exploring the association between hypothalamic activity and patients' clinical features. To better understand the mechanisms underpinning the functional organization of the hypothalamus, I have also investigated longitudinal hypothalamic RS FC changes and their association with clinical measures and disease progression over the years (**Chapter 5**). This study showed that during the interictal phase the hypothalamus modulates the activity of pain and visual processing areas, like the OFG and lingual gyrus, in episodic migraine patients. The functional interplay between the hypothalamus and other brain regions implicated in migraine pathophysiology could influence the frequency of the migraine attacks. In addition, weakened hypothalamic connections with frontal areas of the antinociceptive system may be a prognostic marker for migraine disability. Interestingly, the hypothalamic-cortical interplay changed dynamically over time. Specifically, the interaction between the hypothalamus and OFG was reinforced after 4

years, and the increased RS FC was associated to a lower migraine attack frequency at follow-up, suggesting the implementation of an adaptive coping response that could lower the migraine attack frequency over the years.

Another important unanswered question is whether brain functional and structural imaging alterations revealed in patients with migraine are migraine specific or are common to other headache and chronic pain disorders. During my PhD, combining machine learning techniques and multimodal MRI modalities, I have explored brain structural and functional patterns shared by migraine and cluster headache patients, as well as MRI and clinical biomarkers that accurately differentiate these two types of primary headaches (C**hapter 6**). An interesting result of this study is that the combination of different patterns of brain activation and morphometry yielded the best classification performance in distinguishing migraine and cluster headache patients from controls, supporting the value of combining functional and structural imaging metrics that disclose complementary information regarding the underlying biological processes. Functional biomarkers, including the hypothalamic and PAG networks, were shared by migraine and cluster headache patients. The activity of the PAG networks was significantly associated to patients' clinical features, including pain severity and the presence of cranial autonomic symptoms. Thus, reinforcing the role of the PAG in mediating some of the symptoms of the migraine and cluster headache attack and supporting its potential as a therapeutic target. Interestingly, like the hypothalamic study, this study confirmed a functional interaction between the hypothalamus and brain areas implicated in pain control and visual processing in a different sample of migraine patients and in patients with cluster headache, corroborating the crucial role of the hypothalamus in primary headaches. The low accuracy rate achieved by the MRI model in discriminating migraine and cluster headache patients further supports the presence of common pathophysiological mechanisms in the two forms of headache. Beyond mutual brain networks involved in both migraine and cluster headache, the thalamo-cortical network could represent the neural substrate that differentiates migraine from cluster headache attacks with their specific symptomatology.

8. CONCLUSIONS

Overall, the results obtained during my PhD have strengthened the idea that migraine is not simply a disorder of recurrent pain attacks resulting from vascular changes, but a more complex neurological disease that involves the interplay of multiple brain networks to account for the pain and the wide constellation of symptoms experienced by patients. This PhD project suggests that imaging techniques can unveil migraine predisposing brain traits, as well as dynamic brain changes that influence the course of migraine. Moreover, this project showed that cutting edge MRI techniques can help us to disclose adaptive responses implemented by migraine patients. Finally, during my PhD I have demonstrated that the application of machine learning techniques and multimodal MRI data is a valuable strategy to reduce the unmet needs in the understanding of primary headaches, identify biomarkers that are specific for different headaches, reveal new therapeutic targets and guide the development of new drugs tailored to each form of primary headache.

Future longitudinal studies with longer follow-up and including patients at different stages of the disease (e.g., pediatric, episodic and chronic patients) are needed. In the future, objective imaging biomarkers that might predict patients' therapeutic response to headache treatments should be identified.

9. ADDITIONAL PUBLICATIONS

Original Research

1. Filippi M, **Messina R**, Goadsby PJ, Rocca MA. Author response: Gray matter volume modifications in migraine: A cross-sectional and longitudinal study. Neurology. 2019 Mar 19;92(12):587-588.
2. **Messina R**, Lastarria Perez CP, Filippi M, Goadsby PJ. Candesartan in migraine prevention: results from a retrospective real-world study. J Neurol. 2020 Nov;267(11):3243-3247
3. Colombo B, Cetta I, **Messina R**, Filippi M. Stress in paediatric migraine: a trigger factor? Neurol Sci. 2020 Dec;41(Suppl 2):447-449.
4. Ammirati E, Moroni F, Magnoni M, Rocca MA, **Messina R**, Anzalone N, De Filippis C, Scotti I, Besana F, Spagnolo P, Rimoldi OE, Chiesa R, Falini A, Filippi M, Camici PG. Extent and characteristics of carotid plaques and brain parenchymal loss in asymptomatic patients with no indication for revascularization. Int J Cardiol Heart Vasc. 2020 Aug 20; 30:100619.
5. Barbanti P, Aurilia C, Cevoli S, Egeo G, Fofi L, **Messina R**, Salerno A, Torelli P, Albanese M, Carnevale A, Bono F, D'Amico D, Filippi M, Altamura C, Vernieri F; EARLY Study Group. Long-term (48 weeks) effectiveness, safety, and tolerability of erenumab in the prevention of high-frequency episodic and chronic migraine in a real worls: results of the EARLY 2 study. Headache. 2021 Jul 26.
6. Albano L, Agosta F, Basaia S, Castellano A, **Messina R**, Parisi V, Barzaghi LR, Falini A, Mortini P, Filippi M. Alterations of brain structural MRI are associated with outcome of surgical treatment in trigeminal neuralgia. Eur J Neurol. 2021 Sep 14.

Review

1. Colombo B, **Messina R**, Rocca MA, Filippi M. Imaging the migrainous brain: the present and the future. Neurol Sci. 2019 May;40(Suppl 1):49-54.
2. Filippi M and **Messina R**. The chronic migraine brain: What have we learned from neuroimaging? Front Neurol. 2020 Jan 9; 10:1356.

3. **Messina R** and Filippi M What we gain from machine learning studies in headache patients. Front Neurol. 2020 Apr 9; 11:221.
4. Altamura C, Corbelli I, De Tommaso M, Di Lorenzo C, Di Lorenzo G, Di rienzo A, Filippi M, Jannini T, **Messina R**, Parisi P, Parisi V, Pierelli F, Rainero I, Raucci U, Rubino E, Sarchielli P, Li L, Vernieri F, Vollono C, Coppola G. Pathophysiological bases of comorbidity in migraine. Front Hum Neurosci. 2021 Apr 20; 15:640574.
5. Ashina S, Mitsikostas D, Lee MJ, Yamani N, Wang SJ, **Messina R**, Ashina H, Buse D, Pozo-Rosich P, Jensen R, Diener HC, Lipton R. Tension-type headache. Nat Rev Dis Primers. 2021 Mar 25;7(1):24.

Editorial

1. **Messina R**, Goadsby PJ, Filippi M. Editorial: Functional and Structural Brain Alterations in Headache: A Trait or a State? Front Neurol. 2020 Aug 12; 11:859.

Book chapter

1. Filippi M and **Messina R**. What imaging has revealed about migraine and chronic migraine. In: *Biology of Migraine*. JW Swanson and M Matharu (eds). Elsevier Publishing Company, In Press.

10. REFERENCES

1. Stovner L, Hagen K, Jensen R, Katsarava Z, Lipton R, Scher A, et al. The global burden of headache: a documentation of headache prevalence and disability worldwide. Cephalalgia. 2007;27(3):193-210.

2. Headache Classification Committee of the International Headache Society (IHS) The International Classification of Headache Disorders, 3rd edition. Cephalalgia. 2018;38(1):1-211.

3. Kaniecki RG, Levin AD. Headache in the elderly. Handb Clin Neurol. 2019;167:511-28.

4. Ashina M. Migraine. N Engl J Med. 2020;383(19):1866-76.

5. Ashina M, Katsarava Z, Do TP, Buse DC, Pozo-Rosich P, Ozge A, et al. Migraine: epidemiology and systems of care. Lancet. 2021;397(10283):1485-95.

6. Vetvik KG, MacGregor EA. Sex differences in the epidemiology, clinical features, and pathophysiology of migraine. Lancet Neurol. 2017;16(1):76-87.

7. Collaborators GBDCoD. Global, regional, and national age-sex specific mortality for 264 causes of death, 1980-2016: a systematic analysis for the Global Burden of Disease Study 2016. Lancet. 2017;390(10100):1151-210.

8. May A, Schulte LH. Chronic migraine: risk factors, mechanisms and treatment. Nature reviews Neurology. 2016;12(8):455-64.

9. Lipton RB. Tracing transformation: chronic migraine classification, progression, and epidemiology. Neurology. 2009;72(5 Suppl):S3-7.

10. Altamura C, Corbelli I, de Tommaso M, Di Lorenzo C, Di Lorenzo G, Di Renzo A, et al. Pathophysiological Bases of Comorbidity in Migraine. Frontiers in human neuroscience. 2021;15:640574.

11. Buse DC, Manack A, Serrano D, Turkel C, Lipton RB. Sociodemographic and comorbidity profiles of chronic migraine and episodic migraine sufferers. Journal of neurology, neurosurgery, and psychiatry. 2010;81(4):428-32.

12. Polderman TJ, Benyamin B, de Leeuw CA, Sullivan PF, van Bochoven A, Visscher PM, et al. Meta-analysis of the heritability of human traits based on fifty years of twin studies. Nature genetics. 2015;47(7):702-9.

13. Goadsby PJ, Holland PR, Martins-Oliveira M, Hoffmann J, Schankin C, Akerman S. Pathophysiology of Migraine: A Disorder of Sensory Processing. Physiol Rev. 2017;97(2):553-622.
14. Russell MB, Iselius L, Olesen J. Inheritance of migraine investigated by complex segregation analysis. Hum Genet. 1995;96(6):726-30.
15. Gormley P, Kurki MI, Hiekkala ME, Veerapen K, Happola P, Mitchell AA, et al. Common Variant Burden Contributes to the Familial Aggregation of Migraine in 1,589 Families. Neuron. 2018;99(5):1098.
16. Gormley P, Anttila V, Winsvold BS, Palta P, Esko T, Pers TH, et al. Meta-analysis of 375,000 individuals identifies 38 susceptibility loci for migraine. Nature genetics. 2016;48(8):856-66.
17. Freilinger T, Anttila V, de Vries B, Malik R, Kallela M, Terwindt GM, et al. Genome-wide association analysis identifies susceptibility loci for migraine without aura. Nature genetics. 2012;44(7):777-82.
18. Goadsby PJ. Unique Migraine Subtypes, Rare Headache Disorders, and Other Disturbances. Continuum. 2015;21(4 Headache):1032-40.
19. Sutherland HG, Griffiths LR. Genetics of Migraine: Insights into the Molecular Basis of Migraine Disorders. Headache. 2017;57(4):537-69.
20. Kelman L. The triggers or precipitants of the acute migraine attack. Cephalalgia. 2007;27(5):394-402.
21. Ray BS WH. Experimental studies on headache. Pain-sensitive structures of the head and their significance in headache. Arch Surg. 1940;41:813-56.
22. Levy D, Burstein R. The vascular theory of migraine: leave it or love it? Ann Neurol. 2011;69(4):600-1.
23. Amin FM, Asghar MS, Hougaard A, Hansen AE, Larsen VA, de Koning PJ, et al. Magnetic resonance angiography of intracranial and extracranial arteries in patients with spontaneous migraine without aura: a cross-sectional study. Lancet Neurol. 2013;12(5):454-61.
24. Khan S, Amin FM, Christensen CE, Ghanizada H, Younis S, Olinger ACR, et al. Meningeal contribution to migraine pain: a magnetic resonance angiography study. Brain. 2019;142(1):93-102.

25. Hansen JM, Schankin CJ. Cerebral hemodynamics in the different phases of migraine and cluster headache. J Cereb Blood Flow Metab. 2017:271678X17729783.
26. Akerman S, Romero-Reyes M, Holland PR. Current and novel insights into the neurophysiology of migraine and its implications for therapeutics. Pharmacology & therapeutics. 2017;172:151-70.
27. Moskowitz MA. The neurobiology of vascular head pain. Ann Neurol. 1984;16(2):157-68.
28. Roon KI, Olesen J, Diener HC, Ellis P, Hettiarachchi J, Poole PH, et al. No acute antimigraine efficacy of CP-122,288, a highly potent inhibitor of neurogenic inflammation: results of two randomized, double-blind, placebo-controlled clinical trials. Ann Neurol. 2000;47(2):238-41.
29. Goldstein DJ, Offen WW, Klein EG, Phebus LA, Hipskind P, Johnson KW, et al. Lanepitant, an NK-1 antagonist, in migraine prevention. Cephalalgia. 2001;21(2):102-6.
30. Puledda F, Messina R, Goadsby PJ. An update on migraine: current understanding and future directions. J Neurol. 2017;264(9):2031-9.
31. Charles AC, Baca SM. Cortical spreading depression and migraine. Nature reviews Neurology. 2013;9(11):637-44.
32. Tfelt-Hansen PC. History of migraine with aura and cortical spreading depression from 1941 and onwards. Cephalalgia. 2010;30(7):780-92.
33. Hansen JM, Baca SM, Vanvalkenburgh P, Charles A. Distinctive anatomical and physiological features of migraine aura revealed by 18 years of recording. Brain. 2013;136(Pt 12):3589-95.
34. Sanchez del Rio M, Bakker D, Wu O, Agosti R, Mitsikostas DD, Ostergaard L, et al. Perfusion weighted imaging during migraine: spontaneous visual aura and headache. Cephalalgia. 1999;19(8):701-7.
35. Olesen J, Larsen B, Lauritzen M. Focal hyperemia followed by spreading oligemia and impaired activation of rCBF in classic migraine. Ann Neurol. 1981;9(4):344-52.
36. Karatas H, Erdener SE, Gursoy-Ozdemir Y, Lule S, Eren-Kocak E, Sen ZD, et al. Spreading depression triggers headache by activating neuronal Panx1 channels. Science. 2013;339(6123):1092-5.

37. Lambert GA, Truong L, Zagami AS. Effect of cortical spreading depression on basal and evoked traffic in the trigeminovascular sensory system. Cephalalgia. 2011;31(14):1439-51.
38. Noseda R, Burstein R. Migraine pathophysiology: anatomy of the trigeminovascular pathway and associated neurological symptoms, CSD, sensitization and modulation of pain. Pain. 2013;154 Suppl 1.
39. Viana M, Linde M, Sances G, Ghiotto N, Guaschino E, Allena M, et al. Migraine aura symptoms: Duration, succession and temporal relationship to headache. Cephalalgia. 2016;36(5):413-21.
40. Ashina M, Terwindt GM, Al-Karagholi MA, de Boer I, Lee MJ, Hay DL, et al. Migraine: disease characterisation, biomarkers, and precision medicine. Lancet. 2021;397(10283):1496-504.
41. Goadsby PJ, Edvinsson L, Ekman R. Vasoactive peptide release in the extracerebral circulation of humans during migraine headache. Ann Neurol. 1990;28(2):183-7.
42. Zagami AS, Edvinsson L, Goadsby PJ. Pituitary adenylate cyclase activating polypeptide and migraine. Ann Clin Transl Neurol. 2014;1(12):1036-40.
43. Hansen JM, Hauge AW, Olesen J, Ashina M. Calcitonin gene-related peptide triggers migraine-like attacks in patients with migraine with aura. Cephalalgia. 2010;30(10):1179-86.
44. Schytz HW, Birk S, Wienecke T, Kruuse C, Olesen J, Ashina M. PACAP38 induces migraine-like attacks in patients with migraine without aura. Brain. 2009;132(Pt 1):16-25.
45. Thomsen LL, Kruuse C, Iversen HK, Olesen J. A nitric oxide donor (nitroglycerin) triggers genuine migraine attacks. Eur J Neurol. 1994;1(1):73-80.
46. Guo S, Olesen J, Ashina M. Phosphodiesterase 3 inhibitor cilostazol induces migraine-like attacks via cyclic AMP increase. Brain. 2014;137(Pt 11):2951-9.
47. Kruuse C, Thomsen LL, Birk S, Olesen J. Migraine can be induced by sildenafil without changes in middle cerebral artery diameter. Brain. 2003;126(Pt 1):241-7.
48. Ashina M, Hansen JM, BO AD, Olesen J. Human models of migraine - short-term pain for long-term gain. Nature reviews Neurology. 2017;13(12):713-24.

49. Al-Karagholi MA, Hansen JM, Guo S, Olesen J, Ashina M. Opening of ATP-sensitive potassium channels causes migraine attacks: a new target for the treatment of migraine. Brain. 2019;142(9):2644-54.
50. Al-Karagholi MA, Ghanizada H, Waldorff Nielsen CA, Skandarioon C, Snellman J, Lopez-Lopez C, et al. Opening of BKCa channels causes migraine attacks: a new downstream target for the treatment of migraine. Pain. 2021.
51. Blau JN. Migraine: theories of pathogenesis. Lancet. 1992;339(8803):1202-7.
52. Lai TH, Fuh JL, Wang SJ. Cranial autonomic symptoms in migraine: characteristics and comparison with cluster headache. Journal of neurology, neurosurgery, and psychiatry. 2009;80(10):1116-9.
53. Charles A. The evolution of a migraine attack - a review of recent evidence. Headache. 2013;53(2):413-9.
54. Karsan N, Goadsby PJ. Biological insights from the premonitory symptoms of migraine. Nature reviews Neurology. 2018;14(12):699-710.
55. Giffin NJ, Ruggiero L, Lipton RB, Silberstein SD, Tvedskov JF, Olesen J, et al. Premonitory symptoms in migraine: an electronic diary study. Neurology. 2003;60(6):935-40.
56. Ong JJY, De Felice M. Migraine Treatment: Current Acute Medications and Their Potential Mechanisms of Action. Neurotherapeutics : the journal of the American Society for Experimental NeuroTherapeutics. 2018;15(2):274-90.
57. Schulte LH, Jurgens TP, May A. Photo-, osmo- and phonophobia in the premonitory phase of migraine: mistaking symptoms for triggers? J Headache Pain. 2015;16:14.
58. Karsan N, Bose P, Newman J, Goadsby PJ. Are some patient-perceived migraine triggers simply early manifestations of the attack? J Neurol. 2021;268(5):1885-93.
59. Filippi M, Rocca M.A. Migraine. White Matter Disease: Springer 2020.
60. Schankin CJ, Viana M, Goadsby PJ. Persistent and Repetitive Visual Disturbances in Migraine: A Review. Headache. 2017;57(1):1-16.
61. Viana M, Sances G, Linde M, Ghiotto N, Guaschino E, Allena M, et al. Clinical features of migraine aura: Results from a prospective diary-aided study. Cephalalgia. 2017;37(10):979-89.
62. Charles A. The Migraine Aura. Continuum. 2018;24(4, Headache):1009-22.

63. Hansen JM, Goadsby PJ, Charles AC. Variability of clinical features in attacks of migraine with aura. Cephalalgia. 2016;36(3):216-24.
64. Bose P, Goadsby PJ. The migraine postdrome. Curr Opin Neurol. 2016;29(3):299-301.
65. Giffin NJ, Lipton RB, Silberstein SD, Olesen J, Goadsby PJ. The migraine postdrome: An electronic diary study. Neurology. 2016;87(3):309-13.
66. Camarda C, Monastero R, Pipia C, Recca D, Camarda R. Interictal executive dysfunction in migraineurs without aura: relationship with duration and intensity of attacks. Cephalalgia. 2007;27(10):1094-100.
67. Huang L, Juan Dong H, Wang X, Wang Y, Xiao Z. Duration and frequency of migraines affect cognitive function: evidence from neuropsychological tests and event-related potentials. J Headache Pain. 2017;18(1):54.
68. Chong CD, Starling AJ, Schwedt TJ. Interictal photosensitivity associates with altered brain structure in patients with episodic migraine. Cephalalgia. 2016;36(6):526-33.
69. Vuralli D, Ayata C, Bolay H. Cognitive dysfunction and migraine. J Headache Pain. 2018;19(1):109.
70. Gil-Gouveia R, Oliveira AG, Martins IP. Assessment of cognitive dysfunction during migraine attacks: a systematic review. J Neurol. 2015;262(3):654-65.
71. Dodick DW. Pearls: headache. Seminars in neurology. 2010;30(1):74-81.
72. Sandrini G, Friberg L, Coppola G, Janig W, Jensen R, Kruit M, et al. Neurophysiological tests and neuroimaging procedures in non-acute headache (2nd edition). Eur J Neurol. 2011;18(3):373-81.
73. Silberstein SD. Practice parameter: evidence-based guidelines for migraine headache (an evidence-based review): report of the Quality Standards Subcommittee of the American Academy of Neurology. Neurology. 2000;55(6):754-62.
74. Lipton RB, Silberstein SD. Episodic and chronic migraine headache: breaking down barriers to optimal treatment and prevention. Headache. 2015;55 Suppl 2:103-22; quiz 23-6.
75. Society AH. The American Headache Society Position Statement On Integrating New Migraine Treatments Into Clinical Practice. Headache. 2019;59(1):1-18.

76. Lipton RB, Fanning KM, Serrano D, Reed ML, Cady R, Buse DC. Ineffective acute treatment of episodic migraine is associated with new-onset chronic migraine. Neurology. 2015;84(7):688-95.
77. Goadsby PJ. The pharmacology of headache. Progress in neurobiology. 2000;62(5):509-25.
78. Goadsby PJ, Sprenger T. Current practice and future directions in the prevention and acute management of migraine. Lancet Neurol. 2010;9(3):285-98.
79. Humphrey PP, Goadsby PJ. The mode of action of sumatriptan is vascular? A debate. Cephalalgia. 1994;14(6):401-10; discussion 393.
80. Ahn AH, Basbaum AI. Where do triptans act in the treatment of migraine? Pain. 2005;115(1-2):1-4.
81. Goadsby PJ, Edvinsson L. The trigeminovascular system and migraine: studies characterizing cerebrovascular and neuropeptide changes seen in humans and cats. Ann Neurol. 1993;33(1):48-56.
82. Shields KG, Goadsby PJ. Serotonin receptors modulate trigeminovascular responses in ventroposteromedial nucleus of thalamus: a migraine target? Neurobiology of disease. 2006;23(3):491-501.
83. Weiller C, May A, Limmroth V, Juptner M, Kaube H, Schayck RV, et al. Brain stem activation in spontaneous human migraine attacks. Nat Med. 1995;1(7):658-60.
84. Moreno-Ajona D, Chan C, Villar-Martinez MD, Goadsby PJ. Targeting CGRP and 5-HT1F Receptors for the Acute Therapy of Migraine: A Literature Review. Headache. 2019;59 Suppl 2:3-19.
85. Silberstein SD. Preventive Migraine Treatment. Continuum. 2015;21(4 Headache):973-89.
86. Diener HC, Charles A, Goadsby PJ, Holle D. New therapeutic approaches for the prevention and treatment of migraine. Lancet Neurol. 2015;14(10):1010-22.
87. Ong JJY, Wei DY, Goadsby PJ. Recent Advances in Pharmacotherapy for Migraine Prevention: From Pathophysiology to New Drugs. Drugs. 2018;78(4):411-37.
88. Tepper SJ. CGRP and headache: a brief review. Neurol Sci. 2019;40(Suppl 1):99-105.
89. Barbanti P, Aurilia C, Cevoli S, Egeo G, Fofi L, Messina R, et al. Long-term (48 weeks) effectiveness, safety, and tolerability of erenumab in the prevention of high-

frequency episodic and chronic migraine in a real world: Results of the EARLY 2 study. Headache. 2021.

90. Tepper SJ. History and Review of anti-Calcitonin Gene-Related Peptide (CGRP) Therapies: From Translational Research to Treatment. Headache. 2018;58 Suppl 3:238-75.

91. Puledda F, Shields K. Non-Pharmacological Approaches for Migraine. Neurotherapeutics : the journal of the American Society for Experimental NeuroTherapeutics. 2018;15(2):336-45.

92. Ogawa S, Menon RS, Tank DW, Kim SG, Merkle H, Ellermann JM, et al. Functional brain mapping by blood oxygenation level-dependent contrast magnetic resonance imaging. A comparison of signal characteristics with a biophysical model. Biophys J. 1993;64(3):803-12.

93. Biswal BB. Resting state fMRI: a personal history. Neuroimage. 2012;62(2):938-44.

94. Miletich RS. Positron Emission Tomography and Single-Photon Emission Computed Tomography in Neurology. Continuum. 2016;22(5, Neuroimaging):1636-54.

95. Wong EC. An introduction to ASL labeling techniques. Journal of magnetic resonance imaging : JMRI. 2014;40(1):1-10.

96. Bhaskar S, Saeidi K, Borhani P, Amiri H. Recent progress in migraine pathophysiology: role of cortical spreading depression and magnetic resonance imaging. Eur J Neurosci. 2013;38(11):3540-51.

97. Le Bihan D, Mangin JF, Poupon C, Clark CA, Pappata S, Molko N, et al. Diffusion tensor imaging: concepts and applications. Journal of magnetic resonance imaging : JMRI. 2001;13(4):534-46.

98. Pierpaoli C, Barnett A, Pajevic S, Chen R, Penix LR, Virta A, et al. Water diffusion changes in Wallerian degeneration and their dependence on white matter architecture. Neuroimage. 2001;13(6 Pt 1):1174-85.

99. Messina R, Filippi M, Goadsby PJ. Recent advances in headache neuroimaging. Curr Opin Neurol. 2018;31(4):379-85.

100. Maniyar FH, Sprenger T, Monteith T, Schankin C, Goadsby PJ. Brain activations in the premonitory phase of nitroglycerin-triggered migraine attacks. Brain. 2014;137(Pt 1):232-41.

101. Karsan N, Bose PR, O'Daly O, Zelaya FO, Goadsby PJ. Alterations in Functional Connectivity During Different Phases of the Triggered Migraine Attack. Headache. 2020.
102. Schulte LH, May A. The migraine generator revisited: continuous scanning of the migraine cycle over 30 days and three spontaneous attacks. Brain. 2016;139(Pt 7):1987-93.
103. Schulte LH, Mehnert J, May A. Longitudinal Neuroimaging over 30 Days: Temporal Characteristics of Migraine. Ann Neurol. 2020;87(4):646-51.
104. Maniyar FH, Sprenger T, Schankin C, Goadsby PJ. The origin of nausea in migraine-a PET study. J Headache Pain. 2014;15:84.
105. Maniyar FH, Sprenger T, Schankin C, Goadsby PJ. Photic hypersensitivity in the premonitory phase of migraine--a positron emission tomography study. Eur J Neurol. 2014;21(9):1178-83.
106. Schulte LH, Menz MM, Haaker J, May A. The migraineur's brain networks: Continuous resting state fMRI over 30 days. Cephalalgia. 2020;40(14):1614-21.
107. Denuelle M, Fabre N, Payoux P, Chollet F, Geraud G. Hypothalamic activation in spontaneous migraine attacks. Headache. 2007;47(10):1418-26.
108. Schulte LH, Allers A, May A. Hypothalamus as a mediator of chronic migraine: Evidence from high-resolution fMRI. Neurology. 2017;88(21):2011-6.
109. Hougaard A, Amin FM, Larsson HB, Rostrup E, Ashina M. Increased intrinsic brain connectivity between pons and somatosensory cortex during attacks of migraine with aura. Hum Brain Mapp. 2017;38(5):2635-42.
110. Stankewitz A, May A. Increased limbic and brainstem activity during migraine attacks following olfactory stimulation. Neurology. 2011;77(5):476-82.
111. Younis S, Christensen CE, Vestergaard MB, Lindberg U, Tolnai D, Paulson OB, et al. Glutamate levels and perfusion in pons during migraine attacks: A 3T MRI study using proton spectroscopy and arterial spin labeling. J Cereb Blood Flow Metab. 2021;41(3):604-16.
112. Stankewitz A, Aderjan D, Eippert F, May A. Trigeminal nociceptive transmission in migraineurs predicts migraine attacks. The Journal of neuroscience : the official journal of the Society for Neuroscience. 2011;31(6):1937-43.

113. Amin FM, Hougaard A, Magon S, Sprenger T, Wolfram F, Rostrup E, et al. Altered thalamic connectivity during spontaneous attacks of migraine without aura: A resting-state fMRI study. Cephalalgia. 2017:333102417729113.
114. Maleki N, Szabo E, Becerra L, Moulton E, Scrivani SJ, Burstein R, et al. Ictal and interictal brain activation in episodic migraine: Neural basis for extent of allodynia. PLoS One. 2021;16(1):e0244320.
115. Coppola G, Tinelli E, Lepre C, Iacovelli E, Di Lorenzo C, Di Lorenzo G, et al. Dynamic changes in thalamic microstructure of migraine without aura patients: a diffusion tensor magnetic resonance imaging study. Eur J Neurol. 2013.
116. Coppola G, Di Renzo A, Tinelli E, Di Lorenzo C, Scapeccia M, Parisi V, et al. Resting state connectivity between default mode network and insula encodes acute migraine headache. Cephalalgia. 2017:333102417715230.
117. Coppola G, Di Renzo A, Tinelli E, Di Lorenzo C, Di Lorenzo G, Parisi V, et al. Thalamo-cortical network activity during spontaneous migraine attacks. Neurology. 2016;87(20):2154-60.
118. Amin FM, Hougaard A, Magon S, Asghar MS, Ahmad NN, Rostrup E, et al. Change in brain network connectivity during PACAP38-induced migraine attacks: A resting-state functional MRI study. Neurology. 2016;86(2):180-7.
119. Tfelt-Hansen PC, Koehler PJ. One hundred years of migraine research: major clinical and scientific observations from 1910 to 2010. Headache. 2011;51(5):752-78.
120. Hougaard A, Amin FM, Ashina M. Migraine and structural abnormalities in the brain. Curr Opin Neurol. 2014;27(3):309-14.
121. Kruit MC, van Buchem MA, Hofman PA, Bakkers JT, Terwindt GM, Ferrari MD, et al. Migraine as a risk factor for subclinical brain lesions. Jama. 2004;291(4):427-34.
122. Hamedani AG, Rose KM, Peterlin BL, Mosley TH, Coker LH, Jack CR, et al. Migraine and white matter hyperintensities: the ARIC MRI study. Neurology. 2013;81(15):1308-13.
123. Bashir A, Lipton RB, Ashina S, Ashina M. Migraine and structural changes in the brain: a systematic review and meta-analysis. Neurology. 2013;81(14):1260-8.
124. Cooney BS, Grossman RI, Farber RE, Goin JE, Galetta SL. Frequency of magnetic resonance imaging abnormalities in patients with migraine. Headache. 1996;36(10):616-21.

125. Zhang Q, Datta R, Detre JA, Cucchiara B. White matter lesion burden in migraine with aura may be associated with reduced cerebral blood flow. Cephalalgia. 2017;37(6):517-24.
126. Kruit MC, Launer LJ, Ferrari MD, van Buchem MA. Infarcts in the posterior circulation territory in migraine. The population-based MRI CAMERA study. Brain. 2005;128(Pt 9):2068-77.
127. Kruit MC, van Buchem MA, Launer LJ, Terwindt GM, Ferrari MD. Migraine is associated with an increased risk of deep white matter lesions, subclinical posterior circulation infarcts and brain iron accumulation: the population-based MRI CAMERA study. Cephalalgia. 2010;30(2):129-36.
128. Gaist D, Garde E, Blaabjerg M, Nielsen HH, Kroigard T, Ostergaard K, et al. Migraine with aura and risk of silent brain infarcts and white matter hyperintensities: an MRI study. Brain. 2016;139(Pt 7):2015-23.
129. Palm-Meinders IH, Koppen H, Terwindt GM, Launer LJ, Konishi J, Moonen JM, et al. Structural brain changes in migraine. Jama. 2012;308(18):1889-97.
130. Kurth T, Mohamed S, Maillard P, Zhu YC, Chabriat H, Mazoyer B, et al. Headache, migraine, and structural brain lesions and function: population based Epidemiology of Vascular Ageing-MRI study. Bmj. 2011;342:c7357.
131. Mar S, Kelly JE, Isbell S, Aung WY, Lenox J, Prensky A. Prevalence of white matter lesions and stroke in children with migraine. Neurology. 2013;81(16):1387-91.
132. Porter A, Gladstone JP, Dodick DW. Migraine and white matter hyperintensities. Current pain and headache reports. 2005;9(4):289-93.
133. Lee MJ, Park BY, Cho S, Park H, Chung CS. Cerebrovascular reactivity as a determinant of deep white matter hyperintensities in migraine. Neurology. 2019;92(4):e342-e50.
134. Hoogeveen ES, Arkink EB, van der Grond J, van Buchem MA, Ferrari MD, Terwindt GM, et al. MRI evaluation of the relationship between carotid artery endothelial shear stress and brain white matter lesions in migraine. Journal of cerebral blood flow and metabolism : official journal of the International Society of Cerebral Blood Flow and Metabolism. 2020;40(5):1040-7.

135. Schmitz N, Arkink EB, Mulder M, Rubia K, Admiraal-Behloul F, Schoonman GG, et al. Frontal lobe structure and executive function in migraine patients. Neurosci Lett. 2008;440(2):92-6.
136. Messina R, Rocca MA, Colombo B, Valsasina P, Horsfield MA, Copetti M, et al. Cortical abnormalities in patients with migraine: a surface-based analysis. Radiology. 2013;268(1):170-80.
137. Lakhan SE, Avramut M, Tepper SJ. Structural and functional neuroimaging in migraine: insights from 3 decades of research. Headache. 2013;53(1):46-66.
138. DaSilva AF, Granziera C, Tuch DS, Snyder J, Vincent M, Hadjikhani N. Interictal alterations of the trigeminal somatosensory pathway and periaqueductal gray matter in migraine. Neuroreport. 2007;18(4):301-5.
139. Vereb D, Szabo N, Tuka B, Tajti J, Kiraly A, Farago P, et al. Correlation of neurochemical and imaging markers in migraine: PACAP38 and DTI measures. Neurology. 2018;91(12):e1166-e74.
140. Messina R, Rocca MA, Colombo B, Pagani E, Falini A, Comi G, et al. White matter microstructure abnormalities in pediatric migraine patients. Cephalalgia. 2015.
141. Granziera C, DaSilva AF, Snyder J, Tuch DS, Hadjikhani N. Anatomical alterations of the visual motion processing network in migraine with and without aura. PLoS Med. 2006;3(10):e402.
142. Rocca MA, Pagani E, Colombo B, Tortorella P, Falini A, Comi G, et al. Selective diffusion changes of the visual pathways in patients with migraine: a 3-T tractography study. Cephalalgia. 2008;28(10):1061-8.
143. Schwedt TJ, Chiang CC, Chong CD, Dodick DW. Functional MRI of migraine. Lancet Neurol. 2015;14(1):81-91.
144. Russo A, Tessitore A, Esposito F, Marcuccio L, Giordano A, Conforti R, et al. Pain processing in patients with migraine: an event-related fMRI study during trigeminal nociceptive stimulation. J Neurol. 2012;259(9):1903-12.
145. Schwedt TJ, Chong CD, Chiang CC, Baxter L, Schlaggar BL, Dodick DW. Enhanced pain-induced activity of pain-processing regions in a case-control study of episodic migraine. Cephalalgia. 2014;34(12):947-58.

146. Chen Z, Chen X, Liu M, Dong Z, Ma L, Yu S. Altered functional connectivity of amygdala underlying the neuromechanism of migraine pathogenesis. J Headache Pain. 2017;18(1):7.

147. Yu ZB, Lv YB, Song LH, Liu DH, Huang XL, Hu XY, et al. Functional Connectivity Differences in the Insular Sub-regions in Migraine without Aura: A Resting-State Functional Magnetic Resonance Imaging Study. Front Behav Neurosci. 2017;11:124.

148. Zhang J, Su J, Wang M, Zhao Y, Zhang QT, Yao Q, et al. The sensorimotor network dysfunction in migraineurs without aura: a resting-state fMRI study. J Neurol. 2017;264(4):654-63.

149. Chong CD, Schwedt TJ, Hougaard A. Brain functional connectivity in headache disorders: A narrative review of MRI investigations. J Cereb Blood Flow Metab. 2017:271678X17740794.

150. Russo A, Tessitore A, Silvestro M, Di Nardo F, Trojsi F, Del Santo T, et al. Advanced visual network and cerebellar hyperresponsiveness to trigeminal nociception in migraine with aura. J Headache Pain. 2019;20(1):46.

151. Mainero C, Boshyan J, Hadjikhani N. Altered functional magnetic resonance imaging resting-state connectivity in periaqueductal gray networks in migraine. Ann Neurol. 2011;70(5):838-45.

152. Burstein R, Jakubowski M, Garcia-Nicas E, Kainz V, Bajwa Z, Hargreaves R, et al. Thalamic sensitization transforms localized pain into widespread allodynia. Ann Neurol. 2010;68(1):81-91.

153. Russo A, Esposito F, Conte F, Fratello M, Caiazzo G, Marcuccio L, et al. Functional interictal changes of pain processing in migraine with ictal cutaneous allodynia. Cephalalgia. 2017;37(4):305-14.

154. Stankewitz A, Schulz E, May A. Neuronal correlates of impaired habituation in response to repeated trigemino-nociceptive but not to olfactory input in migraineurs: an fMRI study. Cephalalgia. 2013;33(4):256-65.

155. Russo A, Silvestro M, Trojsi F, Bisecco A, De Micco R, Caiazzo G, et al. Cognitive Networks Disarrangement in Patients With Migraine Predicts Cutaneous Allodynia. Headache. 2020;60(7):1228-43.

156. Moulton EA, Becerra L, Johnson A, Burstein R, Borsook D. Altered hypothalamic functional connectivity with autonomic circuits and the locus coeruleus in migraine. PLoS One. 2014;9(4):e95508.
157. Russo A, Tessitore A, Giordano A, Corbo D, Marcuccio L, De Stefano M, et al. Executive resting-state network connectivity in migraine without aura. Cephalalgia. 2012;32(14):1041-8.
158. Tessitore A, Russo A, Giordano A, Conte F, Corbo D, De Stefano M, et al. Disrupted default mode network connectivity in migraine without aura. J Headache Pain. 2013;14(1):89.
159. Messina R, Goadsby PJ, Filippi M. Editorial: Functional and Structural Brain Alterations in Headache: A Trait or a State? Front Neurol. 2020;11:859.
160. Rocca MA, Messina R, Colombo B, Falini A, Comi G, Filippi M. Structural brain MRI abnormalities in pediatric patients with migraine. J Neurol. 2014;261(2):350-7.
161. Gaist D, Hougaard A, Garde E, Reislev NL, Wiwie R, Iversen P, et al. Migraine with visual aura associated with thicker visual cortex. Brain. 2018.
162. Rocca MA, Ceccarelli A, Falini A, Colombo B, Tortorella P, Bernasconi L, et al. Brain gray matter changes in migraine patients with T2-visible lesions: a 3-T MRI study. Stroke. 2006;37(7):1765-70.
163. Schmitz N, Admiraal-Behloul F, Arkink EB, Kruit MC, Schoonman GG, Ferrari MD, et al. Attack frequency and disease duration as indicators for brain damage in migraine. Headache. 2008;48(7):1044-55.
164. Messina R, Rocca MA, Colombo B, Pagani E, Falini A, Goadsby PJ, et al. Gray matter volume modifications in migraine: A cross-sectional and longitudinal study. Neurology. 2018;91(3):e280-e92.
165. Chen WT, Chou KH, Lee PL, Hsiao FJ, Niddam DM, Lai KL, et al. Comparison of gray matter volume between migraine and "strict-criteria" tension-type headache. J Headache Pain. 2018;19(1):4.
166. Schwedt TJ, Si B, Li J, Wu T, Chong CD. Migraine Subclassification via a Data-Driven Automated Approach Using Multimodality Factor Mixture Modeling of Brain Structure Measurements. Headache. 2017;57(7):1051-64.
167. Dumkrieger G, Chong CD, Ross K, Berisha V, Schwedt TJ. Static and dynamic functional connectivity differences between migraine and persistent post-traumatic

headache: A resting-state magnetic resonance imaging study. Cephalalgia. 2019;39(11):1366-81.

168. Chong CD, Peplinski J, Berisha V, Ross K, Schwedt TJ. Differences in fibertract profiles between patients with migraine and those with persistent post-traumatic headache. Cephalalgia. 2019;39(9):1121-33.

169. Chong CD, Gaw N, Fu Y, Li J, Wu T, Schwedt TJ. Migraine classification using magnetic resonance imaging resting-state functional connectivity data. Cephalalgia. 2017;37(9):828-44.

170. Tu Y. ZF, Lan L., Li Z., Maleki N., Liu B., Chen J., Wang C., Park J., Lang C., Gao Y., Liu M., Fu Z., Zhang Z., Liang F., Kong J. An fMRI-based neural marker for migraine without aura. Neurology. 2019.

171. Schwedt TJ, Chong CD, Wu T, Gaw N, Fu Y, Li J. Accurate Classification of Chronic Migraine via Brain Magnetic Resonance Imaging. Headache. 2015;55(6):762-77.

172. Chong CD, Berisha V, Ross K, Kahn M, Dumkrieger G, Schwedt TJ. Distinguishing persistent post-traumatic headache from migraine: Classification based on clinical symptoms and brain structural MRI data. Cephalalgia. 2021;41(8):943-55.

173. Messina R, Filippi M. What We Gain From Machine Learning Studies in Headache Patients. Front Neurol. 2020;11:221.

174. Filippi M, Messina R. The Chronic Migraine Brain: What Have We Learned From Neuroimaging? Front Neurol. 2019;10:1356.

175. Gaist D, Pedersen L, Madsen C, Tsiropoulos I, Bak S, Sindrup S, et al. Long-term effects of migraine on cognitive function: a population-based study of Danish twins. Neurology. 2005;64(4):600-7.

176. Messina R, Rocca MA, Colombo B, Valsasina P, Meani A, Falini A, et al. Dysregulation of multisensory processing stands out from an early stage of migraine: a study in pediatric patients. J Neurol. 2020;267(3):760-9.

177. Puledda F, Ffytche D, O'Daly O, Goadsby PJ. Imaging the Visual Network in the Migraine Spectrum. Front Neurol. 2019;10:1325.

178. Baschi R, Monastero R, Cosentino G, Costa V, Giglia G, Fierro B, et al. Visuospatial learning is fostered in migraine: evidence by a neuropsychological study. Neurol Sci. 2019;40(11):2343-8.

179. HeadacheClassificationCommitteeoftheIHS. The International Classification of Headache Disorders, 3rd edition (beta version). Cephalalgia. 2013;33(9):629-808.
180. Lines CR, Vandormael K, Malbecq W. A comparison of visual analog scale and categorical ratings of headache pain in a randomized controlled clinical trial with migraine patients. Pain. 2001;93(2):185-90.
181. Stewart WF, Lipton RB, Dowson AJ, Sawyer J. Development and testing of the Migraine Disability Assessment (MIDAS) Questionnaire to assess headache-related disability. Neurology. 2001;56(6 Suppl 1):S20-8.
182. Kosinski M, Bayliss MS, Bjorner JB, Ware JE, Jr., Garber WH, Batenhorst A, et al. A six-item short-form survey for measuring headache impact: the HIT-6. Qual Life Res. 2003;12(8):963-74.
183. Bowie CR, Harvey PD. Administration and interpretation of the Trail Making Test. Nature protocols. 2006;1(5):2277-81.
184. Orsini A, Pezzuti, L. . WAIS-IV. Contributo alla taratura italiana. Firenze: Giunti O.S; 2013.
185. Wechsler D. WAIS---IV: Wechsler Adult Intelligence Scale. San Antonio, TX: Pearson2008.
186. Heaton. Wisconsin Card Sorting Test (Manual). Odessa, Fl1981.
187. Ferracuti F. Benton. Tests di giudizio di orientamento di linee-Manuale. Firenze: SF, editor. Versione italiana. Organizzazioni Speciali O.S. ; 1992.
188. Caffarra P, Vezzadini G, Dieci F, Zonato F, Venneri A. Rey-Osterrieth complex figure: normative values in an Italian population sample. Neurol Sci. 2002;22(6):443-7.
189. TG. SH. Standardizzazione e Taratura Italiana di Test Neuropsicologici: Masson; 1981.
190. Hamilton M. A rating scale for depression. Journal of neurology, neurosurgery, and psychiatry. 1960;23:56-62.
191. Hamilton M. The assessment of anxiety states by rating. The British journal of medical psychology. 1959;32(1):50-5.
192. Sack AT, Kohler A, Bestmann S, Linden DE, Dechent P, Goebel R, et al. Imaging the brain activity changes underlying impaired visuospatial judgments: simultaneous FMRI, TMS, and behavioral studies. Cerebral cortex. 2007;17(12):2841-52.

193. May A. Pearls and pitfalls: neuroimaging in headache. Cephalalgia. 2013;33(8):554-65.
194. Casanova R, Srikanth R, Baer A, Laurienti PJ, Burdette JH, Hayasaka S, et al. Biological parametric mapping: A statistical toolbox for multimodality brain image analysis. Neuroimage. 2007;34(1):137-43.
195. Ungerleider LG, Haxby JV. 'What' and 'where' in the human brain. Curr Opin Neurobiol. 1994;4(2):157-65.
196. Eckert MA, Menon V, Walczak A, Ahlstrom J, Denslow S, Horwitz A, et al. At the heart of the ventral attention system: the right anterior insula. Hum Brain Mapp. 2009;30(8):2530-41.
197. Pedale T, Macaluso E, Santangelo V. Enhanced insular/prefrontal connectivity when resisting from emotional distraction during visual search. Brain structure & function. 2019;224(6):2009-26.
198. Corbetta M, Shulman GL. Control of goal-directed and stimulus-driven attention in the brain. Nature reviews Neuroscience. 2002;3(3):201-15.
199. Nachev P, Kennard C, Husain M. Functional role of the supplementary and pre-supplementary motor areas. Nature reviews Neuroscience. 2008;9(11):856-69.
200. Reynolds NC, Zhong JY, Clendinen CA, Moffat SD, Magnusson KR. Age-related differences in brain activations during spatial memory formation in a well-learned virtual Morris water maze (vMWM) task. Neuroimage. 2019;202:116069.
201. Burks JD, Conner AK, Bonney PA, Glenn CA, Baker CM, Boettcher LB, et al. Anatomy and white matter connections of the orbitofrontal gyrus. Journal of neurosurgery. 2018;128(6):1865-72.
202. Raichle ME, MacLeod AM, Snyder AZ, Powers WJ, Gusnard DA, Shulman GL. A default mode of brain function. Proceedings of the National Academy of Sciences of the United States of America. 2001;98(2):676-82.
203. Singh KD, Fawcett IP. Transient and linearly graded deactivation of the human default-mode network by a visual detection task. Neuroimage. 2008;41(1):100-12.
204. Leech R, Sharp DJ. The role of the posterior cingulate cortex in cognition and disease. Brain. 2014;137(Pt 1):12-32.
205. Tracey I, Mantyh PW. The cerebral signature for pain perception and its modulation. Neuron. 2007;55(3):377-91.

206. Shepherd AJ. Colour vision in migraine: selective deficits for S-cone discriminations. Cephalalgia. 2005;25(6):412-23.

207. Shepherd AJ. Color vision but not visual attention is altered in migraine. Headache. 2006;46(4):611-21.

208. G.B.D.Collaborators. Global, regional, and national incidence, prevalence, and years lived with disability for 310 diseases and injuries, 1990-2015: a systematic analysis for the Global Burden of Disease Study 2015. Lancet. 2016;388(10053):1545-602.

209. Rocca MA, Messina R, Colombo B, Falini A, Comi G, Filippi M. Structural brain MRI abnormalities in pediatric patients with migraine. J Neurol. 2013.

210. Faria V, Erpelding N, Lebel A, Johnson A, Wolff R, Fair D, et al. The migraine brain in transition: girls vs boys. Pain. 2015;156(11):2212-21.

211. Santoro JD, Forkert ND, Yang QZ, Pavitt S, MacEachern SJ, Moseley ME, et al. Brain Diffusion Abnormalities in Children with Tension-Type and Migraine-Type Headaches. AJNR Am J Neuroradiol. 2018;39(5):935-41.

212. Youssef AM, Ludwick A, Wilcox SL, Lebel A, Peng K, Colon E, et al. In child and adult migraineurs the somatosensory cortex stands out ... again: An arterial spin labeling investigation. Hum Brain Mapp. 2017;38(8):4078-87.

213. Xue T, Yuan K, Zhao L, Yu D, Zhao L, Dong T, et al. Intrinsic brain network abnormalities in migraines without aura revealed in resting-state fMRI. PLoS One. 2012;7(12):e52927.

214. Chong CD, Gaw N, Fu Y, Li J, Wu T, Schwedt TJ. Migraine classification using magnetic resonance imaging resting-state functional connectivity data. Cephalalgia. 2016.

215. Schulte LH, May A. Of generators, networks and migraine attacks. Curr Opin Neurol. 2017;30(3):241-5.

216. Maleki N, Gollub RL. What Have We Learned From Brain Functional Connectivity Studies in Migraine Headache? Headache. 2016;56(3):453-61.

217. Allen EA, Erhardt EB, Damaraju E, Gruner W, Segall JM, Silva RF, et al. A baseline for the multivariate comparison of resting-state networks. Frontiers in systems neuroscience. 2011;5:2.

218. Calhoun VD, Adali T, Pearlson GD, Pekar JJ. A method for making group inferences from functional MRI data using independent component analysis. Hum Brain Mapp. 2001;14(3):140-51.
219. Himberg J, Hyvarinen A, Esposito F. Validating the independent components of neuroimaging time series via clustering and visualization. Neuroimage. 2004;22(3):1214-22.
220. Rocca MA, Savoldi F, Valsasina P, Radaelli M, Preziosa P, Comi G, et al. Cross-modal plasticity among sensory networks in neuromyelitis optica spectrum disorders. Multiple sclerosis. 2018:1352458518778008.
221. Jafri MJ, Pearlson GD, Stevens M, Calhoun VD. A method for functional network connectivity among spatially independent resting-state components in schizophrenia. Neuroimage. 2008;39(4):1666-81.
222. Murphy K, Birn RM, Handwerker DA, Jones TB, Bandettini PA. The impact of global signal regression on resting state correlations: are anti-correlated networks introduced? Neuroimage. 2009;44(3):893-905.
223. Martin H, Sanchez del Rio M, de Silanes CL, Alvarez-Linera J, Hernandez JA, Pareja JA. Photoreactivity of the occipital cortex measured by functional magnetic resonance imaging-blood oxygenation level dependent in migraine patients and healthy volunteers: pathophysiological implications. Headache. 2011;51(10):1520-8.
224. Tedeschi G, Russo A, Conte F, Corbo D, Caiazzo G, Giordano A, et al. Increased interictal visual network connectivity in patients with migraine with aura. Cephalalgia. 2016;36(2):139-47.
225. Macaluso E. Orienting of spatial attention and the interplay between the senses. Cortex; a journal devoted to the study of the nervous system and behavior. 2010;46(3):282-97.
226. Buckner RL, Andrews-Hanna JR, Schacter DL. The brain's default network: anatomy, function, and relevance to disease. Annals of the New York Academy of Sciences. 2008;1124:1-38.
227. Martins IP, Gil-Gouveia R, Silva C, Maruta C, Oliveira AG. Migraine, headaches, and cognition. Headache. 2012;52(10):1471-82.

228. Rocca MA, Valsasina P, Martinelli V, Misci P, Falini A, Comi G, et al. Large-scale neuronal network dysfunction in relapsing-remitting multiple sclerosis. Neurology. 2012;79(14):1449-57.
229. Tessitore A, Russo A, Conte F, Giordano A, De Stefano M, Lavorgna L, et al. Abnormal Connectivity Within Executive Resting-State Network in Migraine With Aura. Headache. 2015;55(6):794-805.
230. Mouraux A, Iannetti GD. The search for pain biomarkers in the human brain. Brain. 2018;141(12):3290-307.
231. Peng K, Steele SC, Becerra L, Borsook D. Brodmann area 10: Collating, integrating and high level processing of nociception and pain. Progress in neurobiology. 2018;161:1-22.
232. Lorenz J, Minoshima S, Casey KL. Keeping pain out of mind: the role of the dorsolateral prefrontal cortex in pain modulation. Brain. 2003;126(Pt 5):1079-91.
233. Rea M, Kullmann S, Veit R, Casile A, Braun C, Belardinelli MO, et al. Effects of aversive stimuli on prospective memory. An event-related fMRI study. PLoS One. 2011;6(10):e26290.
234. Li Z, Lan L, Zeng F, Makris N, Hwang J, Guo T, et al. The altered right frontoparietal network functional connectivity in migraine and the modulation effect of treatment. Cephalalgia. 2017;37(2):161-76.
235. Smallwood J, Brown K, Baird B, Schooler JW. Cooperation between the default mode network and the frontal-parietal network in the production of an internal train of thought. Brain research. 2012;1428:60-70.
236. Godwin CA, Hunter MA, Bezdek MA, Lieberman G, Elkin-Frankston S, Romero VL, et al. Functional connectivity within and between intrinsic brain networks correlates with trait mind wandering. Neuropsychologia. 2017;103:140-53.
237. Demarquay G, Mauguiere F. Central Nervous System Underpinnings of Sensory Hypersensitivity in Migraine: Insights from Neuroimaging and Electrophysiological Studies. Headache. 2016;56(9):1418-38.
238. de Tommaso M, Ambrosini A, Brighina F, Coppola G, Perrotta A, Pierelli F, et al. Altered processing of sensory stimuli in patients with migraine. Nature reviews Neurology. 2014;10(3):144-55.

239. Lee MJ, Park BY, Cho S, Kim ST, Park H, Chung CS. Increased connectivity of pain matrix in chronic migraine: a resting-state functional MRI study. J Headache Pain. 2019;20(1):29.
240. Coppola G, Di Renzo A, Petolicchio B, Tinelli E, Di Lorenzo C, Serrao M, et al. Increased neural connectivity between the hypothalamus and cortical resting-state functional networks in chronic migraine. J Neurol. 2020;267(1):185-91.
241. Headache Classification Committee of the International Headache S. The International Classification of Headache Disorders, 3rd edition (beta version). Cephalalgia. 2013;33(9):629-808.
242. Headache Classification Subcommittee of the International Headache S. The International Classification of Headache Disorders: 2nd edition. Cephalalgia. 2004;24 Suppl 1:9-160.
243. Biswal B, Yetkin FZ, Haughton VM, Hyde JS. Functional connectivity in the motor cortex of resting human brain using echo-planar MRI. Magnetic resonance in medicine. 1995;34(4):537-41.
244. Lowe MJ, Mock BJ, Sorenson JA. Functional connectivity in single and multislice echoplanar imaging using resting-state fluctuations. Neuroimage. 1998;7(2):119-32.
245. Hidalgo de la Cruz M, Valsasina P, Mesaros S, Meani A, Ivanovic J, Martinovic V, et al. Clinical predictivity of thalamic sub-regional connectivity in clinically isolated syndrome: a 7-year study. Mol Psychiatry. 2020.
246. Gazerani P, Cairns BE. Dysautonomia in the pathogenesis of migraine. Expert Rev Neurother. 2018;18(2):153-65.
247. May A, Burstein R. Hypothalamic regulation of headache and migraine. Cephalalgia. 2019;39(13):1710-9.
248. Chong CD, Aguilar M, Schwedt TJ. Altered Hypothalamic Region Covariance in Migraine and Cluster Headache: A Structural MRI Study. Headache. 2020;60(3):553-63.
249. Petrovic P, Kalso E, Petersson KM, Ingvar M. Placebo and opioid analgesia--imaging a shared neuronal network. Science. 2002;295(5560):1737-40.
250. Karimi S, Hamidi G, Fatahi Z, Haghparast A. Orexin 1 receptors in the anterior cingulate and orbitofrontal cortex regulate cost and benefit decision-making. Progress in neuro-psychopharmacology & biological psychiatry. 2019;89:227-35.

251. Saper CB. Hypothalamic connections with the cerebral cortex. Progress in brain research. 2000;126:39-48.
252. Schwedt TJ, Chong CD. Medication Overuse Headache: Pathophysiological Insights from Structural and Functional Brain MRI Research. Headache. 2017;57(7):1173-8.
253. Burke MJ, Joutsa J, Cohen AL, Soussand L, Cooke D, Burstein R, et al. Mapping migraine to a common brain network. Brain. 2020;143(2):541-53.
254. Schulte LH, Peng KP. Current understanding of premonitory networks in migraine: A window to attack generation. Cephalalgia. 2019;39(13):1720-7.
255. Kamali A, Ghazi Sherbaf F, Rahmani F, Khayat-Khoei M, Aein A, Gandhi A, et al. A direct visuosensory cortical connectivity of the human limbic system. Dissecting the trajectory of the parieto-occipito-hypothalamic tract in the human brain using diffusion weighted tractography. Neurosci Lett. 2020;728:134955.
256. Schwedt TJ, Berisha V, Chong CD. Temporal lobe cortical thickness correlations differentiate the migraine brain from the healthy brain. PLoS One. 2015;10(2):e0116687.
257. Zielman R, Wijnen JP, Webb A, Onderwater GLJ, Ronen I, Ferrari MD, et al. Cortical glutamate in migraine. Brain. 2017;140(7):1859-71.
258. May A, Schwedt TJ, Magis D, Pozo-Rosich P, Evers S, Wang SJ. Cluster headache. Nature reviews Disease primers. 2018;4:18006.
259. Hoffmann J, Baca SM, Akerman S. Neurovascular mechanisms of migraine and cluster headache. J Cereb Blood Flow Metab. 2017:271678X17733655.
260. Arkink EB, Schmitz N, Schoonman GG, van Vliet JA, Haan J, van Buchem MA, et al. The anterior hypothalamus in cluster headache. Cephalalgia. 2017;37(11):1039-50.
261. Giorgio A, Lupi C, Zhang J, De Cesaris F, Alessandri M, Mortilla M, et al. Changes in grey matter volume and functional connectivity in cluster headache versus migraine. Brain imaging and behavior. 2020;14(2):496-504.
262. Orru G, Pettersson-Yeo W, Marquand AF, Sartori G, Mechelli A. Using Support Vector Machine to identify imaging biomarkers of neurological and psychiatric disease: a critical review. Neuroscience and biobehavioral reviews. 2012;36(4):1140-52.
263. Zhang Q, Wu Q, Zhang J, He L, Huang J, Zhang J, et al. Discriminative Analysis of Migraine without Aura: Using Functional and Structural MRI with a Multi-Feature Classification Approach. PLoS One. 2016;11(9):e0163875.

264. Tso AR, Brudfors M, Danno D, Grangeon L, Cheema S, Matharu M, et al. Machine phenotyping of cluster headache and its response to verapamil. Brain. 2021;144(2):655-64.
265. Hodkinson DJ, Krause K, Khawaja N, Renton TF, Huggins JP, Vennart W, et al. Quantifying the test-retest reliability of cerebral blood flow measurements in a clinical model of on-going post-surgical pain: A study using pseudo-continuous arterial spin labelling. NeuroImage Clinical. 2013;3:301-10.
266. Hodkinson DJ, Khawaja N, O'Daly O, Thacker MA, Zelaya FO, Wooldridge CL, et al. Cerebral analgesic response to nonsteroidal anti-inflammatory drug ibuprofen. Pain. 2015;156(7):1301-10.
267. Detre JA, Rao H, Wang DJ, Chen YF, Wang Z. Applications of arterial spin labeled MRI in the brain. Journal of magnetic resonance imaging : JMRI. 2012;35(5):1026-37.
268. Smith DV, Utevsky AV, Bland AR, Clement N, Clithero JA, Harsch AE, et al. Characterizing individual differences in functional connectivity using dual-regression and seed-based approaches. Neuroimage. 2014;95:1-12.
269. Schwedt TJ, Larson-Prior L, Coalson RS, Nolan T, Mar S, Ances BM, et al. Allodynia and descending pain modulation in migraine: a resting state functional connectivity analysis. Pain Med. 2014;15(1):154-65.
270. Beckmann CF, Smith SM. Tensorial extensions of independent component analysis for multisubject FMRI analysis. Neuroimage. 2005;25(1):294-311.
271. Beckmann CF. Modelling with independent components. Neuroimage. 2012;62(2):891-901.
272. Smith SM, Fox PT, Miller KL, Glahn DC, Fox PM, Mackay CE, et al. Correspondence of the brain's functional architecture during activation and rest. Proceedings of the National Academy of Sciences of the United States of America. 2009;106(31):13040-5.
273. Smith SM, Miller KL, Moeller S, Xu J, Auerbach EJ, Woolrich MW, et al. Temporally-independent functional modes of spontaneous brain activity. Proceedings of the National Academy of Sciences of the United States of America. 2012;109(8):3131-6.
274. Lin C-CCaC-J. LIBSVM: A Library for Support Vector Machines. ACM Trans Intell Syst Technol. 2011;2,3(Article 27).

275. Fagerholm ED, Hellyer PJ, Scott G, Leech R, Sharp DJ. Disconnection of network hubs and cognitive impairment after traumatic brain injury. Brain. 2015;138(Pt 6):1696-709.

276. Doyle OM, Mehta MA, Brammer MJ. The role of machine learning in neuroimaging for drug discovery and development. Psychopharmacology. 2015;232(21-22):4179-89.

277. Beckmann CF, Smith SM. Probabilistic independent component analysis for functional magnetic resonance imaging. IEEE transactions on medical imaging. 2004;23(2):137-52.

278. Leech R, Kamourieh S, Beckmann CF, Sharp DJ. Fractionating the default mode network: distinct contributions of the ventral and dorsal posterior cingulate cortex to cognitive control. The Journal of neuroscience : the official journal of the Society for Neuroscience. 2011;31(9):3217-24.

279. Maleki N, Becerra L, Brawn J, McEwen B, Burstein R, Borsook D. Common hippocampal structural and functional changes in migraine. Brain structure & function. 2013;218(4):903-12.

280. Maleki N, Becerra L, Brawn J, Bigal M, Burstein R, Borsook D. Concurrent functional and structural cortical alterations in migraine. Cephalalgia. 2012;32(8):607-20.

281. Mehnert J, May A. Functional and structural alterations in the migraine cerebellum. J Cereb Blood Flow Metab. 2017:271678X17722109.

282. May A, Bahra A, Buchel C, Frackowiak RS, Goadsby PJ. Hypothalamic activation in cluster headache attacks. Lancet. 1998;352(9124):275-8.

283. Denuelle M, Fabre N, Payoux P, Chollet F, Geraud G. Posterior cerebral hypoperfusion in migraine without aura. Cephalalgia. 2008;28(8):856-62.

284. Schulte LH, Haji AA, May A. Phase dependent hypothalamic activation following trigeminal input in cluster headache. J Headache Pain. 2020;21(1):30.

285. Yang FC, Chou KH, Fuh JL, Lee PL, Lirng JF, Lin YY, et al. Altered hypothalamic functional connectivity in cluster headache: a longitudinal resting-state functional MRI study. Journal of neurology, neurosurgery, and psychiatry. 2015;86(4):437-45.

286. Qiu E, Wang Y, Ma L, Tian L, Liu R, Dong Z, et al. Abnormal brain functional connectivity of the hypothalamus in cluster headaches. PLoS One. 2013;8(2):e57896.
287. Rocca MA, Valsasina P, Absinta M, Colombo B, Barcella V, Falini A, et al. Central nervous system dysregulation extends beyond the pain-matrix network in cluster headache. Cephalalgia. 2010;30(11):1383-91.
288. Messina RR, MA; Valsasina, P; Misci, P; Filippi, M. Clinical correlates of hypothalamic functional changes in migraine patients. Cephalalgia. 2021;0(0):1–12.
289. Jia Z, Tang W, Zhao D, Yu S. Disrupted functional connectivity between the periaqueductal gray and other brain regions in a rat model of recurrent headache. Sci Rep. 2017;7(1):3960.
290. Leone M. Deep brain stimulation in headache. Lancet Neurol. 2006;5(10):873-7.
291. Akerman S, Holland PR, Goadsby PJ. Diencephalic and brainstem mechanisms in migraine. Nature reviews Neuroscience. 2011;12(10):570-84.
292. Pozo-Rosich P, Storer RJ, Charbit AR, Goadsby PJ. Periaqueductal gray calcitonin gene-related peptide modulates trigeminovascular neurons. Cephalalgia. 2015;35(14):1298-307.
293. Bartsch T, Knight YE, Goadsby PJ. Activation of 5-HT(1B/1D) receptor in the periaqueductal gray inhibits nociception. Ann Neurol. 2004;56(3):371-81.
294. Bahra A, May A, Goadsby PJ. Cluster headache: a prospective clinical study with diagnostic implications. Neurology. 2002;58(3):354-61.
295. Noseda R, Jakubowski M, Kainz V, Borsook D, Burstein R. Cortical projections of functionally identified thalamic trigeminovascular neurons: implications for migraine headache and its associated symptoms. The Journal of neuroscience : the official journal of the Society for Neuroscience. 2011;31(40):14204-17.
296. Ku J, Lee YS, Chang H, Earley CJ, Allen RP, Cho YW. Default mode network disturbances in restless legs syndrome/Willis-Ekbom disease. Sleep medicine. 2016;23:6-11.
297. Yoshida T, Mori T, Yamazaki K, Sonobe N, Shimizu H, Matsumoto T, et al. Relationship between regional cerebral blood flow and neuropsychiatric symptoms in dementia with Lewy bodies. International journal of geriatric psychiatry. 2015;30(10):1068-75.

298. Alsop DC, Detre JA, Golay X, Gunther M, Hendrikse J, Hernandez-Garcia L, et al. Recommended implementation of arterial spin-labeled perfusion MRI for clinical applications: A consensus of the ISMRM perfusion study group and the European consortium for ASL in dementia. Magnetic resonance in medicine. 2015;73(1):102-16.
299. Davies C. Treatment of Individuals at Clinical High Risk for Psychosis: King's College London; 2019.
300. Cardoso MJ, Modat M, Wolz R, Melbourne A, Cash D, Rueckert D, et al. Geodesic Information Flows: Spatially-Variant Graphs and Their Application to Segmentation and Fusion. IEEE transactions on medical imaging. 2015;34(9):1976-88.
301. Sudre CH, Cardoso MJ, Bouvy WH, Biessels GJ, Barnes J, Ourselin S. Bayesian model selection for pathological neuroimaging data applied to white matter lesion segmentation. IEEE transactions on medical imaging. 2015;34(10):2079-102.
302. Prados F, Cardoso MJ, Kanber B, Ciccarelli O, Kapoor R, Gandini Wheeler-Kingshott CAM, et al. A multi-time-point modality-agnostic patch-based method for lesion filling in multiple sclerosis. Neuroimage. 2016;139:376-84.
303. Modat M, Ridgway GR, Taylor ZA, Lehmann M, Barnes J, Hawkes DJ, et al. Fast free-form deformation using graphics processing units. Comput Methods Programs Biomed. 2010;98(3):278-84.
304. Forkel SJ, Thiebaut de Schotten M, Dell'Acqua F, Kalra L, Murphy DG, Williams SC, et al. Anatomical predictors of aphasia recovery: a tractography study of bilateral perisylvian language networks. Brain. 2014;137(Pt 7):2027-39.
305. Chang LC, Walker L, Pierpaoli C. Informed RESTORE: A method for robust estimation of diffusion tensor from low redundancy datasets in the presence of physiological noise artifacts. Magnetic resonance in medicine. 2012;68(5):1654-63.
306. Cox RW. AFNI: software for analysis and visualization of functional magnetic resonance neuroimages. Computers and biomedical research, an international journal. 1996;29(3):162-73.
307. Posse S, Wiese S, Gembris D, Mathiak K, Kessler C, Grosse-Ruyken ML, et al. Enhancement of BOLD-contrast sensitivity by single-shot multi-echo functional MR imaging. Magnetic resonance in medicine. 1999;42(1):87-97.
308. Kundu P, Brenowitz ND, Voon V, Worbe Y, Vertes PE, Inati SJ, et al. Integrated strategy for improving functional connectivity mapping using multiecho fMRI.

Proceedings of the National Academy of Sciences of the United States of America. 2013;110(40):16187-92.

309. Kundu P, Santin MD, Bandettini PA, Bullmore ET, Petiet A. Differentiating BOLD and non-BOLD signals in fMRI time series from anesthetized rats using multi-echo EPI at 11.7 T. Neuroimage. 2014;102 Pt 2:861-74.

310. Kundu P, Benson BE, Baldwin KL, Rosen D, Luh WM, Bandettini PA, et al. Robust resting state fMRI processing for studies on typical brain development based on multi-echo EPI acquisition. Brain imaging and behavior. 2015;9(1):56-73.

311. Dipasquale O, Sethi A, Lagana MM, Baglio F, Baselli G, Kundu P, et al. Comparing resting state fMRI de-noising approaches using multi- and single-echo acquisitions. PLoS One. 2017;12(3):e0173289.

312. Dipasquale O, Martins D, Sethi A, Veronese M, Hesse S, Rullmann M, et al. Unravelling the effects of methylphenidate on the dopaminergic and noradrenergic functional circuits. Neuropsychopharmacology. 2020;45(9):1482-9.

Roberto Messina